



UNIVERSIDADE D
COIMBRA

Felipe Augusto Gomes Ferreira

**ELECTROMAGNETIC FIELD SURVEY FOR
ELECTROMAGNETIC COMPATIBILITY IN
DEEC-UC**

Dissertação no âmbito do Mestrado em Engenharia Electrotécnica e de Computadores, Área de Especialização em Energia, orientada pelo Professor Doutor António Paulo Mendes Breda Dias Coimbra e pelo Professor Doutor Tony Richard de Oliveira de Almeida e apresentada ao Departamento de Engenharia Electrotécnica e de Computadores da Faculdade de Ciências e Tecnologia da Universidade de Coimbra.

Fevereiro 2023



Departamento de Engenharia Electrotécnica e de Computadores
Faculdade de Ciências e Tecnologia
Universidade de Coimbra

A Dissertation
for Graduate Study in MSc Program
Master of Science in Electrical and Computer Engineering

Electromagnetic field survey for Electromagnetic Compatibility in DEEC-UC

Felipe Augusto Gomes Ferreira

Research Developed Under Supervision of
Prof. Dr. António Paulo Mendes Breda Dias Coimbra and
Prof. Dr. Tony Richard de Oliveira de Almeida

Jury

President: Prof. Dr. Jaime Batista dos Santos
Vocal: Prof. Dr. Henrique Leonel Gomes
Vocal: Prof. Dr. António Paulo Mendes Breda Dias Coimbra

February 2023

Thanks

Do not be surprised by the height of the flight. The higher, the further from danger. The higher you rise, the more time there is to recognize a breakdown. It is when you are close to the ground that you should be suspicious
(Alberto Santos Dumont)

First and foremost, I express my gratitude to the almighty God, that from the height of His redemption and wisdom blesses me in countless ways and guides me on my spiritual life journey. I thank my advisors, Dr. Paulo Coimbra and Dr. Tony Almeida for their patience and assistance during the development of this dissertation. I equally praise the supervisors at my job, Humberto and Nuno, for the opportunity given to me in the beginning of my career.

I thank my parents Eliane and Carlos, brothers, uncles, aunts, great aunts, cousins and other Brazilian and Portuguese family members for all the support provided, and also to Boo for covering me with her affection all this time. I also mention the camaraderie of the colleagues from Olaria, Pio XI, CEFET/RJ, MUN's, Viseu, Aachen, along with all the ones I met as a volunteer, and other friends on this journey who, in one way or another, helped me get here.

And last but no least, I nominally express my gratitude for my friends Ephraim, Carol, Fabian and also to Engineer Fábio and Professor Humberto Jorge for the help provided during the manual activities carried out in this dissertation.

Abstract

With the advent of the industrial society and popularization of electric equipment and RF telecommunication devices to foster the comfort of everyday life, complex multifrequency scenarios of non-ionizing radiation have become common in any working or household environment. Efforts have been developed throughout the last decades to identify possible health hazards in both short and long electromagnetic fields (EMF) exposure, establishing legislation for the definition of maximum exposure reference levels. Furthermore, the effects of Electromagnetic Interference (EMI) in electronic devices is one of the major topics investigated nowadays, studying in which EMF exposure conditions there is degradation in the performance of this.

The work presented in this dissertation was primarily oriented to environmentally characterize the DEEC facilities in terms of Electromagnetic Compatibility (EMC). Either in terms of spatial variation, temporal variation and spectrum occupation; or in terms of LF or HF electric and magnetic fields. For this objective, a series of non-overlapping broadband and frequency screening methods were employed, and the results were compared with the corresponding compatibility level for a given disturbance degree phenomena for public environments, prescribed in IEC 61000-2-5 standard. Moreover, the dosimetric levels of the DEEC population were assessed in conformity with ICNIRP reference levels for general-public exposure, also comparing to the most recent publications and national EMF legislation.

An overview of all results indicates compliance at both the EMC and human exposure levels, for all spaces investigated, for all the moments researched. The power frequency magnetic fields are higher the closer a room is to Tower B, confirming the prevalence of the power line over the DEEC, with a measured maximum of $1.97 \mu\text{T}$ in Tower B roof. However, there are several rooms within the $0.4 \mu\text{T}$ limit, which would indicate the inability a real state development in the department's land in accordance with the legislation of other European countries. Moreover, all indoor electric fields measured were below 3.5 V/m , and the electric field measured below the power line, 3 m in front at the main DEEC's Main Entrance, is 36.2 V/m . A temporal-variation

Dynamic range factor of 3 dB was measured for 50 Hz magnetic fields, as well as a variation of 10 dB for HF EMF.

A new method of interpolation graphic representation of ULF Magnetic Fields spatial-variation was also proposed, from measurements made at the central point and the middle of each halved diagonals. The representations were reliable, with good representation of the influence of the power line and electrical distribution boards, and one can consider a fast and robust alternative to traditional Mapping grid methods. There was also a correlation factor of 0.94 in the pairs defined between the central points and each corner of each environment. This suggests that the geometric center measurement can be defined as a good snapshot of the magnetic fields of a given location at that moment.

The HF spectrum occupation occurs mainly in the telecommunications frequency bands. The maximum values of HF electric fields occurred in locations outside the department, with a maximum of 1.73 V/m at the DEI promenade. However, there is a triangular signal, peaking at 97 dB/m and centered at 4 GHz, whose source is unknown.

Regarding the EMC conducted noise in the department, it was not found adequate literature to measure disturbances injected by the mains network in the 0.15-30 MHz frequency range. To this end, an innovative equipment called LISN+I was designed, built and tested. Through measurements at power outlets at various points of the DEEC, the results obtained were credible and easily visualized in a spectrum analyzer, becoming an interesting pedagogical asset and subject to a future paper publication. The measurements indicated Average and Peak values above the emissions limits of Average and Quasi-peak of Class B CISPR 32.

Finally, the Shielding Effectiveness (SE) of DEEC's RF Shielded Chamber, located in the underground parking lot, was measured according to the IEEE 299-2006 standard adapted. The SE curves at points near the wall, corner and door show that the Chamber does not have good shielding for power frequency and low frequency EMF, having values above 40 dB only for incident EMF above 450 MHz. Moreover, the SE behavior at the corner and wall are similar, but the door's SE is noticeably lower for all tested frequencies, which may be an indication that door gaskets need maintenance or replacement.

Keywords: Electromagnetic Environment, Electromagnetic Compatibility, IEC 61000-2-5, EMC conducted noise, RF Shielded Chamber

Resumo

Ao longo do desenvolvimento da eletrónica e popularização de equipamentos de telecomunicação por rádio-frequência, níveis cada vez mais complexos de radiação não-ionizante multifrequência são encontrados, seja em ambientes residenciais ou laborais. Esforços têm sido empreendidos nas últimas décadas para identificar possíveis efeitos biológicos devido a exposição a campos eletromagnéticos, estabelecendo legislação para a definição de níveis máximos de exposição. Ademais, os efeitos de Interferência Eletromagnética (EMI) em equipamentos elétricos é um dos principais temas investigados atualmente, estudando em que condições, duração e intensidade de exposição há degradação no desempenho deste.

Desta forma, o trabalho conduzido nesta dissertação foi orientado para caracterizar ambientalmente as instalações do Departamento de Engenharia Electrotécnica da Universidade de Coimbra em termos de Compatibilidade Eletromagnética (CEM). Quer em termos de variação espacial ou temporal, seja para a gama de baixa ou alta frequência. Para tal objetivo, foi empregado uma série de métodos de pesquisa através de detetores de campos de banda larga e análise espectral. Os resultados foram comparados com os máximos *Compatibility Levels* para ambientes comerciais e públicos da norma IEC 61000-2-5, para fins de CEM. Ademais, os níveis dosimétricos de exposição do DEEC foram verificados em conformidade com os níveis máximos de referência do ICNIRP para padrões de exposição do público geral, realizando referências pontuais a legislação nacional de membros da UE para a respectiva temática.

Os resultados obtidos indicam total conformidade com os máximos *Compatibility Levels* e dosimetria humana, para todos os ambientes e em todos os momentos investigados. De um modo geral, os níveis de indução magnética à frequência da rede são maiores quão mais a Este esteja uma localidade, a confirmar a preponderância da linha de transmissão sobre a Torre B, com um valor máximo medido de $1,97 \mu\text{T}$ na torre deste. Ademais, todos os campos elétricos à frequência da rede registados dentro do DEEC possuem magnitude abaixo dos $3,5 \text{ V/m}$, com a exceção do ponto medido 3 m em frente à entrada principal do DEEC, cujo valor medido foi de $36,2 \text{ V/m}$.

Foi registado um *Dynamic range*, fator de variação temporal, de 3 dB para campos magnéticos a 50 Hz, e um fator de 10 dB para os campos eletromagnéticos entre 150 MHz e 6 GHz.

Um novo método de interpolação gráfica para a representação de campos magnéticos a 50 Hz foi proposto. Os resultados foram credíveis, sendo tal método uma alternativa robusta e rápida a métodos tradicionais como representação em grelha. Um factor de correlação de 0.94 também foi obtido entre os pares definidos pelos pontos centrais e cada um dos cantos de cada ambiente, sugerindo que o ponto central pode ser tido como um bom indicativo da intensidade do campo magnético em todo ambiente.

A ocupação espectral às altas frequências acontece majoritariamente nas faixas de telecomunicação. Os maiores níveis de campos elétricos medidos nesta faixa foram registado na parte externa do departamento, com um máximo de 1,73 V/m no ponto em frente à entrada principal do Departamento de Engenharia Informática. No entanto, há um sinal triangular, com um pico de $97 \text{ dB}\mu\text{V/m}$ centrado em 4 GHz, cuja origem é incerta.

Para a avaliação dos distúrbios conduzidos na gama de frequências de CEM, 150 kHz-30 MHz, há inexistência de literatura técnica sobre o ruído presente globalmente na rede eléctrica. Desta forma, um equipamento inovador batizado LISN+I foi concebido e testado. Através de medições em fichas em diferentes pontos do DEEC, os resultados obtidos foram credíveis e facilmente visualizáveis através de um analisador de espectro, tornando-se portanto uma interessante adição pedagógica e passíveis de publicação futura. Os resultados indicaram valores de *Average* e *Peak* acima dos limites de emissão da Classe B da norma CISPR 32 para *Average* e *Quasi-peak*, respectivamente.

Por fim, a *Shielding Effectiveness* (SE) da câmara blindada do ISR, presente no estacionamento subterrâneo do DEEC, foi medida com adaptações da norma IEEE 299-2006. A análise das curvas de SE indicam que a câmara não possui blindagem adequada para campos eletromagnéticos de baixa frequência. Valores de SE acima de 40 dB somente ocorrem para campos incidentes acima de 450 MHz. Entretanto, embora o comportamento das curvas da quina e parede sejam similares, a porta notoriamente possui os menores valores de SE para as frequências testadas, indicando que os seus *gaskets* possam precisar de manutenção ou substituição.

Palavras-chave: Ambiente Electromagnético, Compatibilidade Eletromagnética, Câmara blindada, IEC 61000-2-5, Distúrbio conduzido para CEM, RF Câmara blindada

Acronyms and symbols

Abbreviation	Meaning
AF	Antenna factor
ANSI	American National Standards Institute
CISPR	Comité International Spécial des Perturbations Radioélectriques
DEEC	Departamento de Engenharia Electrotécnica e de Computadores
DoC	Declaration of Conformity
EBF	Equivalent B-field
EEF	Equivalent Electric Field
EMBF	Equivalent Majorant Magnetic flux density
EMC	Electromagnetic Compatibility
EME	Electromagnetic Environment
EMEF	Equivalent Majorant Electric Field
EMF	Electromagnetic fields
EMI	Electromagnetic Interference
EMP	Electromagnetic Pulse
EN	European Standard
EPW	Equivalent Plane Wave
ERP	Effective Radiated Power
ESD	Electrostatic Discharge
EUT	Equipment under test
FCC	United States Federal Communications Commission
GER	Global Exposure Ratio
GND	Ground
HF	High Frequency
HV	High Voltage
IARC	International Agency for Research on Cancer
ICNIRP	International Commission on Non-ionizing Radiation Protection
IEC	International Electrotechnical Commission
IEEE	Institute of Electrical and Electronics Engineers
IEP	Instituto Electrotécnico Português

Abbreviation	Meaning
ILC	Interlaboratory Comparisons
LISN	Line Impedance Stabilization Network
LF	Low Frequency
LV	Low Voltage
OATS	Open Area Test Site
POW	Power Frequency
QP	Quasi-Peak
RBW	Resolution Bandwidth
RF	Radio Frequency
RFI	Radio Frequency Interference
RFR	Radio Frequency Resource
RMS	Root Mean Square
SE	Shielding Effectiveness
ULF	Ultra Low Frequency
WDTS	Wideband Data Transmission Systems

Symbol	Meaning
dBm	decibel miliWatt
\hat{V}_P	Voltage drop in standard 50Ω resistor between phase and ground conductor
\hat{V}_N	Voltage drop in standard 50Ω resistor between neutral and ground conductor
\hat{I}_P	Current in standard 50Ω phase resistor
\hat{I}_N	Current in standard 50Ω neutral resistor

Contents

1	Introduction	1
1.1	Motivations and Objectives	1
1.2	Document structure	3
2	EMC theoretic framework	5
2.1	Electromagnetic Environment	8
2.2	Biological effects	10
3	Radiated Emissions Survey	14
3.1	Broadband Measurements	16
3.1.1	Low Frequency Magnetic Field Measurements	16
3.1.2	Low Frequency Electric Fields levels measurement	18
3.1.3	Possibilities on data representation	20
3.2	Frequency Screening Analysis	22
3.2.1	Radiometric survey	22
3.2.2	Long-range temporal variation Survey	25
3.2.3	Spatial-averaging power frequency human exposure assessment approach	26
3.2.4	Aaronia NF-5040 and HF-6060V4 specifications	28
4	Conducted electromagnetic pollution survey	30
5	Chamber Shielding Effectiveness Calculation	34

5.1	Shielding effectiveness estimation of electromagnetic Shielded Chamber	35
6	Characterization survey results	39
6.1	Broadband approach survey	39
6.2	Frequency Screening results	48
6.3	EMC conducted noise measurements	57
6.4	Chamber's Shielding Effectiveness measurement	59
7	Conclusion	62
7.1	Conclusions	62
7.2	Future Work	64
	References	65
A	IEC 61000-2-5 overview of compatibility levels, disturbance degrees and levels for location classes	71
B	ICNIRP reference levels for general-public exposure to time-varying EMF	76
C	EMF radiated survey equipment characteristic and additional results	77
D	Shielding Effectiveness testing site configurations and additional results	83
E	Additional results and Datasheet	86

List of Figures

2.1	Electromagnetic Interference phenomenon concept.	6
2.2	IEC 61000-2-5 archetypes of location classes.	10
2.3	ICNIRP reference levels for exposure to time-varying magnetic flux density.	12
2.4	ICNIRP reference levels for exposure to time-varying electric fields.	12
3.1	Radiated EMF survey protocol fluxogram.	15
3.2	Five-point and Mapping methods	17
3.3	Geometries of typical free-body electric field meter.	19
3.4	NF-5020 single axis E-field sensor and External survey for Vertical E-fields.	19
3.5	Interpolations and extrapolation techniques assessment for Five-point LF magnetic-fields methods.	21
3.6	Radiometric survey measurement flowchart.	23
3.7	Six-measurement grid for Human spatial-averaging compliance.	27
4.1	Ordinary LISN topology.	31
4.2	Adapted LISN internal circuit.	32
5.1	FCC Radiated emission and immunity test facilities.	35
5.2	Shielding effectiveness tests configuration protocol.	38
6.1	Maximum magnetic flux density in each location surveyed in the Five-point method.	41
6.2	Scatter chart of magnetic flux density at the center of each environment versus other points at the same environment.	42

6.3	Magnetic field density obtained in the survey along the corridors of the second and fourth floor of DEEC.	44
6.4	Magnetic field density obtained in the survey along the Third floor Study aisle and the 3A corridor.	44
6.5	Magnetic flux density mapping at the Second Floor Entrance Atrium (left) and Sixth Floor Tower B Study Room(right).	46
6.6	Power frequency B-field interpolation and extrapolation at the Entrance Atrium. .	47
6.7	Power frequency B-field interpolation and extrapolation at the Tower B Study Room third subspace.	47
6.8	Power frequency B-field interpolation and extrapolation at the Tower B Roof - Outdoor.	48
6.9	Power frequency spectrum signatures with MinMax and RMS detector type at different locations in DEEC.	51
6.10	HF spectrum signatures with MinMax and RMS detector type at different locations in DEEC at different locations in DEEC.	52
6.11	0.15-1 MHz spectrum signatures with MinMax and RMS detector type at different locations in DEEC.	53
6.12	200-500 Hz spectrum signatures with MinMax and RMS detector type at different locations in DEEC.	54
6.13	65-110 Hz spectrum signatures with MinMax and RMS detector type at different locations in DEEC.	55
6.14	Dynamic range in 50 Hz 24 hour temporal variation Survey in 3A.23 office. . . .	56
6.15	Dynamic range in the HF 24 hour temporal variation Survey in 3A.21 office. . . .	57
6.16	EMC conducted noise at power outlet outside Shielded Chamber along with the EN 55022 class A and class B limits.	58
6.17	EMC conducted noise at power outlet with filter inside Shielded Chamber along with the EN 55022 class A and class B limits.	58
6.18	EMC conducted noise at power outlet in T4.2 classroom along with the EN 55022 class A and class B limits.	59

6.19	ULF Power frequency SE versus incident \vec{B} field.	60
6.20	Maximum and minimum chamber's SE per frequency and location.	61
C.1	Magnetic field density obtained in the survey along the East and West Third Floor corridors.	78
C.2	Bar's Lateral Mapping	80
C.3	Power frequency B-field interpolation and extrapolation at the Secretary first sub-space.	80
C.4	Power frequency B-field interpolation and extrapolation at the NEEC second sub-space.	81
C.5	Power frequency B-field interpolation and extrapolation at the Bar.	81
C.6	Power frequency B-field interpolation and extrapolation at the Parking - Drivers Zone.	82
C.7	Power frequency B-field interpolation and extrapolation at the 3A.23 Office.	82
D.1	ULF Power frequency SE in different loading test configurations.	84
D.2	Chamber's SE scenario with Signal generator emitting fields with a strength of 15dBm 15dB.	84
D.3	Shielding effectiveness tests configuration protocol for chamber's door, corner and wall.	85
E.1	EMC conducted noise at power outlet in Bar along with the EN 55022 class A and class B limits.	86
E.2	EMC conducted noise at power outlet in Third floor Study Aisle along with the EN 55022 class A and class B limits.	86
E.3	EMC conducted noise at power outlet in R1.2 laboratory at 17:41h along with the EN 55022 class A and class B limits.	87
E.4	EMC conducted noise at power outlet in R1.2 laboratory at 22:54h along with the EN 55022 class A and class B limits.	87
E.5	Example of expansion joint in DEEC.	88

E.6	Wavelength spatial-variation hypothesis graphic results.	89
E.7	LISN+I equipment.	89
E.8	Front page of Five-point method Datasheet.	90
E.9	Back page of Five-point method Datasheet.	91
E.10	Front page of ULF B-field time-variation Datasheet.	92
E.11	Back page of ULF B-field time-variation Datasheet.	93
E.12	LF Radiometric Survey Datasheet.	94
E.13	HF Radiometric Survey Datasheet.	95
E.14	Electric fields survey Datasheet	96

List of Tables

2.1	CISPR 32 Requirements for conducted emissions of Class B equipment	8
2.2	CISPR 32 Requirements for radiated emissions for Class B equipment	8
3.1	Radiometric survey equipment parameters	25
6.1	Five-point method in single space environments	40
6.2	Five-point method in locations with multiple subspace.	40
6.3	B-field temporal-variation assessment in Spot points at the Fourth Floor corridor.	41
6.4	B-field temporal-variation assessment in Spot points at the Entrance Atrium. . . .	42
6.5	Power frequency magnetic flux density at the windows.	43
6.6	Power frequency magnetic flux density at points in the outside of DEEC.	43
6.7	Electric field survey at power frequency at different locations with EFM160. . . .	45
6.8	Radiometric survey LF overview with MinMax detector type.	49
6.9	Radiometric survey HF overview with MinMax detector type.	49
6.10	Radiometric survey LF overview with RMS detector type.	49
6.11	Radiometric survey HF overview with RMS detector type.	49
6.12	Spatial-averaging power frequency human exposure assessment magnetic flux density.	56
6.13	HF Shielding Effectiveness results per location.	60
A.1	Disturbance degrees and maximum compatibility levels for LF magnetic fields at various frequencies	71
A.2	Disturbance degrees and maximum compatibility levels for LF electric fields	72

A.3	Disturbance degrees in the commercial/public location class	72
A.4	Disturbance degrees and maximum compatibility levels of induced continuous-wave conducted voltages with ground reference	72
A.5	Disturbances degrees and maximum compatibility levels for conducted oscillatory transients in low-voltage AC power systems	73
A.6	Disturbance degrees, maximum compatibility levels for HF RF wideband devices and distance to source	73
A.7	Disturbance degrees, maximum compatibility levels for HF RF terminal wideband devices and distance to source	74
A.8	Disturbance degrees, maximum compatibility levels for Base stations and distance to source	74
A.9	Disturbance degrees, levels for Mobile and portable phones and distance to source	75
A.10	Disturbance degrees, maximum compatibility levels for HF radiated electric fields and distance to source	75
A.11	Types of Location Classes	75
B.1	ICNIRP reference levels for general-public exposure to time-varying electric and magnetic fields.	76
C.1	Aaronia SPECTRAN NF-5020 Spectrum Analyzer	77
C.2	Aaronia SPECTRAN HF-6060V4 Spectrum Analyzer	77
C.3	SYPRIS 4080 ELF handheld meter characteristic	77
C.4	EFM 160 Power Frequency Electric Field Sensor	78
C.5	Electric field survey at power frequency at different locations with EFM160 and Aaronia NF5020.	78
C.6	Five-point method measurements summary	79
D.1	Shielding effectiveness frequency test specifications.	83
D.2	Shielding effectiveness at Power-frequency conditions with testing set incandescent load configuration.	83

E.1	LISN+I toggle switches configuration modes	88
E.2	LISN+I insulation verification tests.	88
E.3	Wavelength spatial-variation hypothesis results.	88

Chapter 1

Introduction

1.1 Motivations and Objectives

The number of Electromagnetic fields (EMF) produced by artificial sources, intentionally or non-intentionally, has been increasing dramatically in the last few years. Electronic devices, electric machines, electric power transmission lines, atmospheric events and even cosmic discharges might lead to the emission of electric, magnetic and electromagnetic fields. Furthermore, any contemporary working and household environment are equipped with RF telecommunication systems, leading to a scenario with a multi-frequency EMF composition.

This complex framework consists of what is called an Electromagnetic Environment (EME). In such context, the EMF emitted by any electric device might affect the operation of any other equipment present in a same site, a phenomenon called Electromagnetic Interference (EMI), classified as an environmental pollution and a crucial concern factor in any currently designed electronic product [1]. While operating in a hypothetical EME, an equipment is said susceptible if it does not operate satisfactorily on it. Therefore, the term Electromagnetic Compatibility (EMC) consists on the capacity of a given device to be insusceptible on its EME, as well as do not provoke intolerable electromagnetic disturbances to other device in that same environment [2]. The transferred energy between an EMI source and the affected device might be a **conductive** coupling, through its AC power cord, a **radiated** coupling, over electric, magnetic and electromagnetic fields propagation through the medium, and also **capacitive** and **inductive** [1].

According to the 2014/30/EU directive, a manufacturer or importer must state a Declaration of Conformity (DOC) over any electrical equipment sold in the EU common market. This

compliance states that the results of emission and immunity tests and EMC tests that address respectively the EMI and susceptibility of such device are below the standards maximum level allowed [2]. Because of this, a certification process is conducted in special test facilities, where the equipment under test (EUT) and testing measurement devices involved are ideally isolated from the external EME. Reverberation chambers, anechoic and semi-anechoic chambers and shielded enclosure chambers are the commonly facilities used in this process, each on its own advantages and disadvantages, as referenced on specific standards [3].

The hazards of an EMF are also observed on human health. Intense exposure to electromagnetic energy affects human tissues, although the extent of the direct and indirect effects and the frequency range related to each type of damage are a controversial topic on epidemiological studies, representing a major concern on research papers [4, 5]. Since exposure to intense electromagnetic energy over a long period of time is proven to damage human tissues, regulatory standards have been defined by international bodies and national legislation authorities, concerning the levels of energy that may be considered dangerous, as well as the effort to classify time exposure and the environmental conditions for it [6, 7]. The ICNIRP general-public guidelines limits exposure up to 300 GHz, based on known evidence of immediate and long-term harmful effects on human health through non-ionizing radiation¹ [8]; it is the main reference and legally binding standard in Europe [2, 6].

Due to the constant student and staff presence, schools and universities have been classified by the World Health Organization as EMF highly sensitive zones, whilst major efforts have been conducted to assess EMF pollution and their long-term biological effects [9, 10]. Alleged cognitive skills and negative pedagogical outcomes have been reported, an effect called electrical sensitivity, however, there is no confirmation of a link between these symptoms with EMF exposition [11]. In addition, the diversity of EMF sources and the intermittence of their emissions, existing somewhere such as the Department of Electrical and Computer Engineering of University of Coimbra, foreseen an hypothesis of an especially complex EME. Electrical machines on Laboratories, WLAN Access Points, swarming human occupation in common areas, telecommunications antennas on the terrace and a high voltage (HV) power line over the building makes globally forecasting the EMF fields by theoretical calculations a nearly impossible task due the spatial and time variation. The EMF time-varying natural aspect, along with factors such as

¹Ionizing radiation is defined as the energy capable of removing an electron from an atom. Regarding human tissues, ionizing radiation is specially dangerous as it is able to provoke mutations on genoma

intrinsic methodological errors, as well as surveyor expertise and field interaction with objects nearby make measuring EMF one of the least precise measurements in physics [12].

Considering the motivations thus exposed, the main goal of this dissertation is to execute an EME characterization of the DEEC-UC building. In regard to the EMF radiated pollution, a spectrum signature survey throughout a frequency screening methodology was carried, covering a bandwidth up to 6 GHz, as well as a low frequency (LF) electric and magnetic flux density survey protocol was developed, where both were compared to the IEC 61000-2-5 Compatibility Levels for commercial/public location class. A dosimetric evaluation on DEEC's population was also performed, based on ICNIRP guidelines. An innovative LF magnetic field spatial representation is also proposed, through interpolation and extrapolation numeric methods. Spatial-variation metrics were also tested, adapting the Interlaboratorial Comparisons [13].

In respect to the conducted disturbances, although abundant literature on emissions in an EUT, scarce studies are found on the measurement of noise present in a given electrical network in a frequency range of 150 kHz to 30 MHz, the EMC conducted bandwidth required by *Comité International Spécial des Perturbations Radioélectriques* (CISPR) standard 32 and IEC 61000-4-8 standards [14, 15]. In this way, an innovative device called LISN+I is designed, built and tested, checking the noise conducted in several outlets along the building.

Lastly, a radio frequency shielded chamber, kindly donated by the *Instituto Electrotécnico Português* (IEP), will be evaluated as an EMC testing site from its Shielding Effectiveness (SE) characterization. Following the IEEE Std 299-2006 adapted to the equipment available in the EMC laboratory [16], becoming a source of potential pedagogical importance and value to the academic community of DEEC-UC.

1.2 Document structure

This dissertation is composed by seven chapters and their respective appendixes, with the introduction as the first Chapter. The second chapter discusses an EMC overview, biological hazards prescribed on epidemiological reports and the IEC 61000-2-5 standard. Chapter 3 displays the methodology adopted on the Radiated EMF survey, the spatial-variation metrics related, considerations about the results data exposure and technical features of the equipment employed in the enterprise. Chapter 4 addresses the proposed topology of the Line Impedance Stabilization

Network Interface (LISN+I). The fifth chapter exposes the method of calculating the Shielded Chamber's SE, in accordance with IEEE Std 299-2006 guide. Chapter 6 presents and discusses the results obtained in radiated and conducted emissions, as well as the results of Shielded Chamber measurement. Finally, chapter 7 addresses the conclusion of the development of the dissertation and presents a possible pathway for future work related to the subject.

Chapter 2

EMC theoretic framework

Along with the evolution of electronics over the last century, unwanted effects or even damage has been reported regarding electric equipment whilst exposed to other devices installed nearby, a phenomenon called Electromagnetic interference¹. It led to the advent of the scientific area of Electromagnetic Compatibility, a jargon that stands for the ability of a given device to operate satisfactorily in its Electromagnetic Environment (EME), without instigating unacceptable electromagnetic disturbances to other devices in the same site [2].

Three concepts are vital for EMC comprehension, and solving one of them might lead to a correct system operation. Electromagnetic disturbance is the first of them, meaning any electromagnetic phenomenon able to degrade the performance of equipment [2]. This can be electromagnetic noise, an unwanted signal or a change in the propagation medium itself. The concept of electromagnetic disturbance is related to the notion of **Emissions**, that is, electromagnetic energy unleashed to environment, intentionally or not, which can even be generated by natural forces (as Earth's magnetic field)[17]. The second related concept is **susceptibility**, meaning ineffectiveness of a given device, equipment or system to operate without degradation in the presence of an electromagnetic disturbance. In addition, *immunity* denotes how able a certain device is to perform correctly, without degradation, while affected by an electromagnetic disturbance [1, 2]. The third concept is the coupling mechanism, the pathway in which the disturbance flows from an electromagnetic interference (EMI) source to the victim. It consists on inductive, capacitive, conductive or radiated couplings, as the figure 2.1 illustrates[18].

An inductive coupling refers to magnetic fields originated from a current flow source near the

¹Also called Radio-frequency Interference

victim, conceptualized as a power transformer. The capacitive coupling phenomenon arises from electric potential difference between source and victim, given electric field related and shaped as a capacitor. The third type, also referred as resistive coupling, is defined by an electric current flowing through a power cord up to the victim. It is divided into Common Mode and Differential Mode currents and also might be responsible for radiated emissions. The conductive coupling will be discussed thoroughly on chapter 4.

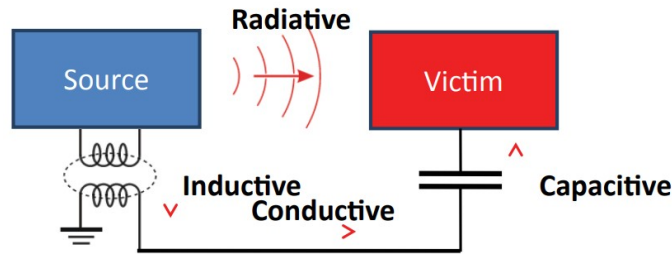


Figure 2.1: Electromagnetic Interference phenomenon concept[18].

Lastly, the radiated coupling refers to electromagnetic fields propagation supposing far-field conditions. In this way, a magnetic field flux variation would incur into an electric field change, which in turn would affect the magnetic field as well. In other words, these conditions imply that electric and magnetic fields are interdependent and perpendicular to each other, and may be approximated by a plane-wave model[6]. For EMC purposes, the boundary where the far field region begins can be defined from the distance to the source of origin, according to equation 2.1, where λ is the EMF wavelength. Due to this, if free space propagating conditions are considered, the electric E and magnetic H field magnitude are orthogonally attached and mathematically related, as equation 2.2 exemplifies, where Z_0 is the characteristic impedance of vacuum (approximately 377Ω)[6, 17].

$$Far\ field_{Boundary}(m) = \frac{5\lambda}{2\pi} \quad (2.1)$$

$$|E| (V/m) = |H| (A/m) \times Z_0 (\Omega) \quad (2.2)$$

Therefore, because of the increasingly congested electromagnetic in any working or living facility, the multitude of equipment available and the speed at which new technologies are introduced, enforcing EMC legislation become a major concern worldwide [19]. In Europe, the 2014/53/EU directive is the legally binding legislation in regards with EMC protection. The law

states that any manufacturer or importer must emit a Declaration of Conformity (DoC) stating that its equipment is in conformity with Emission and Immunity compliance limits, referencing directly the Comité Européen de Normalisation Électrotechnique (CENELEC) standards [2]. The CENELEC is the body for harmonisation of standards in EU, as well as the voluntary preparation of electrotechnical standards.

The EN 550032 standard is the main reference for EMC emission requirements in Europe, being a modified version of IEC/CISPR 32[20]. It specifies procedures methods, equipment and repeatability of results applied to any industrial, scientific and medical equipment with a rated supply voltage not exceeding 600 V and operating frequency from 0 Hz up to 400 GHz, except when specific standards are available [2]. Overall, the standard prescribes that any unnatural signal with frequency above 10 kHz is subject to regulation. Moreover, the emissions levels are lower than immunity limits, placing a buffer margin in order to allow tolerance against any additional potential coupling mechanisms that were not considered in situ events[1].

However, the certifying testing frequency range prescribed by EN 550032 and CISPR 32, concerning conducted and radiated emissions, are not equal. The conducted emissions are tested in a frequency range of 150 kHz to 30 MHz, as the effects of power switching are prominent in such bandwidth. The radiated frequency, nevertheless, is assessed in a bandwidth from 30 MHz up to 6 GHz, due to the number of RF communication devices with transmission ranges above 1 GHz[20].

The non-specifically categorized devices in both standards (such as medical equipment) are classified into two main classes: Class A, covering products labeled for industrial and commercial use only, and Class B, more restricted and labeled for residential use, assuming lack of knowledge of EMC effects and, thus, a greater difficulty to mitigate any EMI question. As DEEC population is in general lay regarding EMF effects, the obtained values during the environmental survey for EMC standards conducted in this dissertation will be compared with the Class B limits, as reference in tables 2.1 and 2.2 for conducted and radiated emissions, respectively[20].

Table 2.1: CISPR 32 Requirements for conducted emissions of Class B equipment

Frequency range (MHz)	Coupling device	Detector type/ bandwidth	Class B limits $\text{dB}\mu\text{V}$
0.15 - 0.5	AMN	Quasi Peak/9 kHz	66 - 56
0.5 - 5	AMN	Quasi Peak/9 kHz	56
5 - 30	AMN	Quasi Peak/9 kHz	60
0.15 - 0.5	AMN	Average/9 kHz	56 - 46
0.5 - 5	AMN	Average/9 kHz	46
5 - 30	AMN	Average/9 kHz	50

NOTE: AMN means Artificial Mains Network or LISN

Table 2.2: CISPR 32 Requirements for radiated emissions for Class B equipment

Frequency range (MHz)	Distance (m)	Detector type/ bandwidth	Class B limits $\text{dB}\mu\text{V}/\text{m}$
30 - 230	10	Quasi Peak/120 kHz	30
230 - 1000	10	Quasi Peak/120 kHz	37
30 - 230	3	Quasi Peak/120 kHz	40
230 - 1000	3	Quasi Peak/120 kHz	47
1000 - 3000	3	Average 1 MHz	50
3000 - 6000	3	Average 1 MHz	54
1000 - 3000	3	Peak 1 MHz	70
3000 - 6000	3	Peak 1 MHz	74

2.1 Electromagnetic Environment

The expression Electromagnetic environment refers to the totality of all electromagnetic phenomena observable in a given site, such as frequency, amplitude, rising time, modulation, as well as their propagation characteristics [2]. A proper knowledge of EME is crucial for accomplishing EMC conformity of an equipment or system, disposing the appropriate immunity levels selection for a correct performance in such environment [21]. Any EME phenomena might be divided in low-frequency (Up to 9 kHz) and high-frequency events (above 9 kHz), as well as ESD, which will not be addressed in this dissertation.

The act of obtaining a total EME description and comparing it to standardized immunity limits, however, is a challenging task due to time and spatial dependence. Completely assessing the whole LF and HF spectrum for susceptibility conformity purposes in a given location might

not as well be required, taking into account that certain EMI disturbance phenomena are most statistically likely to happen on certain specific sites [21]. Moreover, the EME on an specific site is not long-term constant due the constant technology evolution and equipment replacement. Therefore, the IEC 61000-2-5 is the most recently introduced standard regarding an EME classification protocol, providing a correlation degree between a determined location and their potential EMI sources and location boundaries, through eight different location classes, as referenced in table A.11 [21].

The IEC is an international body for standardization of electrical, electronic and related technology areas. Their guidelines are optional, although serving as a reference for national authorities worldwide. The IEC 61000-2-5 referenced classes are characterized by its compatibility levels, consisting on the “specified maximum electromagnetic disturbance level expected to be impressed on a device, equipment or system operated in particular conditions”² [22]. They are constructed based on each specific disturbance degree, a terminology proposed meaning: ”a specified and quantified intensity within a range of disturbance levels, corresponding to a particular electromagnetic phenomenon encountered in the EME of interest coordinating the setting of emission and immunity limit” [22].

As suggested by Jaekel et al, they might be condensed in three non-exclusive archetypes: industrial, residential and office/public, as figure 2.2 shows[15]. Due to overlapping of these, however, a facility might be categorized in more than one archetype. For practical comparison purposes, DEEC facilities will be classified as a commercial/public Location Class. Two different sets of tables are provided: The location-oriented table A.3 provides an archetype of the disturbance degrees and compatibility levels correlation, as well as phenomena-oriented tables A.1-A.10 imposes maximum levels per disturbance degrees for a given phenomenon [21, 22].

²The Maximum, however, must not be understood literally but in a probabilistic sense, on occurrence and its parameters, with very low expectations to actually happen.

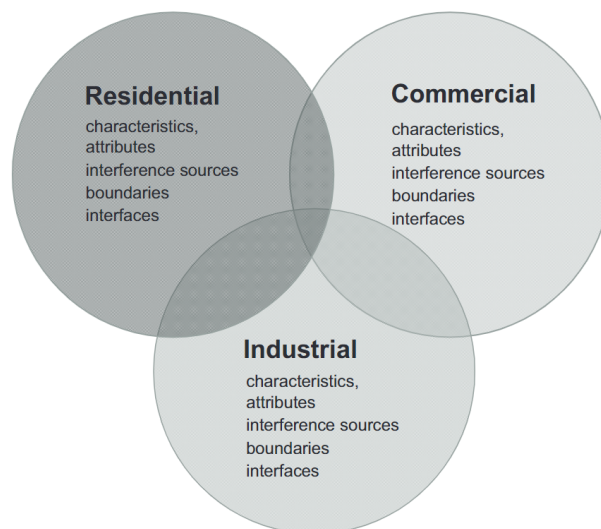


Figure 2.2: IEC 61000-2-5 archetypes of location classes[15].

2.2 Biological effects

Regarding non-ionizing radiation, direct and indirect health hazards are prescribed both on epidemiological literature and exposure legislation [6]. Indirect coupling consists on the resultant contact current, where a human body approaches an object with a different electrical potential [5]. The direct coupling mechanisms, although, are composed by LF electric fields, LF magnetic fields and energy absorption, incurring also in electrical dipoles reorientation and induced internal electrical fields [5].

The biological EMF effects below 100 kHz are mostly related with induction current in the tissues [23]. In addition, an extensive epidemiological literature relates neurological diseases, such as Leukemia, Glioma and brain carcinoma, to long exposure for low frequency electric and magnetic fields. The intensity and exposure duration of hazardous EMF, however, is a controversial topic on its respective literature [5, 24]. Regarding EMF above 100 kHz, thermal effects are the main cause of biological damaging [5]. The higher the frequency, the more superficial is the field penetration and more energy is absorbed, due to skin effect. Hyperthermia and burn injuries are the most common wound related by this effect[25]. Indirect effects are related to interactions with entities with a distinct electrical potential from the human body [6].

In relation to HF EMF, energy absorption is the main factor of concern due to rise in body temperature, although studies linking long exposure to EMF emitted by RF telecommunication devices to glioma [26]. As stated by International Commission on Non-Ionizing Radiation Pro-

tection (ICNIRP) guideline, while exposed to EMF with frequencies in the range from 20 MHz to 300 MHz, a whole body absorption is expected to be seen [6]. Fields below 20 MHz and above 100 kHz might provoke absorption on the neck, trunk and legs. And been exposed to EMF above 300 MHz might cause non-uniform hazardous absorption [5, 6].

Due to these factors, enforcing legislation concerning EMF human exposure is a major public opinion preoccupation [7]. The 1999/519/EU recommendation, originated from ICNIRP 1998 exposure guidelines, introduces basic restrictions for general public to EMF (up to 300 GHz), and is legally binding by Portuguese legislation.[6, 27]. Occupational exposure comprises adults well informed about their EME conditions and trained for taking appropriated mitigating actions, while public exposure covers non-technical reported citizens of all ages and health conditions, unaware of the exposure conditions and possible EMF safety measures. As a consequence, two classes of exposure metrics guidance are established: Basic restrictions and reference levels. The first class is related to time-varying EMF restrictions directly linked to health effects, consisting on induced and contact currents (mA/m^2), SAR (W/Kg) and Power Density (W/m^2).

Nevertheless, the reference levels were established for practical survey purposes and, thus, will be the main Dissertation reference for estimation of human dosimetry. If an electromagnetic survey provides measurements below all reference levels on appropriated timing and averaging conditions, that EME is stated by guideline as being in accordance with the root mean square (RMS) electric and magnetic fields basic magnitude restrictions, as figures 2.3 and 2.4 show, respectively. They consist on maximum electric field strength ($|\vec{E}|$), magnetic field strength ($|\vec{H}|$), magnetic flux density ($|\vec{B}|$) and Power Density (W/m^2), reference on table B.1 [6]. Nonetheless, the EME spectrum generally is multi-frequency composed and their effects are additive [6]. For assessing the conformity over this, the guideline establishes the following requirements:

From 1 to 10 MHz, where the basic restrictions regarding the current density and electrical stimulation are prominent, the equation 2.3 establishes that:

$$\sum_{i=1Hz}^{1MHz} \frac{E_i}{E_{Li}} + \sum_{i>1MHz}^{10MHz} \frac{E_i}{a} \leq 1 \text{ and } \sum_{i=1Hz}^{65kHz} \frac{H_j}{H_{Lj}} + \sum_{i>65kHz}^{10MHz} \frac{H_j}{b} \leq 1 \quad (2.3)$$

Where E_i and H_j are, respectively, the electric and magnetic fields strength at the frequency i ; E_{Li} and H_{Lj} , respectively, the electric and magnetic field reference level mentioned in table B.1 ; a is an electric field constant (87 V/m for general public exposure) and b is a magnetic field constant (0.25 mT for general public exposure). From 100 MHz up to 300 GHz, where the

thermal effects are the prominent, the requisites to be assessed are described by equation 2.4:

$$\sum_{i=100kHz}^{1MHz} \left(\frac{E_i}{c}\right)^2 + \sum_{i>1MHz}^{300GHz} \left(\frac{E_i}{E_{Li}}\right)^2 \leq 1 \text{ and } \sum_{i=100kHz}^{1MHz} \left(\frac{H_j}{d}\right)^2 + \sum_{i>1MHz}^{300GHz} \left(\frac{H_j}{H_{ji}}\right)^2 \leq 1 \quad (2.4)$$

Where E_i and H_j are, respectively, the electric and magnetic fields strength at the frequency i ; E_{Li} and H_{ji} are, respectively, the electric and magnetic field reference level mentioned in table B.1; c is an electric field variable ($87/\sqrt{f}$ for general public exposure); and d is a magnetic field variable ($0.73/f$ for general public exposure).

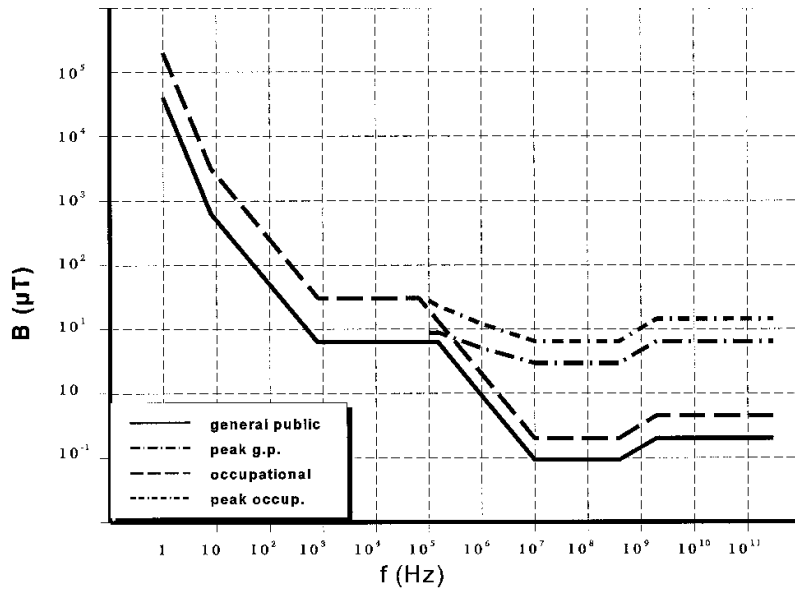


Figure 2.3: ICNIRP reference levels for exposure to time-varying magnetic flux density[6].

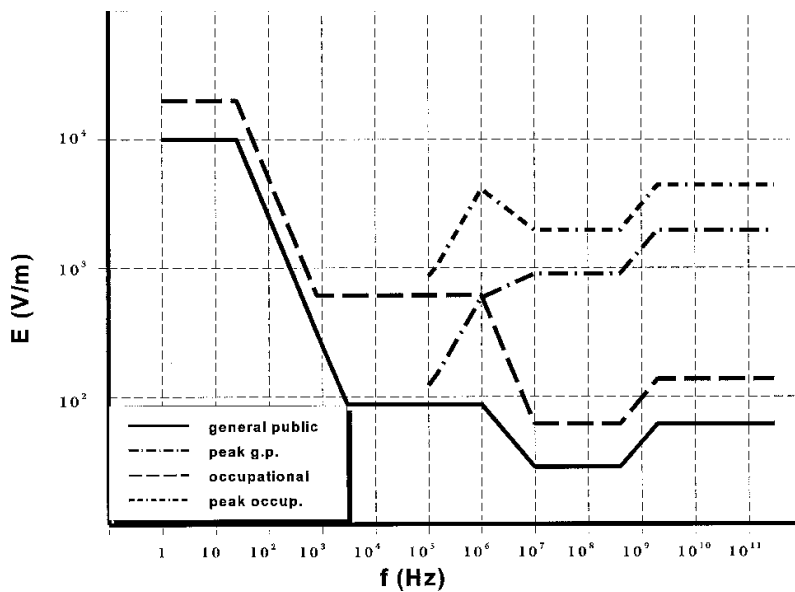


Figure 2.4: ICNIRP reference levels for exposure to time-varying electric fields[6].

Indeed, certain countries adopt significantly smaller limits, both in the residential and occupational levels, with respect to power frequency electric and magnetic exposure. Alleged studies claim childhood leukaemia, breast cancer and melanoma damage increase while exposed continuously to ULF magnetic fields over $0.2 \mu T$ [28]. Swiss and Italian legislation, for instance, enforce a maximum 50 Hz magnetic induction over facilities near overhead power lines to $1 \mu T$ and $3 \mu T$, respectively, along with the governments of Netherlands, Belgium and Finland (as stated by Finnish Radiation safety Authority) recommendation for rejecting new real state developments in a "0.4 μT limit" near power lines[7, 27].

Chapter 3

Radiated Emissions Survey

Concerning radiated EMF environmental survey, two independently techniques are the most accepted: the Broadband approach and the Frequency selective [9]. The first technique uses a broadband field strength meter, providing an unique field strength field, cumulative over their given frequency range. In turn, frequency selective approach uses a spectrum analyzer, providing a set of field strength measurements over each frequency individually (in accordance with frequency range and resolution bandwidth/RBW selected), required by ICNIRP exposure guidelines and by EMC standards [9].

In addition, using devices with isotropic probes is recommended, since no polarization and harmonic content characteristics are previously known [29]. These devices contain three-axis coils, obtaining directly the **resultant** field through three orthogonal spatial components of a given EMF vector. If only a single-axis equipment is available, the prescribed protocol is first to orientate its axis until a **maximum** reading is indicated, and then taking two additional measures in the perpendicular directions [17, 29]. The equivalent majorant electric or magnetic flux density, thus, would be indicated by equation 3.1. However, they would only be equal to the resultant field if the three components are in phase. If the surveyed EMF has circular or elliptically polarization, most common when assessing EMF produced by three-phase power lines or multiple sources in residential/office facilities, the majorant field will not be equal because vector components have distinct phases. Thus, it provides a majorant higher than the true magnitude of the field vector (where the difference is up to 41% relatively to circularly polarized fields) [29, 30].

$$EMEF = \sqrt{E_x^2 + E_y^2 + E_z^2} \text{ and } EMBF = \sqrt{B_x^2 + B_y^2 + B_z^2} \quad (3.1)$$

Among the Broadband meters, True RMS detectors are most commonly used for power frequency measurements[29]. They consist on a rectifier detector circuit, that rectifies the input signal and calculate the RMS for the intended frequency. Nonetheless, the presence of harmonics in a given EMF incur the device will not indicate the true RMS value of the assessed frequency [29]. In this case, if no integrator stage is displaced prior the circuit that performs the RMS math calculation, the numeric output inevitably will be distorted. It also affects device’s frequency response, concurring for a flat response over the bandwidth required[29].

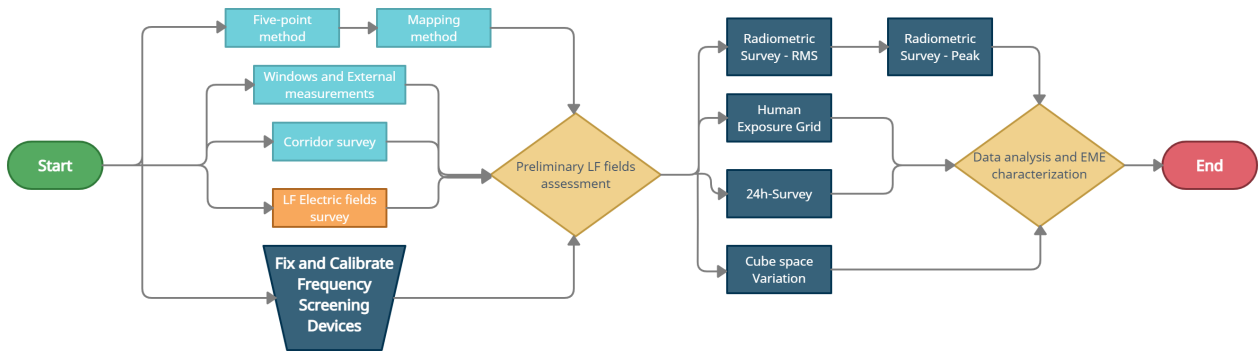


Figure 3.1: Radiated EMF survey protocol fluxogram.

Both of the techniques were applied on survey carried out in this chapter. The SYPRIS 4080 triaxial gaussmeter and EFM 160 are broadband meters for measuring ULF magnetic induction and electric fields, respectively, and their respective characteristic are described on tables C.3 and C.4. Frequency selective analysis, on the other hand, used the Aaronia NF-5020 and HF-6060 V4 handheld spectrum analyzers, whose technical specifications are in tables C.1 and C.2, respectively, and special considerations regarding their operation are described in sub chapter 3.2.4.

For this, a complete survey protocol for radiated EMF was developed, indicated in figure 3.1. Seven complimentary approaches were considered, with distinct objectives regarding the evaluation of EMC susceptibility and human dosimetric levels. Time and spatial-varying parameters, intrinsic to any EME, are also especially evaluated and will be explained in detail in the protocol description below. Moreover, since the DEEC environments measured in each approach are distinct, they will be named in each respective sub chapter or results table in chapter 6.

3.1 Broadband Measurements

3.1.1 Low Frequency Magnetic Field Measurements

The methods described in this subsection are purposed to assess of indoor DEEC ULF magnetic flux density. Under ideal conditions, magnetic fields produced by single conductors in a balanced three-phase system would cancel each other[31]. Nonetheless, the presence of ULF magnetic fields in public environments is common as electrical indoor installations have phase conductors branched for different areas from Distribution board, distinct chart configurations (PEN conductor, PE+N separated, etc) and different power flows in conductors[31].

The Five-point and Mapping methods are the first to be presented, whose objective is not catalog all possible sources in a given environment, but to focus on measuring the background ambient [30]. Based on IEEE California Protocol for measuring LF residential magnetic fields, these methods are called spot measurements because they provide a "snapshot" view of the magnetic induction at a certain location and time, not providing information about aspects of time variation in such environment[30, 31].

The five-point method is a most generalist survey, where five measurement points are selected on a given location for levels and spatial variation characterization: in center of the room and in the middle of each halved diagonals (or as close as possible), as figure 3.2 indicates[31]. Using SYPRIS 4080 meter, each spot point was measured with a height of 1 m, average height of human abdomen[31, 32]. Available electrical equipment and human occupation must be kept intact to assess the EME in its normal operation. A 30-second period over each measurement register was also defined[29]. For this, a register datasheet was prepared and exposed in annex E.8, where an outline of the researched ambient format should be drawn[29]. The surveyed locations are presented in the table C.6, where each of them was surveyed up to three times over different date. Ultimately, if the measured room shape is irregular, or its area is considerably large, a division of this in rectangular subspaces was made.

Aiming to appraise the spatial-variation, the five-point measurements were observed through ISO/IEC 43 guide Interlaboratory Comparisons [33]. Following the ILC standard, the $\delta 1$ and $\delta 2$ dispersion metrics are provided, respectively, in equation 3.2 [13], where s is standard deviation and X the average calculated.

The Mapping approach is a more detailed and traditional technique to evaluate the spatial

variation of magnetic fields in a given space. In accordance with the figure 3.2, a grid is created where the measurement distance of each point is set to 1 m and its dependent on the shape of the room, provided that it respects a minimum distance of 0.5 m from any wall or obstacle. The 1 m measurement height and 30-second measurement period prescribed previously is used again[31].

$$\delta 1 = \frac{sd.100\%}{X} \quad \text{and} \quad \delta 2 = \frac{(result_{max} - result_{min}).100\%}{X} \quad (3.2)$$

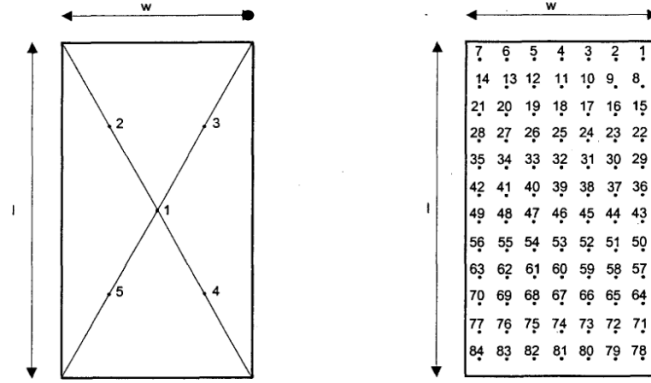


Figure 3.2: Five-point and Mapping methods[34].

Furthermore, since SYPRIS 4080 provides a cumulative magnetic flux density and no harmonic content is provided, the Serbian Electromagnetic Field Monitoring Network (SEMONT) exposure boundaries approach will be employed. Using endmost frequency response values, it is possible to determine global exposure ratio (GER) boundaries, as equation 3.3 shows, since the real human exposure is between the GER_{LOW} and GER_{UP} established by SEMONT, referred in equation 3.4 [9]. Where B_m is the broadband measured value of magnetic flux density; and $B_{refMAX}(f_1)$ and $B_{refMIN}(f_2)$ are respectively the maximum and minimum ICNIRP reference levels, and f_1 and f_2 are the minimum and maximum limits of the frequency response of the instrument used.

$$GER_{LOW} = \frac{B_m}{B_{refMAX}(f_1)} \quad \text{and} \quad GER_{UP} = \frac{B_m}{B_{refMIN}(f_2)} \quad (3.3)$$

$$GER_{LOW} \leq GER_{real} \leq GER_{UP} \quad (3.4)$$

The DEEC corridors were surveyed using a different procedure, adapted from hospital corridor RF methods for medical EMC compliance [35, 36]. Using this procedure, were prospected the

2nd floor corridor, 3 and 3A corridors, the third floor study aisle and 4th floor corridor were evaluated. The survey was performed along their central axes, spaced equally by 0.5 m from each measurement point, on the first ten measurements on westbound direction, and 1 m interval in remaining spots, also with 1 m measurement height and 30-second measurement period. This guidance was chosen because the Five-point method measurements indicated a higher magnetic induction magnitude in the rooms located in the eastern part, presumably due to the power line over the Tower B, and evaluate field's attenuation over distance of this specific source would be a valuable asset on EMC characterization [35, 36, 37].

Lastly, survey routines for the department windows and also its external perimeter were conducted, following the prescribed on California Protocol for survey in residential facilities[30]. The appeal on a specific survey for building windows lies in the fact that they usually have the highest measured magnetic induction levels [17]. The apertures were measured length-centralized, with no electrical devices below them and 1.7 m height over the ground, beyond a 30-second measurement period. On other hand, the measurements for outdoor profile were taken 1 m above floor. Starting from of the corners, sketch a parallel line distant 0.5m to 3m from the wall, taking a measurement on a 3 m pace[30].

3.1.2 Low Frequency Electric Fields levels measurement

In respect of ULF EMF, electric and magnetic fields must always be measured separately, because they are contained in near-field region, where \vec{E} and \vec{B} have reactive properties and do not present the radiated characteristics explained formerly[25]. Therefore, a survey was conducted for evaluating electrical fields levels at 50Hz, on the indoor and external spots mentioned on table 6.7. For this, the EMF 160 and Aaronia NF-5020 equipment were used in a comparative approach, due to construction principles and measurement constancy distinction.

The EMF 160 device is a True-RMS free-body meter. This type of meter works according to the displacement current principle, where two parallel conductive electrodes, if immersed in a time-varying electric field and connected together electrically, will incur into a field-proportional current flux between the two plates due to the electric charge redistribution caused by this alternating magnetic field[25]. A guard ring surrounding the plates is also presented, where this displacement current is sensed and converted to the numerical value corresponding to the electric field[25]. Typical electric field meter geometries are presented in figure 3.3. The Aaronia

NF-5020, in turn, is a frequency screening handheld device that contains a single electrical field sensor, whose direction is indicated by the figure 3.4[17].

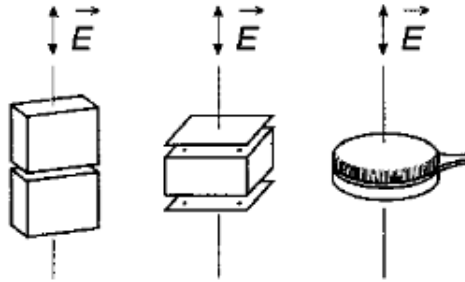


Figure 3.3: Geometries of typical free-body electric field meter[32].

Nonetheless, despite the category of device chosen, \vec{E} are exceptionally sensible on measurements as the human body, metallic objects and vegetation nearby embed perturbations on device's probes[25, 38]. The IEEE C95.3.1 Recommended Practice for Measurements of electric, magnetic and electromagnetic fields from 0 kHz to 100 kHz dissuades the presence of any metallic cable connection on the device in use, as well as recommends a distance of at least 2 m from the surveyor to equipment[25]. Weather aspects are also important for an electric field survey reliability, since humidity and temperature conditions might lead to appearance of static charges on probes. Performing a survey with relative humidity conditions above 70% or with low relative values, as well as in the in the presence of dew, is not advisable[17, 25].



Figure 3.4: NF-5020 single axis E-field sensor and External survey for Vertical E-fields[17].

Moreover, \vec{E} generated by high-voltage equipment sources and power lines are mainly vertical. The IEEE C95.3.1 standard references on its electric fields level characterization methods that the equipment in use must be rotated until it indicates the maximum field value, and then taking two additional orthogonal measurements[25]. Thus, it was agreed for this survey to obligatorily retrieve a measurement in vertical direction (stipulated as axis z), as well as two additional perpendicular directions on ground plane, on eastbound and northbound directions (respectively axis x and y), all taken at 1 m height above ground. Subsequently, the EMEF result will be obtained from the three orthogonal axis recordings.

Aiming to mitigate the human body effects on measurements, the EFM 160 device was hold on each spot by an isolated 1-m long rod during a period of one-minute per axis, where the surveyor held it by holding the opposite end of rod, in a squatting position[38]. Since the observable values showed a significant fluctuation over the recording period and the device does not have an averaging-values mode, the minimum and maximum values obtained were registered in the datasheet. The NF-5020 equipment, nevertheless, was settled on his onboard tripod, in turn supported 1 m height over the floor through a non-conductive tube, as figure 3.4 illustrates. The mains power (50 Hz/60 Hz) preset was chosen, with a 45-65 Hz bandwidth, a 3 Hz RBW filter and 5s sample time, as well as HOLD key selected, enabling the recording of maximum RMS field strength value over the period assessed[17].

3.1.3 Possibilities on data representation

The EME survey focused on human dosimetric evaluation, carried out with broadband equipment, are generally conducted on time-weighted-average approach or continuous evaluation chart[31, 39]. In the first case, measurements are averaged over prescribed by the standard followed (a six-minute-averaging period in ICNIRP guidelines)[6], while the second shows the fluctuation over a given period[31].

The five-point and mapping methods, nevertheless, qualify interest aspects of spatial-variation evaluation. The results obtained in a Mapping grid approach, for instance, allows a heat-map development over the researched environment, providing an accurate fields distribution overview and a best visualization of EMF internal sources to the environment itself[40]. A Scatter plot of the data obtained in Five point method is also possible, observing the dispersion plot between the pairs of the center-of-room measurements versus each of the lateral spots. In this way, a high

dispersion of the measurements might indicate the presence of significant EMF source appliances in this environment, along with a high-correlation factor may indicate a high prominence of an external EMF source[29]. However, the most common representation in such approaches is to construct a bar chart with the maximum measurements obtained in each environment.

In addition, given the simplicity and speed inherent of the Five-point method, the prospect of using interpolation and extrapolation numeric methods to assess the spatial distribution across an entire surveyed room was also evaluated. For this, two possibilities were evaluated in Matlab: Using a *griddata* surface or a *scatteredInterpolant* math function. The first possibility fits a surface of the form $z = f(x, y)$, obtained with data from non-uniform vectors (where the surface inevitably passes through the data points). This technique does not enable numeric extrapolation, and interpolation might be chosen among *linear*, *cubic* and *nearest* methods.

On the other hand, the *scatteredInterpolant* returns an interpolant function for the given data set provided (2D or 3D vectors). This function does not necessarily traverse the obtained measurement data, although it enables extrapolation over a determined area. The interpolation method in this case might be *nearest*, *linear* or *natural*, as well as extrapolation can be chosen between *nearest*, *linear* or *none*.

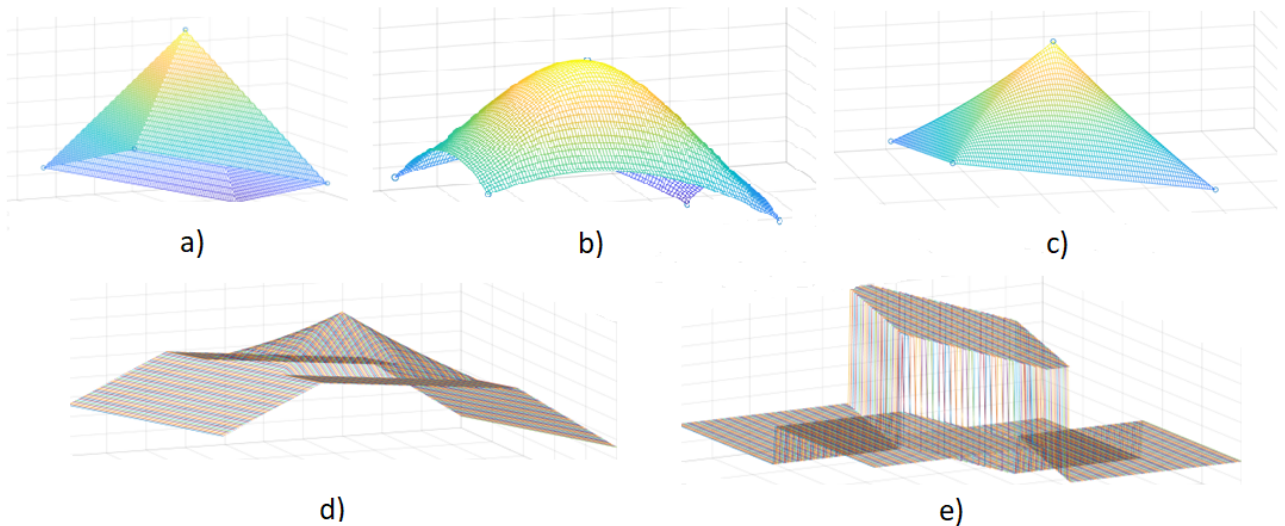


Figure 3.5: Interpolations and extrapolation for Five-point LF magnetic fields method using Matlab's *GridData* and *ScatteredInterpolant* commands: a) *GridData* with *linear* interpolation; b) *GridData* with *cubic* interpolation; c) *GridData* with *natural* interpolation; d) *ScatteredInterpolant* with *natural* interpolation and *linear* extrapolation; and e) *ScatteredInterpolant* with *nearest* interpolation and *nearest* extrapolation.

Different graphic configurations were tested over a hypothetical room with five distinct measurements, and the scatteredInterpolant option with *natural* interpolation and *linear* extrapolation demonstrated the most aesthetic and reliable results in extrapolated area.

The figure 3.5 illustrates the obtained plot for Five-point LF magnetic-fields for: a) GridData with *linear* interpolation; b) GridData with *cubic* interpolation; c) GridData with *natural* interpolation; d) ScatteredInterpolant with *natural* interpolation and *linear* extrapolation; and e) ScatteredInterpolant with *nearest* interpolation and *nearest* extrapolation.

3.2 Frequency Screening Analysis

3.2.1 Radiometric survey

A Radiometric survey is the core of the Frequency selective approach[9], and most complete method regarding a comprehensive representation of existing electromagnetic events, although it is not indicated for spatial and temporal variation assessment. It is aimed to characterize the field strength of each frequency or bandwidth individually within the spectrum considered, as well as identify the frequency harmonics and eventually signal modulation[41, 42].

Therefore, the frequency band occupation and RF usage in a given environment might be determined from the spectrum signature produced[43]. The effects of intentional and non-intentional radiated pollution combined and the contribution of each frequency range on human exposure, also, can be more properly identified, as stated in equations 2.3 and 2.4 in accordance with ICNIRP reference levels [6, 44]. And aiming to characterize the EME in terms of any possible EMI question, the equivalent electromagnetic field of frequency bands whose sources are more likely to occur, will be compared to the Compatibility levels for commercial/public location class of IEC 61000-2-5 standard, as explained in sub chapter 2.1.

The term equivalent electromagnetic field means the equivalent electric field (*EEF*) or magnetic induction (*EBF*) which would result from a source producing as much power density as the power density cumulative sum on a given band, as equation 3.5 defines.[45] Where $EMF(f_i)$ is the electric or magnetic field strength value at frequency f_i , and also f_{start} and f_{final} are the frequency range boundaries.

$$EEF = \sqrt{\sum_{f_i=f_{start}}^{f_{final}} E(f_i)} \quad \text{and} \quad EBF = \sqrt{\sum_{f_i=f_{start}}^{f_{final}} B(f_i)} \quad (3.5)$$

Thus, a spectrum analyzer device is required for a purposed radiometric survey. This type of device might directly measure an incident EMF signal in frequency domain, using an internal probe, or attached to an antenna[42]. Two equipment were used in the Radiometric Survey: The Aaronia NF-5020 analyzer was used to measure magnetic flux density in ULF, LF and medium frequency ranges, from 45 Hz up to 1 MHz, in conjunction with the Aaronia HF-6060V4, which was used to survey HF EMF frequency ranges, from 10 MHz up to 6 GHz[17].

For this, the flowchart represented in figure 3.6 illustrates the measurement process involved. The EMF present in the selected frequency band in the environment are detected by the internal testing probes or, if the incident EMF are over 700MHz, through the attached OmniLog 70600 antenna. In sequence, the spectrum analyzer measurement settings are configured in the MCS software, Aaronia’s real time spectrum analysis software[17]. For this, the spectrum analyzer in use was connected to a PC via a special USB cable with high EMC ferrite performance, allowing the observable data to be registered and exported in a *csv* file format. The characteristics of Aaronia spectrum analyzers are present in appendix C and further considerations were discoursed in sub chapter 3.2.4.

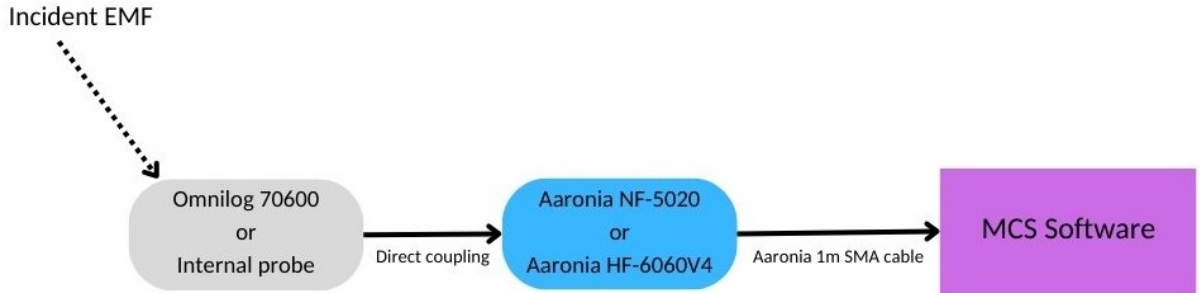


Figure 3.6: Radiometric survey measurement flowchart.

The spectrum analyzers were mounted on a non-conductive support, placed 1 m above the ground, the average of a human abdomen height, and centralized in the surveyed room. Five indoor and three external locations were chosen. The DEEC’s Bar, Third floor study aisle, Entrance Atrium and R5.2 Laboratory were selected since they are commonly inhabited public spaces. In turn, the terraces of Towers B and R were chosen due telecommunication basis installed in Tower’s B roof, as well as the promenade of Department of Computer Engineering

(DEI) building, due to the proximity of antennas installed in the building of the Faculty of Civil Engineering (DEC). Lastly, the underground Parking site also evaluated for comparative intentions due to the assumption of high-frequency EMF sources absence, and also to check the EME in the vicinity of the RF shielded chamber.

Moreover, the low/medium and high-frequency Radiometric surveys required different strategies regarding the frequency range sweep, due to accuracy issues. This issue is due the question of zero-span noise floor, mainly in NF-5020 analyzer, which will be detailed in sub chapter 3.2.4[17].

In the HF survey the results were saved in $dB\mu V/m$ (the physical quantity of the CISPR 32 emission limits), and oriented to perform a global sweep from 150 MHz up to 6 GHz, recorded over a 6-min period. Additional measurements were made in smaller frequency ranges, among those in use by telecommunication devices, recorded over a 1-min period. The low and medium frequency research, although, had frequency-oriented sweeps towards power-frequency magnetic induction sources and their respective harmonics, recorded over an 1-min period each in T physical unit. Additionally, two sweeps were performed over a 6-min period in the frequency ranges of 1.5-150 kHz and 0.15-1 MHz. All frequency range sweeps performed, possible EMF source of interest, RBW and sampletime used are presented in table 3.1[44, 46].

Table 3.1: Radiometric survey equipment parameters

NF 5020				HF 6060-V4			
Frequency Range (Hz)	Possible EM Source	RBW (Hz)	Sample-time(s)	Frequency Range (MHz)	Possible EM Source	RBW (MHz)	Sample-time(s)
45-65	Power frequency systems	3	5	650-950	GSM900 DTV LTE800	1	0.5
65-110	<i>Sub-harmonics</i>	3	5	1650-2000	GSM1800 UMTS LTE1800	1	0.5
110-200	<i>3rdharmonic</i>	10	5	2500-2700	WLAN Access-Point LTE2600	1	0.5
200-500	<i>5th, 7th and 9th harmonics</i>	30	5	3400-3800	Others	1	0.5
		30	5	3800-4400	Others	1	0.5
500-1500	<i>11thharmonic and subsequent</i>	300	3	10-50	Radio Broadcast	1	0.5
1.5k-150k	Monitors	1k	0.7	50-150	FM Radio	1	0.5
150k-1M	<i>Supra-harmonics</i> AM Radio	1k	0.7	400-650	Others	1	0.5
				150-6000	Global Sweep	3	0.2

In conclusion, since the EMF signals registered are not necessarily periodic, in addition to the possibility of recording transient and sparks signals, each specific frequency range was registered with RMS and MIN/MAX detector types (on different dates). In all NF-5020 and HF-6060V4 measurements, it should be noted, an isotropic triaxial sensor probe was adopted. A radius of 2 meters without human bodies and RF telecommunication devices (including cellphones) was established from measurement setting, and the laptop used was set to flight mode. Both laptop and spectrum Analyzer were charged exclusively by its own batteries.

3.2.2 Long-range temporal variation Survey

The therm temporal-variation is related to the change of EMF levels in a given environment over time[29]. Aiming to measure this temporal variation, the power frequency magnetic fields and HF EMF were measured over a 24-hour regular workday journey, according to the following methodology. In regards with power frequency B-field variation, a significant variation was expected since they are produced and directly proportional by load and ground currents with

time[25]. Given the prominence of the power line installed over Tower B, this LF survey was conducted in 3A.23 room, an eastern office and one of the hotspots obtained in the Five-point method. For this, Aaronia NF-5020 mains power (50 Hz/60 Hz) preset was over chosen, with a sample rate of 5 seconds.

The HF EMF 24-hour survey was carried out in 3A.21 office, in view of the presence of an Access Point, investigating a possible correlation with human occupancy rates or traffic variation over a schedule[47]. A frequency range from 150 MHz to 6 GHz was selected in Aaronia HF-6060 V4, with a RBW of 3 MHz and 0.5 second sample rate, allowing to observe possible a time-variation in the frequency range of Wi-Fi and other RF telecommunications technologies. Aiming to compare the temporal variation of the RF signals assessed, a dynamic range (DR_f) metric is defined, where it means the ratio, per frequency, of maximal momentary EMF value ($E_{MAX,f\ 24h}$) to the minimum ($E_{MIN,f\ 24h}$) considered on this 24-hour interval, as equation 3.6 shows[47].

$$DR_f = 20 * \log\left(\frac{E_{MAX,f\ 24h}}{E_{MIN,f\ 24h}}\right) \quad (3.6)$$

For such method, the Aaronia devices were placed on a lateral bench 1 meter above the ground and 80cm from the eastern wall of each respective office, configured with triaxial probes. The power frequency survey used the RMS detector type, although the HF survey considered Min/Max values, given the modulation and non-periodicity of the researched signals. Lastly, it is noteworthy that it was the only Frequency Selective method where both computer and Aaronia chargers were attached, due battery time-constraint questions.

3.2.3 Spatial-averaging power frequency human exposure assessment approach

Epidemiological studies exposing harmful effects due to exposure to ultra low frequency (ULF) magnetic fields are based on a time-weighted-average (TWA) approach, being a viable metric for assessment of dosimetric levels prescribed on respective reference guideline[6, 25]. This technique mixes both spatial and temporal variation precepts, where a series of measurements is performed geometrically as a way to emulate the human trunk. Moreover, the measured values are averaged over a six-minute averaging period, following the ICNIRP main reference guideline[6].

Moreover, this human body spatial-averaging method is also described in EN 50492, the *Basic standard for the in-situ measurement of electromagnetic field strength related to human exposure in the vicinity of base stations*, indicating human body exposure to EMF radiation as accurate as possible[48]. This method is oriented to be performed at points with high B-field levels or in work environments, due to long periods of exposure. Thus, this survey was carried out in the 3A.23 office, in T4.2 (representing a model classroom) and on a dining table in the geometric center of the Bar.

For this, the EN 50492 determines six measurements at the heights indicated in figure 3.7, performing a common human trunk with reduced uncertainty[48]. Furthermore, the results for each measurement site must be averaged in accordance with equation 3.7, where the sum of the squares is divided by the number of measures and than square root[48].

$$B_{Spatialaveraging} = \sqrt{\frac{\sum_{i=1}^N B_i^2}{N}} \quad (3.7)$$

For this purpose, the Aaronia NF-5020 configured with its mains power preset, triaxial probe, RMS detector type, and settled with a 3 Hz RBW filter and 5 s sample time. Cable-connected into a computer, a six-minute survey was conducted in the spots prescribed through MCS software, and data results assessed in Matlab. The values in each measurement point on grid were averaged over each individual frequency registered. And from each resulting spectrum signature, its *EBF* was calculated and proceeded to equation 3.7, as well as the ICNIRP cumulative sum, previously mentioned in equation 2.3 in sub chapter 2.2.

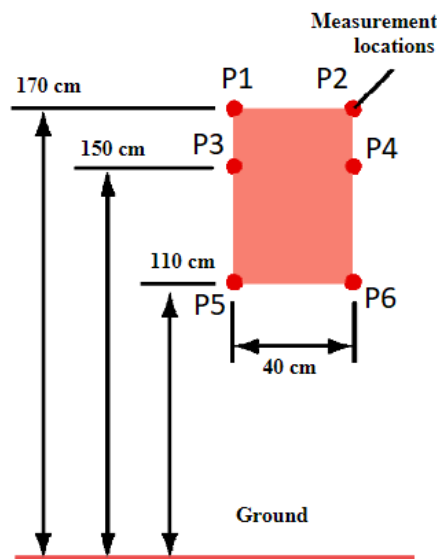


Figure 3.7: Six-measurement grid for Human spatial-averaging compliance[48].

3.2.4 Aaronia NF-5040 and HF-6060V4 specifications

The first aspect mentioned is the need for both spectrum analyzers to be positioned out of the called "close up range", being at least three probe lengths and ten wavelengths (if the case of HF EMF) away from any eventual corresponding EMF source, in order to avoid any distortion in the measurement probe and also avoid the Near-field region[17, 25].

Moreover, the NF-5020 and HF-6060V4 can be operated autonomously in handheld configuration, or connected to a computer, with its settings configured through Aaronia's MCS spectrum Analysis software. Both analyzers are factory-assembled with a list of **hotkeys** presets, oriented to the most common researched frequency bands. In fact, the only used preset in this dissertation was the **mains power (50/60 Hz)** preset, that shows the magnetic flux density in Tesla(T), at a frequency range from 45 Hz to 65 Hz, 3 Hz of Resolution Bandwidth and 5 s sample time. In theory, all settings can be changed configured within manufacturing limits without measurement distortions. An warning, however, must be stated regarding the choice of frequency range, RBW and sample time due to Low-Frequency Spike and Noise-Floor question[17].

The Noise-floor is a term referred to a lower range where measurements below this limit are physically impossible. This floor, following Aaronia's manual considerations, is as large as it approaches the minimum operating frequency of the equipment. It is specially noticed in NF-5020, where measurements settings with a wide frequency span and starting frequency close to 0 Hz have a strong spectrum noise and, thus, are totally unreliable[17]. Due to this factor, there were drafted specific frequency ranges oriented to Power frequency systems and their harmonics, in the LF 10-100 MHz, in the Radiometric survey. In the mains power preset specifically, only 0.3 Hz, 1 Hz or 3 Hz RBW filters can be used.

Furthermore, it is recommended to use a large sample time if the frequency range Span is 20 times larger than the resolution bandwidth. The higher the sweep, more accurate the measurement will be, consisting in a trade-off with the measurement period. In addition, adopting a smaller a RBW is suggested as equipment's sensitivity proportionally increases. It should be noted, however, that a too narrow RBW has inherent phase noise[17]. In addition, sweeps starting close to 0 Hz in NF-5020 device will take a considerably long processing time. However, if some special setting conditions are matched, a very fast DFT sweep mode is activated. This is only possible when the chosen RBW filter is 0.3 Hz, 1 Hz or 3 Hz; frequency Span is simultaneously smaller than 200 Hz and multiple of 15; and the sample time limited to 5 s. For larger RBW

filters, NF-5020 manual recommends using a 700ms Sample time period for 1kHz RBW and a 3 s Sample time for a 300 Hz RBW[17].

Regarding the internal attenuator, it should be set in Auto mode in HF-6060V4, because there is no prior knowledge if the EMF levels found might cause overload in the internal circuitry[17]. In the case of NF-5020, in opposition, a 0 dB setting was used since the Broadband Measurements indicated no levels above the internal overload limit. The **Dot** key is also emphasized, since it allows recording only the maximum electric or magnetic field strength found until it is reset.

Also, both devices allow the selection of how many and which probe axes will be used in the survey, with the exception of the Electric field probe in NF-5020, as previously related in figure 3.4. The high-frequency analyzer probe, nonetheless, is a power meter RF detector, registering the measurement data only in dBm. Following Aaronia instructions, the internal probe is an Active MDF antenna, and according to its antenna factor pattern, the measured dBm values might be converted into dBA/m (and later in $dB\mu V/m$) through the equation 3.8[17].

$$H_{dBm} - 35 = H_{dBA/m} \quad \text{and} \quad H_{A/m} = 10^{\left(\frac{H_{dBA/m}}{20}\right)} \quad (3.8)$$

Moreover, using the Omnilog 76000 external antenna is required in HF surveys above 600MHz, due to initial empirical measurements indicated high inaccuracy where such probe has not been employed. When it is attached, the antenna calibration settings in MCS Software must be changed from *None* to *Omnilog 76000*, otherwise distortions in the antenna factor estimation will occur. The probe detectors types can be selected between RMS and Min/Max values, where this last compares the current sample ($I^2 + Q^2$) with the formerly strongest registered sample[17].

Regarding the accuracy of the equipment, the NF-5020 has $\pm 3\%$ and HF-6060V4 ± 3 dB of typical equipment accuracy. Both equipment are in conformity with calibration requirements, as they were recalibrated and certified by Aaronia's factory in April 19, 2022. The accuracy warranty, however, is only valid if the researched environment has a relative humidity factor larger than 20% and smaller than 60%.

In conclusion, the spectrum signature visualized in MCS software can be stored in a *mdr* file format. In order to convert this file to an Excel *csv* format, the surveyor must load the recorded *mdr* data in the Load Measurement File Menu, reject the Sweep Delay suggestion and start a new recording in *csv* format. After this process, an Excel file output will be generated.

Chapter 4

Conducted electromagnetic pollution survey

Throughout the research process for the construction of the state-of-art of this present dissertation, no significant literature was found about measuring EMI disturbances coming from the power grid in the EMC conducted frequency range. Assessing the conducted emissions and disturbance generated by an EUT, using an Artificial Mains Network (AMN), is a widely studied topic and referenced by CISPR 32 standard, as well as are found studies about the introduced EMI disturbance in aggregate loads in the range of power frequency harmonics or supra-harmonics, but none with respect of 150 kHz-30 MHz conducted EMC frequency range[49].

Due to this context, a heuristic and innovative equipment named Line Impedance Stabilization Network Interface (LISN+I) is proposed, adapting a standardized LISN model, thus enabling the electrical network itself to become the EUT. In this way, the EMC conducted Emissions compliance standards might be used to check possible EMI disturbances introduced in the DEEC's power network, evaluating globally the effects of the electrical appliances present throughout the department.

A AMN is an equipment used in conducted EMC emissions and susceptibility tests in an EUT reliably. Its purpose is supply the EUT with the voltage and frequency levels from the grid, at the same time that presents a constant impedance between phase conductor and safety rail and also between the neutral cord and safety wire, having the results observable through an output connected to a spectrum analyser. This is due the impedance observed into an AC power output varies over the frequency range measured in each different facility, and also block any external

noise coming from the mains network. which in such a way could distort the EMC tests[49]. The figure 4.1 illustrates the basic topology of a standard LISN.

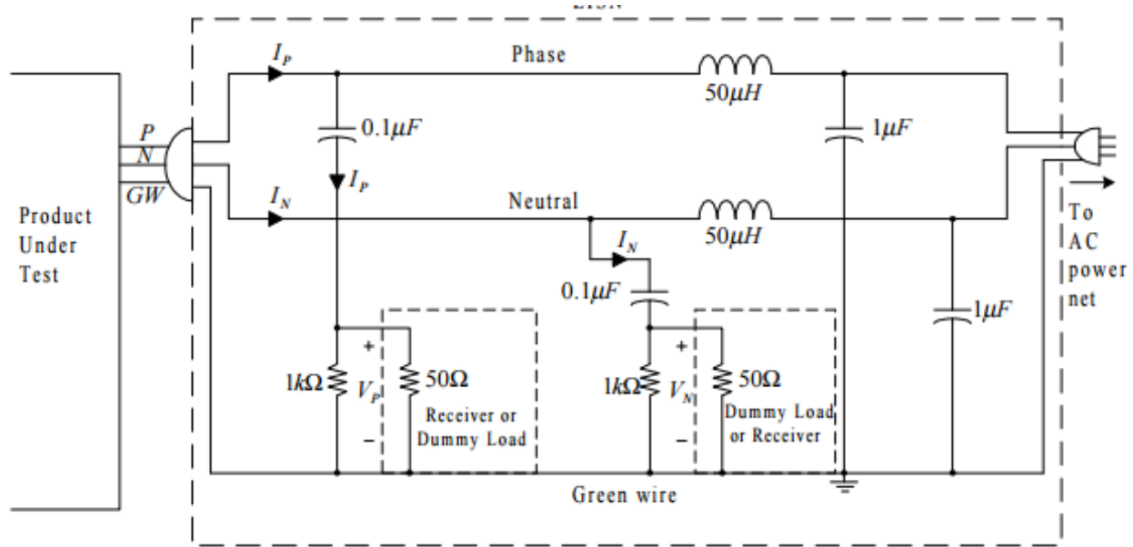


Figure 4.1: Ordinary LISN topology[49].

However, it is intended in the EMC environmental characterization of this Dissertation to measure any disturbances present in the mains network, observing the effects that the multitude of devices would provoke. Therefore, the conceived solution was adapt a regular LISN topology so that the "EUT side" would becomes the only input of the device (and therefore connected into a regular 220 V/50 Hz power outlet), as well as eliminate the inductors and capacitors designed to filter the now desired external noise[49]. Thus, the proposed new topology layout then is presented in figure 4.2, having some concepts adapted from the homemade LISN built by David Pereira in his 2016 Msc. Dissertation work[49].

The 100 nF capacitors (200 pF per phase as they are connected in parallel) are intended to prevent any DC overload of the test receiver. They are 650 V *X-caps* type, which means capacitors that have special insulation properties approved by safety standards and are adequate to be used in a line-to-line disposition[49]. They are associated each with a 1 kΩ dummy resistor, whose proposal is serve as static discharge path for each respective pair of capacitors when the 50 Ω resistor is disconnected[49]. This 50 Ω commercial resistor is placed as a dummy load that guarantees that the impedance seen between the phase conductor and safety rail and also between the neutral conductor and safety wire is always 50 Ω at all frequency range operation, in collusion with the 50 Ω receiver's input impedance[49]. Either way, the capacitors might be simplified as short-circuits over the frequency band of EMC conducted tests. A 100 mA fuse was

placed per phase for overcurrent protection, and also a 275 V varistor and 90 V gas discharge tube were placed to protect the RF path input against any voltage spike damage[49].

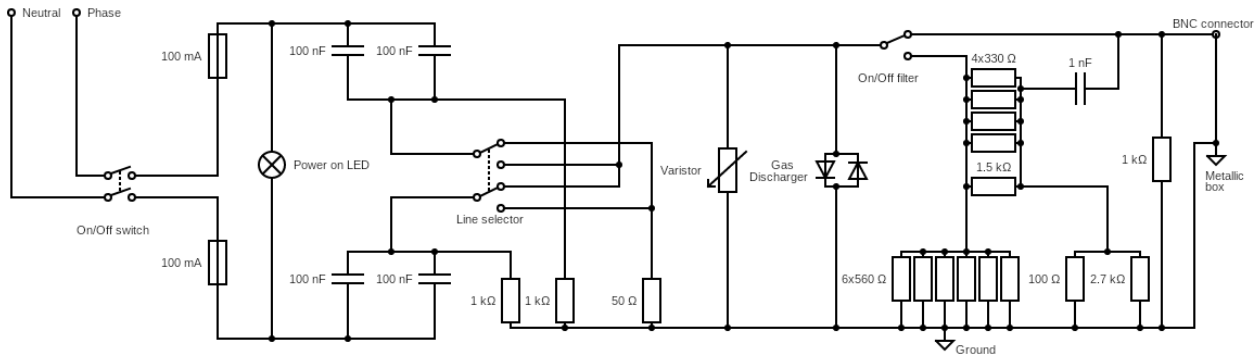


Figure 4.2: Adapted LISN internal circuit.

Moreover, three switches were conceived for the operation of the tests. The first is a simple On/Off switch. The second is a double pole oriented for selecting the line (phase or neutral) to be measured. Lastly, the latter is a toggle switch which enables or disables a set of attenuator and a high pass filter built in Delta, as previously proposed by David Pereira, designed to protect the receiver input from high amplitude pulse transients and attenuate the grid harmonics, respectively[49]. Nevertheless, the measurements of EMC conducted noise present in this Chapter were made without this High-pass filter, having its characterization recommended as future work.

A red warning AC LED is also displaced in the fuse cartridges output, informing when the equipment is energized. After this, the RF path output will be connected to the Receiver through a BNC output, where receiver's impedance will be in parallel with a $1\text{ k}\Omega$ dummy load. The BNC carcass and the metallic case of the equipment, which in turn is electrically connected to the circuit's ground, and is also accessible by an external connection.

In addition, as in a common LISN, the purpose of the designed equipment is register the voltage spectrum signature, between the phase conductor and safety wire (\hat{V}_P) and also between neutral conductor and safety wire (\hat{V}_N). For this, the voltage drop in the $50\ \Omega$ standardized receiver's input impedance is used. Record the voltage value at each frequency is desirable as the CISPR 32 EMC conducted emissions limits are prescribed in Volts, despite logically being associated with noise currents and easily obtained through Ohm's law, in accordance with equation 4.1. Where \hat{I}_P and \hat{I}_N are, respectively, phase and neutral currents[49].

$$\hat{V}_P = 50.\hat{I}_P \quad \text{and} \quad \hat{V}_N = 50.\hat{I}_N \quad (4.1)$$

Using a multimeter, a series of insulation and electrical continuity tests were performed between Phase and Neutral inputs, Phase and BNC ground, Phase and BNC signal port, Neutral and BNC ground, and Neutral and BNC signal port. The results can be consulted in table E.2 and were considered adequate.

The NARDA PMM EMI 7010 spectrum analyzer was the receiver used for this experiment and, therefore, connected to LISN+I BNC output. This spectrum analyzer was then connected to an USB port of a PC and having its settings configured through the manufacturer's software. For this, a frequency range of 150 kHz - 30 MHz and a RBW of 9 kHz settings were chosen, as stated in CISPR 32 standard emissions limits. Thus, the Average (Avg) and peak (Pk) values were registered and then compared with the Avg and Quasi-peak (QP) Class B reference levels of CISPR 32.

At last, the test setup of this survey is considerably simpler than an EMI disturbance test done with a LISN. No ground floor is required and the reference probe of the receiver is connected to the equipment's ground via the BNC output. Its basic operating protocol is then:

- (1) Place the PMM 7010 receiver and the LISN+I on a flat surface, initially without power cable connections to mains supply and with their Power On switches disabled;
- (2) Connect the respective power cords in a common 230 V/50 Hz outlet of the surveyed environment and activate the equipment's power on switch,
- (3) If the warning red LED is on, turn on the Receiver and connect it to the device's BNC port;
- (4) Ensure that no other electrical equipment connected to nearby outlets;
- (5) Connect the Receiver to a computer and take measurements using NARDA's software;
- (7) When the test is complete, turn off all appliances and remove them from the outlet mains network.

Chapter 5

Chamber Shielding Effectiveness Calculation

In order to verify compliance of an equipment with EMC/EMI immunity, susceptibility and emission tests, there are several facilities prescribed in Federal Communications Commission (FCC) and CENELEC standards[3]. All of them have distinct EME characteristics such as propagation mode, polarization, absorption, reverberation, reflection and Shielding Effectiveness per frequency[3, 16]. Regardless their construction type, they are intended to mitigate external EMF, providing reliable testing conditions and ensuring that the equipment tested are suitable for the most diverse functions, including medical and military devices. The flowchart illustrated in figure 5.1 exemplifies the three main groups and environment types of facilities used.

Among the most used types of facilities, the RF shielded chamber is an enclosure where the walls are metallic and all internal surfaces are filled with an internal skin, in order to shield against spurious EMI or RF signals. In this way, it resembles an almost perfect Faraday cage[3].

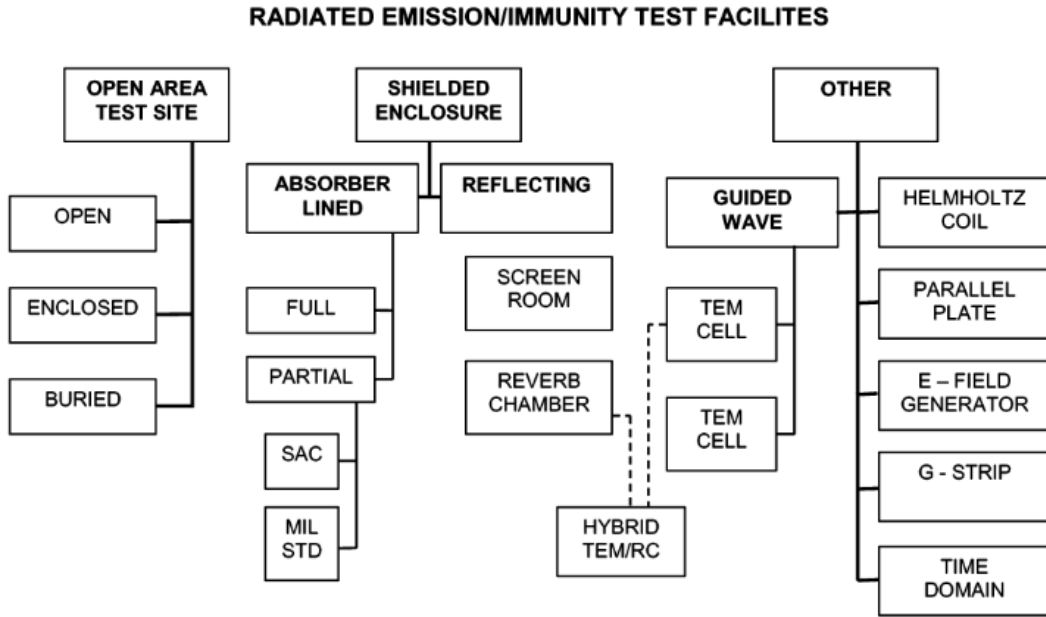


Figure 5.1: FCC Radiated emission and immunity test facilities[50].

In 2019, the *IEP* kindly donated to the ISR an ECCOSHIELD KPG RF Shielded Chamber and Shielded Door, which are currently assembled in DEEC's underground Parking site. Thus, the objective of the method described in this Chapter will be to measure the SE at different points of the Chamber through the IEEE 299-2006 standard adapted to the equipment available in the EMC laboratory[16, 51].

5.1 Shielding effectiveness estimation of electromagnetic Shielded Chamber

The ECCOSHIELD KPG is a RF shielded chamber, enclosed with a single Knife Edge RF Shielded Door. Its dimensions are 2.45 m of length and width, and 2.5 m of height. The term Shielding Effectiveness is referred to the ratio between the magnitude of an incident EMF at the shielding boundary with the field transmitted through the shielding, as equation 5.1 determines[16, 51]. Where B_1 magnitude and E_1 are referred to the incident field, usually in dB, and the SE_B and SE_E are referred to magnetic and electric incident fields shielding effectiveness, respectively.

This factor might be compounded as a result of reflection loss (important for HF fields), absorption loss (significant for near-field conditions) and multiple reflections within the material[16].

$$SE_B = 20 \log_{10} \frac{|B_1|}{|B_2|} \quad \text{and} \quad SE_E = 20 \log_{10} \frac{|E_1|}{|E_2|} \quad (5.1)$$

Considering the the unavailability and high cost of purchase of the antenna types described for the calculation LF and HF Shielding Effectiveness in IEEE 299-2006, a protocol was developed to adapt such equipment to those available in the EMC laboratory. For this proposal, it was measured the EMF magnitude with and without the with shielding.

The test frequencies were chosen according to the recommendations of the standard, cited in table D.1, in frequency bands with high occupancy. No tests were conducted in the medium frequency range (300 kHz-10 MHz), due to the absence of EMF Emitters in such range in the laboratory. In addition, assessing frequency bands below f_r was discarded since none of the available antennas produced measurable signals.

Furthermore, a warning about not conducting tests on chamber's resonance frequency (f_r) is issued by IEEE 299-2006 std, due to this phenomenon leading to distorted SE measurements. Following the provided equation 5.2, this factor was estimated in 85.4 MHz, where a and b are respectively shielding's height and width (in meters)[16, 51].

$$f_r(MHz) = 150 \sqrt{\frac{1}{a^2} + \frac{1}{b^2}} = 85.4 MHz \quad (5.2)$$

For the power-frequency magnetic SE tests a 860 μ H circular coil employed, with 30 spirals and a radius of 25 cm. This coil was connected in series with a variable load of incandescent lamps, whose purpose was to control the coil current and, consequently, the generated B-field [16]. According to Ampere's law, in a free space the math correspondence between them is described in equation 5.3, where μ_0 is vacuum permeability (H/m), N is the number of spirals, I is the coil current(A), R is its radius (m) and z is the distance between the center of the coil and the point where the field is measured (m). In this case, the direction of the B-field will be perpendicular to the coil's center[16]. The possible load configurations and respective calculated theoretical values are present in table D.2.

$$|B_{coil}| = \frac{\mu_0 * I * N * R^2}{2 * (R^2 + z^2)^{3/2}} \quad (5.3)$$

Nevertheless, for HF Shielding Effectiveness measurement, the reference EMF were emitted from a signal generator. The Aaronia BPSG5 HF Signal Generator, with a frequency range from 20 MHz up to 6 GHz, was attached to a BicoLOG 30100 or HyperLOG 7060 antenna. The first type is a biconic antenna with active dipole, and was employed in tests up to 450MHz, since its operating frequency is lower than HyperLOG. In turn, the second type is a broadband LogPer antenna and has better frequency response in EMF above 1 GHz. Thus, the HyperLOG 7060 was set to the tests from 900 MHz up to 6 GHz[17]. Their characteristics are displayed in appendix C.

In addition, the figure 5.2 illustrates the SE measurement protocol applied to all spots within the Shielded Chamber. The emitter of the reference signal has been positioned at 30cm from the outer part of the shielding, having the Normal vector of such EMF emitter being positioned in the direction perpendicular to the surface of the shield. On the other hand, the Aaronia NF-5020 or HF-6060V4 spectrum analyzer probe was positioned aligned with the direction of emitted fields at 30 cm from the inner wall, registering the incident EMF as in the Radiometric Survey.

Immediately before, the EME noise inside the chamber was registered with the same settings at each frequency test point considered. After this, the signal emitter was turned on and positioned in a distance of 62 cm from the analyzer without any shielding surface (as the thickness of the Shielded Chamber wall is to 2 cm), enabling the calculation method described in equation 5.1[16, 51].

In addition, the ECOSHIELD chamber was donated to ISR without any type of operations manual, as there are no technical references or technical support available to public consultation on the internet. Thus, despite the assumption that the shielding material is ferromagnetic, through a simple test with magnets, it would be good practice to evaluate the SE in different conditions of incident electric or magnetic fields. For this purpose, each one of the HF Shielding Effectiveness assessments was done with the signal generator emitting EMF reference signals with a transmission power of +1 dBm, +7 dBm, +12 dBm, +15 dBm and +18 dBm, as well as the power frequency SE assessment was performed in a set of nine increasing loads, as table D.2 shows[16].

Finally, the IEEE 299-2006 recommends evaluating the SE magnitude in distinct points of the surveyed facility, checking for possible points of shielding failure[51]. Thus, the developed measurement protocol described previously was applied in front of Chamber's door, in one of its corners and next to a massive wall (without any aperture), as figure D.3 in appendix D illustrates.

All measurements were carried out at a 0.9m height from the ground, or 0.8m from chamber's floor perspective. In the power frequency SE test, the NF-5020 **mains power** preset was used, and all HF SE tests were configured centered in the desired frequency with a 10 MHz Span, 1 MHz RBW and 500 ms sampletime, over a 30 s measurement period each. For the SE calculation, only the maximum absolute EMF values recorded in this period were considered.

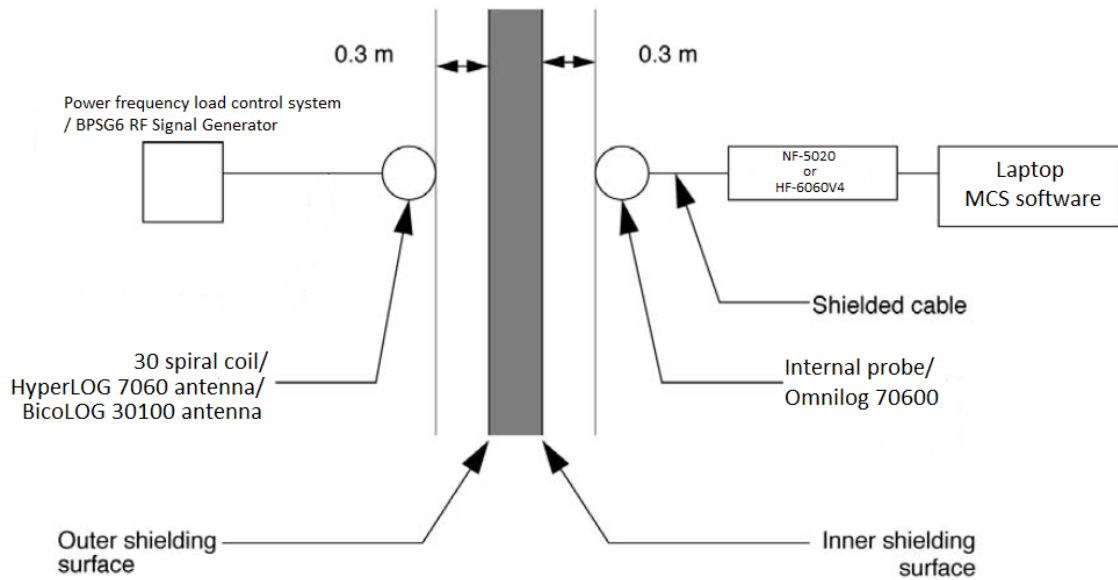


Figure 5.2: Shielding effectiveness tests configuration protocol.

Chapter 6

Characterization survey results

6.1 Broadband approach survey

The broadband measurements were the first milestone conducted in the DEEC electromagnetic characterization survey. All LF magnetic field measurements were made during the first semester of 2022, while the survey of LF electric fields levels were executed in July and August.

As regards the Five-point method, 23 environments were assessed, comprising a total of 65 registers and 325 spot measurements. The results for environments with a single subspace are shown in the table 6.1, for multiple subspace environments in table 6.2, as well as a general summary is presented in table C.6. The maximum values recorded in each environment can be observed in the figure 6.1. As a general rule, it can be inferred that the further east and the higher the floor of a given environment, the higher the values recorded for ULF magnetic fields will be.

Regarding human safety, all maximum recorded values are far below the $100\mu T$ power frequency B-field limit prescribed in table B.1. Even when considering the hypothesis of the presence of harmonics or spurious signals in the response range of the SYPRIS 4080 meter (25 Hz to 1 kHz), whose maximum records were treated by the SEMONT approach and can be observed in the table C.6, all maximum and minimum boundaries are below the limits of the epidemiological literature. However, it is noteworthy that environments located closer to the power line, such as the 3A.23 Office and the study room of tower B, are above the previously mentioned "0.4 μT limit", in accordance with the national legislation of other EU countries, as explained previously in chapter 2.2.

Table 6.1: Five-point method in single space environments

Location	First Register			Second Register			Third Register			Ratio (AVG Max /AVG Min)
	Avg (uT)	$\delta 1$ (%)	$\delta 2$ (%)	Avg (uT)	$\delta 1$ (%)	$\delta 2$ (%)	Avg (uT)	$\delta 1$ (%)	$\delta 2$ (%)	
3A.23 Office	0.032	32.1	83.3	-	-	-	-	-	-	-
Second floor West Terrace	0.014	35.0	71.4	0.010	63.2	200.0	-	-	-	1.40
Second floor East Terrace	0.026	18.8	38.5	0.160	30.3	62.5	-	-	-	6.15
East Third floor corridor	0.171	42.9	124.2	-	-	-	-	-	-	-
East 3A floor corridor	0.229	72.6	225.3	-	-	-	-	-	-	-
East Study Aisle	0.036	22.2	55.6	0.026	30.8	76.9	-	-	-	1.38
West Study Aisle	0.022	34.0	90.9	0.008	50.0	125.0	-	-	-	2.75
Bar	0.158	56.8	151.9	0.102	36.9	98.0	-	-	-	1.55
T4.2	0.014	35.0	71.4	0.040	90.8	250.0	-	-	-	2.86
T5.4	0.010	0.0	0.0	-	-	-	-	-	-	-
T6.4	0.040	15.8	50.0	-	-	-	-	-	-	-
Tower B Roof - Outdoor	1.642	1.5	4.3	-	-	-	-	-	-	-
Tower B Roof - Indoor	0.028	26.7	71.4	-	-	-	-	-	-	-
Chamber	0.000	-	-	-	-	-	-	-	-	-
Parking - Inverters zone	0.012	33.3	83.3	0.016	50.0	125.0	0.016	50.0	125.0	1.33
Electric vehicle parking lot	0.064	41.5	109.4	0.036	22.2	55.6	0.058	42.8	120.7	1.78
Parking - Power Station Room	0.117	101.2	298.8	0.121	101.6	296.5	0.109	87.4	248.7	1.11
R1.2	0.008	93.5	250.0	0.006	133.3	333.3	-	-	-	1.33
Tower A 6th Floor	0.060	38.5	100.0	-	-	-	-	-	-	-
Tower R terrace	0.012	33.3	83.3	-	-	-	-	-	-	-

Considering the approach for EMC compliance purposes through IEC 61000-2-5 Compatibility Levels, one should consult the Disturbance Degree for each respective frequency range and physical quantity in the table A.3, and then check their respective maximum compatibility level to which such environment might be subject. As an example, the Disturbance Degree for LF B-fields in commercial/public environments is 2, which in turn will indicate a compatibility level of up to 10 A/m (12.56 μT in free space). In this way, all the environments surveyed are in accordance with the standard.

Table 6.2: Five-point method in locations with multiple subspace.

Location	Subspace 1			Subspace 2			Subspace 3			Subspace 4		
	Avg (uT)	$\delta 1$ (%)	$\delta 2$ (%)	Avg (uT)	$\delta 1$ (%)	$\delta 2$ (%)	Avg (uT)	$\delta 1$ (%)	$\delta 2$ (%)	Avg (uT)	$\delta 1$ (%)	$\delta 2$ (%)
2nd Floor Corridor (Sub 1 - Sub 4)	0.106	14.1	37.7	0.066	15.5	45.5	0.062	12.1	32.3	0.032	23.4	62.5
2nd Floor Corridor (Sub 5 - Sub 6)	0.024	33.33	83.33	0.012	33.33	83.33	-	-	-	-	-	-
4th Floor Corridor East	0.218	55.5	146.8	0.068	39.9	117.6	0.062	31.3	96.8	-	-	-
4th Floor Corridor West	0.049	50.9	144.1	0.024	72.5	205.9	0.020	37.8	100.0	-	-	-
R5.2 Classroom	0.008	93.5	250.0	0.022	44.5	136.4	-	-	-	-	-	-
Tower B 6th Floor Study Room	0.577	15.9	46.8	0.460	14.2	41.3	0.252	42.3	107.2	0.140	21.7	64.3
DEEC Secretary	0.168	31.1	95.1	0.168	11.5	29.8	-	-	-	-	-	-
Entrance Atrium - 1st Register	0.090	22.2	66.7	0.068	17.2	44.1	-	-	-	-	-	-
Entrance Atrium - 2nd Register	0.118	25.4	67.8	0.062	21.4	64.5	-	-	-	-	-	-
NEEC - 1st Register	0.012	97.2	250.0	0.018	173.6	444.4	-	-	-	-	-	-
NEEC - 2nd Register	0.000	-	-	0.034	142.4	382.4	-	-	-	-	-	-

In the case of spatial variation, the ILC dispersion metrics do not produce reliable trends for

environments with B-field averages close to the SYPRIS 4080 scale division ($0.01 \mu T$). Considering only those environments whose average is more than 10 times the minimum scale, it is noted that $\delta 1$ assumes values above 40% only in long length environments, such as DEEC corridors, as well as spaces containing electrical distribution boards or some significant source of magnetic fields (notoriously the Parking area near the Power Station room).

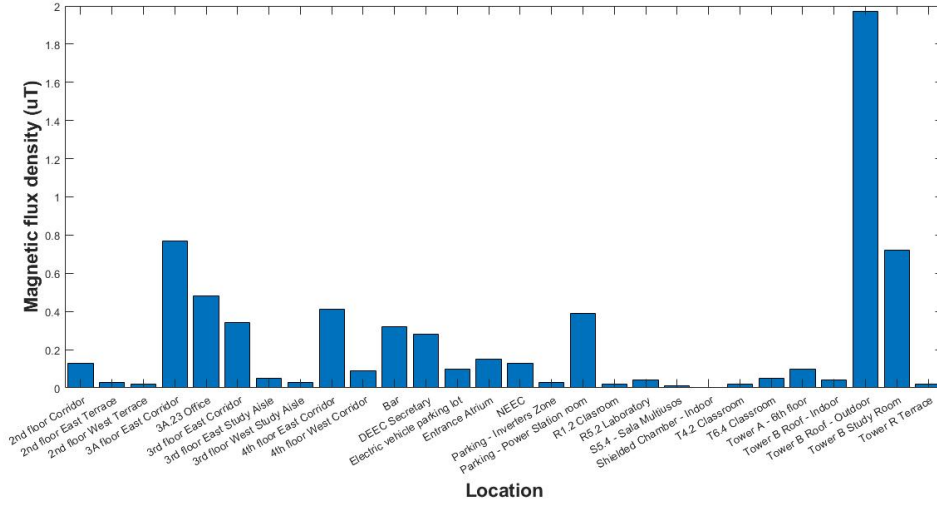


Figure 6.1: Maximum magnetic flux density in each location surveyed in the Five-point method.

The tables 6.3 and 6.4 shows the results in the two spots considered for the temporal variation analysis, with measurements taken at different dates throughout 2022. The 4th floor corridor and the Entrance Atrium were chosen due to their high human presence and higher B-field values compared to other environments considered in the five-point method. In the first case, Spot A represents the boundary between the Bar and the corridor, Spot B is located 1 m from A (centered in the aisle) and Spot C is the orthogonal projection of B, read 30 cm from the glass panel. In the Atrium, spot A is the geometric center and spot B in the southwest corner of the space. In any case, it is observed that the Std. deviation varies between 7% and 18.5% of their respective average.

Table 6.3: B-field temporal-variation assessment in Spot points at the Fourth Floor corridor.

Date	Time	Temperature (°C)	Humidity (%)	Spot A (uT)	Spot B (uT)	Spot C (uT)
07/fev	16:23	21	51	0.4	0.42	0.78
14/fev	10:45	19.4	59	0.39	0.4	0.54
24/fev	16:15	21	62	0.42	0.42	0.75
07/mar	09:18	16.9	51	0.4	0.4	0.65
08/mar	12:15	20.2	55	0.47	0.46	0.72
08/mar	19:05	17.9	60	0.49	0.5	0.78
31/mai	23:05	25.4	55	0.38	0.41	0.64
09/jun	11:09	24.5	65	0.4	0.43	0.57
Average (uT)				0.42	0.43	0.68
Standard Deviation (uT)				0.04	0.03	0.09

Table 6.4: B-field temporal-variation assessment in Spot points at the Entrance Atrium.

Date	Time	Temperature (°C)	Humidity (%)	Spot A (uT)	Spot B (uT)
06/fev	17:12	22	54	0.08	0.54
07/fev	15:41	21	51	0.09	0.62
14/fev	10:54	19.4	59	0.11	0.31
24/fev	16:21	21	62	0.1	0.59
07/mar	09:25	16.9	51	0.09	0.53
08/mar	12:07	20.2	55	0.11	0.61
08/mar	19:13	17.9	60	0.12	0.66
31/mai	22:58	25.4	55	0.09	0.47
09/jun	11:14	24.5	65	0.1	0.49
Average (uT)				0.10	0.54
Standard Deviation (uT)				0.01	0.10

Moreover, as stated in the subchapter 3.1.3, the Spatial variation in DEEC as a whole can also be evaluated from scatter plot of the combination of center-of-room versus each corner registered in Five-point measurements, whose results are observable in figure 6.2 through its 260 pairs. There is a high correlation, above 0.94, which together with the results seen so far can be inferred that ULF magnetic in the whole building tends to come from an external source, presumably the power line over tower B, just as the center point snapshot is a good representation of the whole magnetic field distribution of each space.

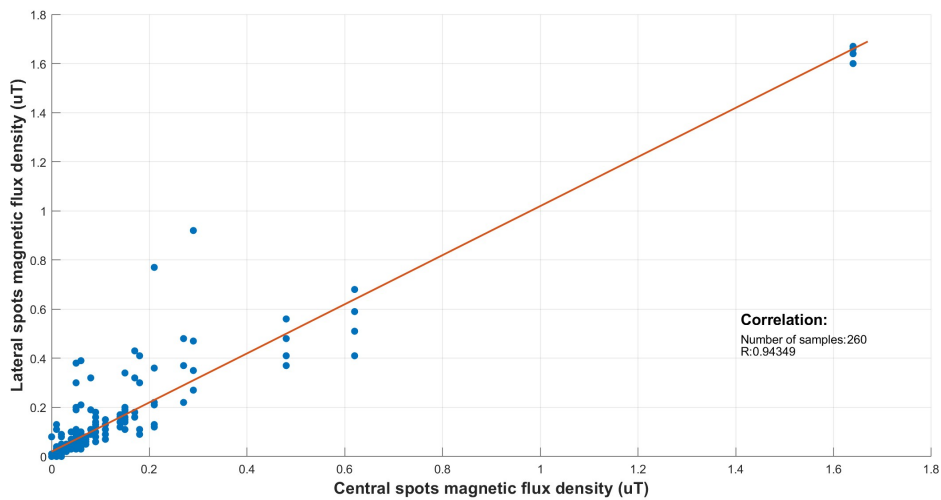


Figure 6.2: Scatter chart of magnetic flux density at the center of each environment versus other points at the same environment.

Proceeding in the Broadband analysis, a total of 26 windows were measured, whose records are in table 6.5. The results indicate that the values of magnetic flux density in the window are equal to or greater than the maximum values of each researched environment.

Table 6.5: Power frequency magnetic flux density at the windows.

Location	B-field (uT)	Measurement description	Location	B-field (uT)	Measurement description
Bar	0.15	20cm away from the East door	Tower S 6th floor	0.02	20cm away from the East glass panel
Bar	0.12	Centralized 20cm away from the West door	Tower S 5th floor	0.03	20cm away from the East glass panel
Study Aisle corridor	0.03	20cm away from the East 3rd floor terrace door	Tower S 6th floor	0.02	20cm away from the East glass panel
Study Aisle corridor	0.02	20cm away from the West 3rd floor terrace door	Fourth floor corridor	0.57	20cm away from the glass panel at the Anomaly point
T4.2 Classroom	0.01	20cm away from the West door	Fourth floor corridor	0.1	20cm away from the Tower B auditorium entrance
Tower T 5th floor	0.06	20cm away from the East glass panel	Fourth floor corridor	0.04	20cm away from the East 4th floor terrace door
Tower T 6th floor	0.06	20cm away from the East glass panel	Fourth floor corridor	0.02	20cm away from the West 4th floor terrace door
Second floor terrace	0.01	20cm away from the West 2nd floor terrace door	NEEC	0.01	Centralized 20cm away from the west window
Second floor terrace	0.02	20cm away from the East 2nd floor terrace door	ISR first floor aisle	0.11	Centralized 20cm away from the east glass panel
Entrance atrium	0.13	20cm away from the East door	Secretary	0.15	20cm away from the East window
Entrance atrium	0.22	Centralized 20cm away from South main's entrance	Secretary	0.16	20cm away from the West window
ISR floor 0	0.07	20cm away from the East entrance	R1.2 Laboratory	0.04	20cm away from North's main door
Tower S 5th floor	0.04	20cm away from the East glass panel	R1.2 Laboratory	0.05	20cm away from the East door
Additional information					
All measures were taken in 29/08/2022, with the SYPRIS 4080 gaussimeter located 1.7m above the ground					
The Anomaly point is a spot located in fourth floor corridor where the values of Electric field and Magnetic field strength are the highest recorded indoor DEEC's building. It's					
This Anomaly point is located 1.2m away from the eastend of the fourth floor corridor.					

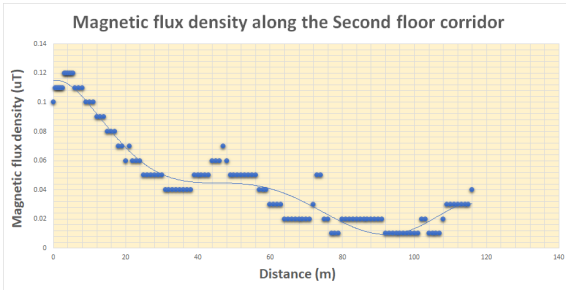
Table 6.6 indicates the results made to the outer perimeter of the terrace of the Bar and the main entrance, made spaced in a step of 3 m. The average of the three records was basically the same ($0.23 \mu\text{T}$), having however the terrace of the Bar registered the highest value ($0.54 \mu\text{T}$).

Table 6.6: Power frequency magnetic flux density at points in the outside of DEEC.

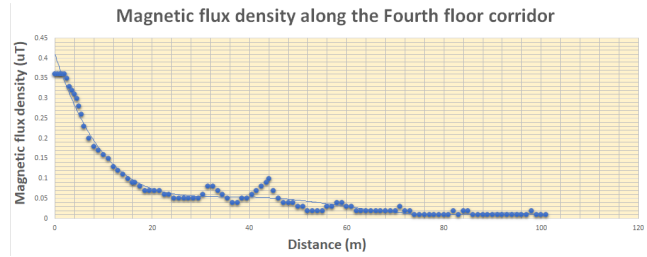
Data	Hour	Location	Number of points	Min (uT)	Max (uT)	Avg (uT)	Observation
06/02/2022	17:41	Exterior of the entrance Atrium	11	0.15	0.33	0.23	The highest value was recorded 3m away from the western point of the Entrance's glass panel.
09/06/2022	11:03	Exterior of the entrance Atrium	11	0.18	0.29	0.22	The highest value was recorded 3m away from the western point of the Entrance's glass panel.
09/06/2022	11:15	Fourth floor bar terrace perimeter	27	0.15	0.54	0.23	The highest value recorded 3m away from the Bar's west door
Additional information							
All measures were taken with the SYPRIS 4020 gaussimeter located 1.7m above the ground.							

In addition, the B-field distribution along the corridors of the second and fourth floors are present in figure 6.3, the figure 6.4 shows the survey for the 3A floor corridor and the Third floor Study aisle, as well as the East and West Third Floor corridor chart are represented in figure C.1. The origin of the X-axis is the easternmost point of each corridor, just as the trendline in each chart represents an interpolation by a fifth degree equation.

This confirms the tendency seen earlier that, as it is further east in the Department, the more intense the magnetic induction. The highest measurement is in the fourth floor corridor, with a $0.35 \mu\text{T}$ B-field magnitude in the eastern point. However, despite the notorious decay as it moves west in each corridor, magnetic induction peaks are observed in this trajectory. Such phenomenon was observed near the UPS power frames, as well some of the the expansion joints between the towers, illustrated in Figure E.5. This leads to believe that such spaces are used as a power cable path, whose magnetic fields in the vicinity are at safe levels for human exposure and EMC purposes, but are observable and not negligible.

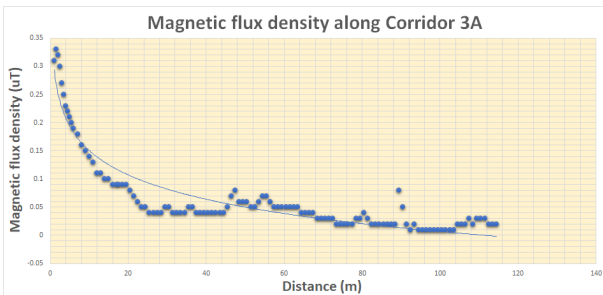


(a) Second floor corridor chart.

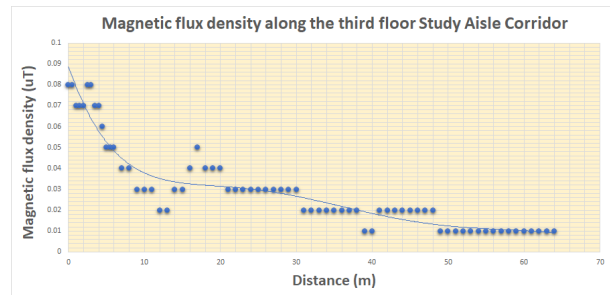


(b) Fourth floor corridor chart.

Figure 6.3: Magnetic field density obtained in the survey along the corridors of the second and fourth floor of DEEC.



(a) Floor 3A corridor chart.



(b) Third floor Study aisle chart.

Figure 6.4: Magnetic field density obtained in the survey along the Third floor Study aisle and the 3A corridor.

The broadband survey of ULF electric fields was made in July and August. Although both EMF160 and Aaronia NF5020 were employed for this duty, it was decided to discard the measurements of the latter due to inconsistency of the magnitude values per axis recorded when rotating the probe coil at 180 degrees. In this way, the table 6.7 indicates the values of electric fields in different locations of the Department with EFM160 measurements, and the table C.5 in the appendix provides a comparison between the records of both equipment.

In addition, it was decided to record the maximum and minimum value obtained with the EMF-160, due to the variability of the electric field read on the display over the 1-min measurement period. With this, each axis average and the EMEF per location was obtained. From the majorant field, it is noted that the electric fields in indoor environments have low magnitude, not exceeding 3.5 V/m. Even at an external point, opposite the main entrance and almost vertical from the power line, the maximum EMEF is 36.19 V/m.

Thus, all observed electric fields are well below the 5 kV/m limit established by ICNIRP

guideline, referred in table B.1, as well as below the E-field compatibility level presented in table A.4, in accordance with public environments Disturbance Degrees of IEC 61000-2-5.

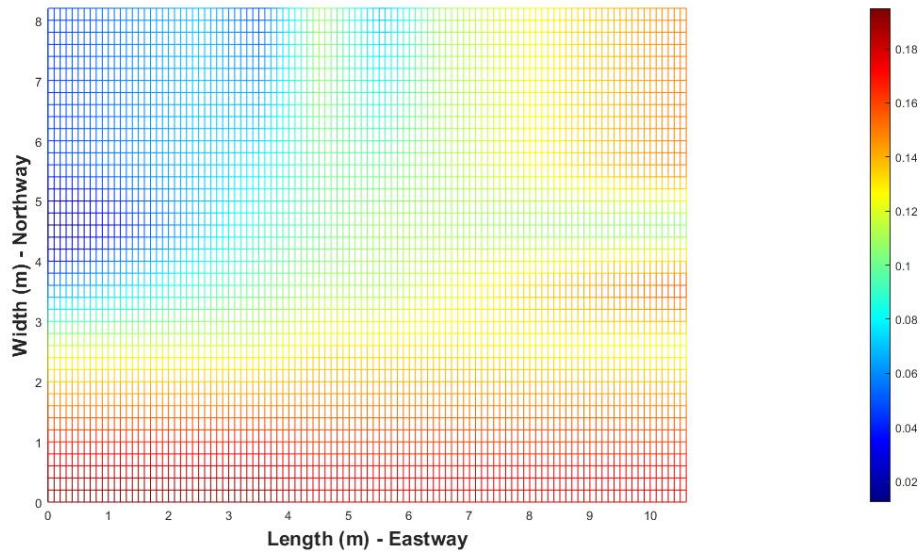
Table 6.7: Electric field survey at power frequency at different locations with EFM160.

Time	Axis X			Axis Y			Axis Z			Equivalent Majorant Electric Field (EMEF)		
	Min (V/m)	Avg (V/m)	Max (V/m)	Min (V/m)	Avg (V/m)	Max (V/m)	Min (V/m)	Avg (V/m)	Max (V/m)	Min (V/m)	Avg (V/m)	Max (V/m)
Location: Bar. Measured at the geometrical center												
18:00	0.89	0.94	1.00	0.89	1.33	1.78	1.00	1.56	2.11	1.61	2.26	2.94
Location: Terrace 4th floor. Measured 3m away from Bar's entrance, centered on the perspective of the door												
18:10	1.33	1.61	1.89	1.00	1.61	2.22	0.89	1.33	1.78	1.89	2.64	3.42
Location: Entrance Atrium. Measured at the geometrical center												
18:20	0.00	0.39	0.78	0.00	0.33	0.67	0.00	0.39	0.78	0.00	0.64	1.29
Location: 3A Corridor. Measured 1m from the eastend of corridor 3A												
18:50	0.11	0.22	0.33	0.67	1.17	1.67	1.11	1.50	1.89	1.30	1.91	2.54
Location: East Terrace. Measured at the geometrical center												
18:40	0.00	0.44	0.89	0.11	0.56	1.00	0.78	0.89	1.00	0.79	1.14	1.67
Location: DEEC's main entrance - Outdoor. Measured 3m away from DEEC's main Entrance, centered on the perspective of the door												
18:30	23.89	24.33	24.78	22.11	22.33	22.56	11.89	12.78	13.67	34.65	35.41	36.19
Location: R1.2 Laboratory. Measured at the geometrical center.												
19:00	0.00	0.11	0.22	0.00	0.11	0.22	0.78	0.83	0.89	0.78	0.85	0.94
Additional information: All measurements were taken 1m above the ground, on 07/19/2022												

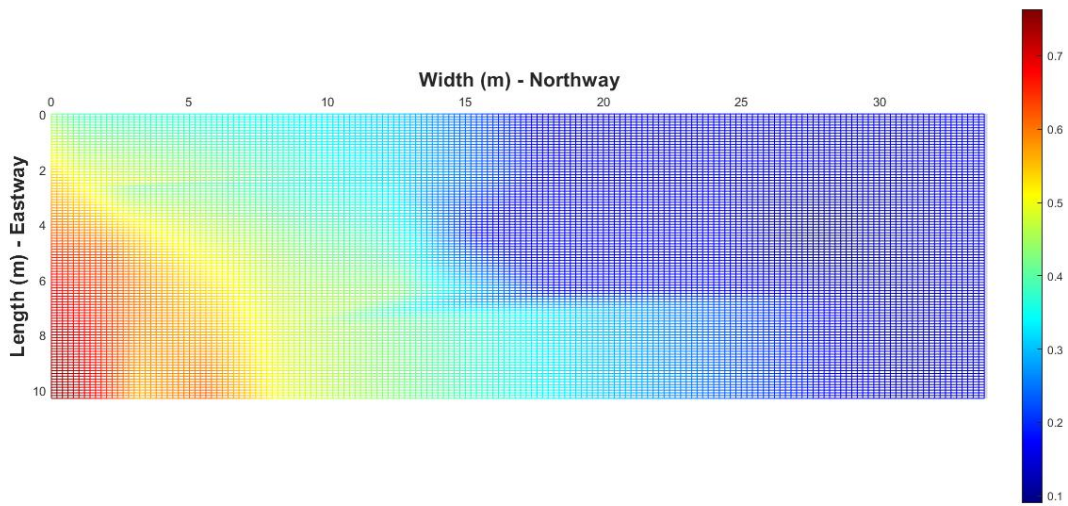
Regarding the graphical representation of power frequency magnetic fields via Mapping, the Entrance Atrium and Tower B Study Room were chosen due to its large area and proximity to the power line, available in figure 6.5. The Bar's lateral was also mapped, due to the distribution board located in its northern part, whose plot is available in figure C.2 in appendix.

Finally, figures 6.7, C.7, 6.8 ,C.3, C.4, C.5 and C.6 show some examples of natural interpolation and linear extrapolation of the rooms surveyed with the Five-point method, obtained using the *scattered interpolant* function in Matlab. The greater the length or width of a certain coordinate, the further east and north it will be, respectively. Furthermore, the figure 6.6 illustrates a comparison between the characterization made via Mapping and that obtained with this new method, having both the same trend and similar values.

Generally speaking, such approach allows from a rapid measurement process to visualize the preponderance of an external source of dominant magnetic fields, as well as assess whether there is any possible switchboard or electrical appliance within such an environment that generates significant fields throughout the space.



(a) 25-point Mapping grid in Entrance Atrium



(b) 32-point Mapping grid in Sixth Floor Tower B Study Room

Figure 6.5: Magnetic flux density mapping at the Second Floor Entrance Atrium (left) and Sixth Floor Tower B Study Room(right).

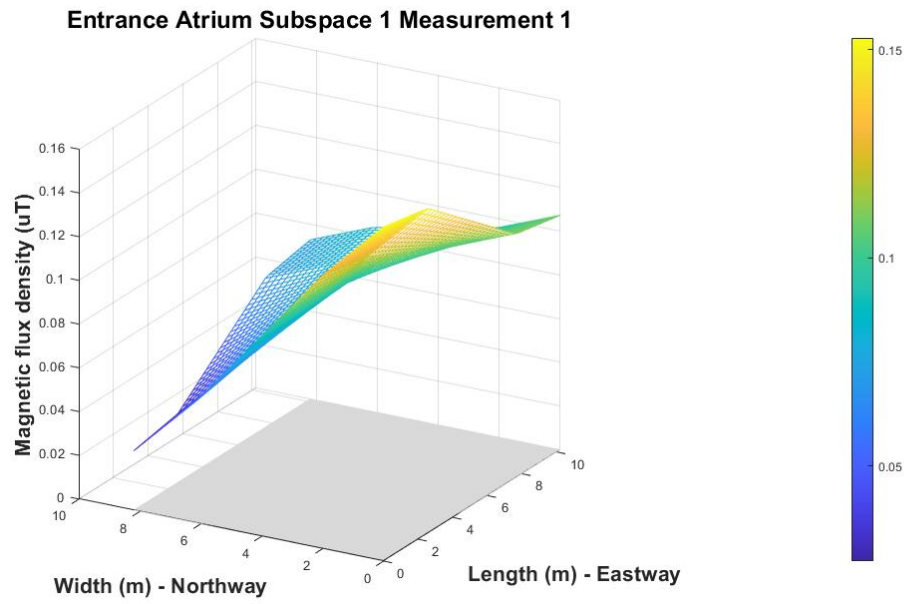


Figure 6.6: Power frequency B-field interpolation and extrapolation at the Entrance Atrium.

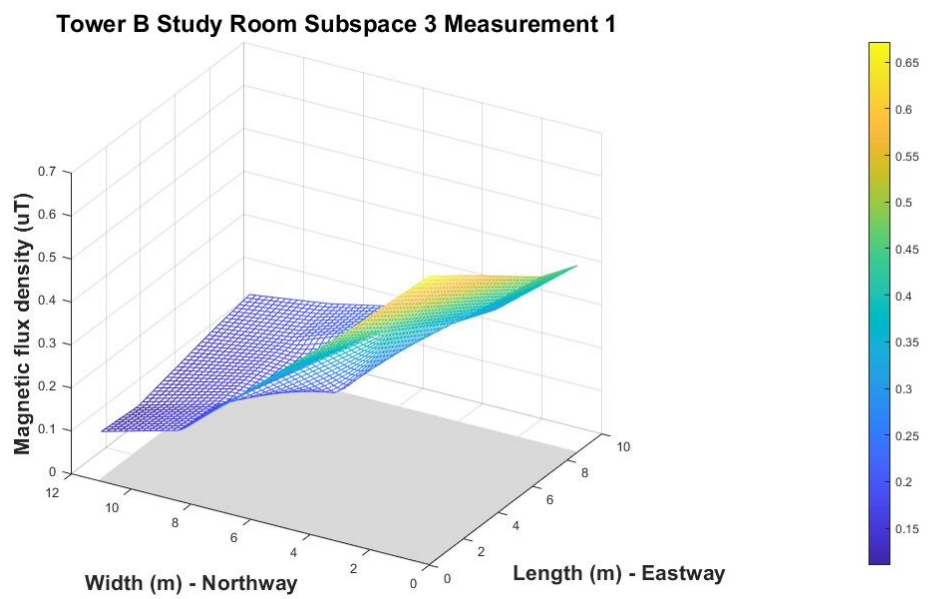


Figure 6.7: Power frequency B-field interpolation and extrapolation at the Tower B Study Room third subspace.

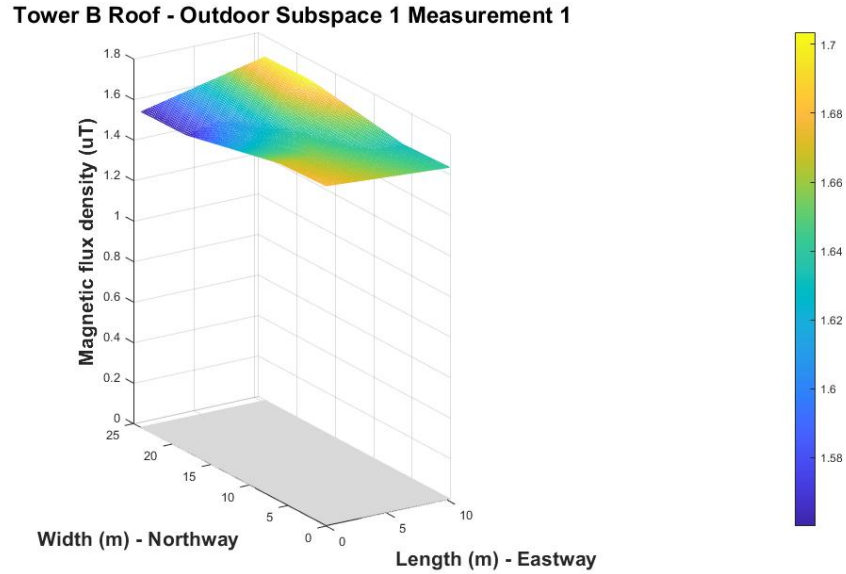


Figure 6.8: Power frequency B-field interpolation and extrapolation at the Tower B Roof - Outdoor.

6.2 Frequency Screening results

Tables 6.8 and 6.9 show the Radiometric Survey results with MinMax detector type for the Low-frequency and High-frequency range, respectively, while tables 6.10 and 6.11 show the results using the RMS detector type. All Radiometric Survey was performed between June and September 2022. For each frequency sweep and location, each record was made in a period of 1 minute. With this, through the maximum values recorded in each frequency in in that period, the equivalent electric or magnetic field (using the equation 3.5) and the sum for human dosimetric assessment, as established by ICNIRP and using the equations 2.3 and 2.4. In general, the physical quantities surveyed are higher with the MinMax Detector type.

Regarding the LF B-field Radiometric survey, in all locations and frequency range considered the dosimetric levels are below that established by ICNIRP guidelines, and all equivalent magnetic field in the power frequency sweep are below the $12.56 \mu\text{T}$ power frequency IEC Compatibility Level for commercial/public environments. The most intense magnitudes of power frequency magnetic flux density were found on Tower B Terrace. Meanwhile, for the range of 150 kHz to 1 MHz, the highest values were recorded in the Bar.

Concerning the HF Radiometric Survey, the DEI promenade showed the highest dosimetric

and EEF values for all frequency range surveyed, counting with EEF levels of 1.13 V/m in the 650-950 MHz frequency sweep e a global EEF of 1.74 V/m, in the case of the MinMax detector type. Locations with population continuously using telecommunication devices, as in the case of Entrance Atrium and Study Aisle, did not demonstrate higher exposure to EMF in the frequency bands considered. The lowest EMF levels were recorded in the underground parking lot.

In any case, the human dosimetric assessment for all locations and frequency range are far below the guideline limits. As well as all EEF levels are below 3 V/m, the corresponding electric field of the third Disturbance Degree, due to the phenomenon of External Radio and Base stations of phones for commercial/public location class in table A.3.

Table 6.8: Radiometric survey LF overview with MinMax detector type.

Freq Sweep (Hz)	Bar			DEI			Entrance Atrium			Parking			Study Aisle			Tower R			R5.2 Laboratory		
	Max (T)	EBF (T)	ICNIRP	Max (T)	EBF (T)	ICNIRP	Max (T)	EBF (T)	ICNIRP	Max (T)	EBF (T)	ICNIRP	Max (T)	EBF (T)	ICNIRP	Max (T)	EBF (T)	ICNIRP	Max (T)	EBF (T)	ICNIRP
45-65	3.13E-08	1.38E-07	9.48E-06	4.75E-08	1.93E-07	1.26E-05	3.86E-08	1.64E-07	1.09E-05	1.69E-08	9.03E-08	6.79E-06	2.00E-08	9.80E-08	7.25E-06	1.70E-08	8.89E-08	6.65E-06	1.70E-08	8.43E-08	6.36E-06
65-110	1.50E-07	8.62E-07	1.05E-04	4.99E-08	2.72E-07	3.27E-05	4.96E-08	2.72E-07	3.27E-05	4.84E-08	2.73E-07	3.31E-05	4.87E-08	2.74E-07	3.32E-05	4.84E-08	2.73E-07	3.31E-05	4.86E-08	2.71E-07	3.28E-05
110-200	3.64E-07	1.94E-06	4.09E-04	1.16E-07	6.21E-07	1.32E-04	9.13E-08	4.86E-07	1.03E-04	1.15E-07	6.18E-07	1.31E-04	1.15E-07	6.16E-07	1.30E-04	1.15E-07	6.16E-07	1.30E-04	1.16E-07	6.17E-07	1.31E-04
200-500	1.85E-08	4.64E-08	1.65E-05	1.80E-08	1.21E-05	3.73E-04	1.06E-08	1.82E-08	2.97E-06	1.68E-08	3.44E-08	1.10E-05	1.63E-08	3.27E-08	1.02E-05	1.71E-08	3.39E-08	1.04E-05	1.63E-08	3.34E-08	1.04E-05
500-1500	3.50E-09	1.39E-08	4.87E-06	1.77E-09	5.76E-09	2.00E-06	1.99E-09	8.82E-09	2.82E-06	1.95E-09	6.11E-09	2.12E-06	1.79E-09	5.72E-09	1.96E-06	1.71E-09	5.65E-09	2.00E-06	1.79E-09	5.64E-09	1.98E-06
1.5k-150k	5.12E-09	1.43E-08	0.0093	3.67E-09	1.02E-08	0.0056	4.28E-09	1.12E-08	0.0063	4.65E-09	1.07E-08	0.0054	3.67E-09	9.35E-09	0.0053	3.76E-09	1.01E-08	0.0055	3.53E-09	9.68E-09	0.0056
150k-1M	2.39E-09	3.28E-08	0.2011	1.01E-09	2.26E-09	0.0068	1.52E-09	1.21E-08	0.0759	1.56E-09	1.20E-08	0.0748	1.66E-09	1.15E-08	0.0715	1.49E-09	1.09E-08	0.0672	1.73E-09	1.24E-08	0.0772
Total	-	2.125E-06	2.11E-01	-	1.216E-05	1.26E-02	-	5.81E-07	8.24E-02	-	6.82E-07	8.04E-02	-	6.82E-07	7.70E-02	-	6.81E-07	7.29E-02	-	6.80E-07	8.30E-02

Table 6.9: Radiometric survey HF overview with MinMax detector type.

Freq Sweep (MHz)	Bar			DEI			Entrance Atrium			Parking			Study Aisle			Tower R			R5.2 Laboratory		
	Max (V/m)	EEF (V/m)	ICNIRP	Max (V/m)	EEF (V/m)	ICNIRP	Max (V/m)	EEF (V/m)	ICNIRP	Max (V/m)	EEF (V/m)	ICNIRP	Max (V/m)	EEF (V/m)	ICNIRP	Max (V/m)	EEF (V/m)	ICNIRP	Max (V/m)	EEF (V/m)	ICNIRP
650-850	0.0174	0.0684	2.92E-12	0.3878	1.1372	8.44E-10	0.1263	0.391	9.34E-11	0.0015	0.0245	3.84E-13	0.0031	0.0314	6.29E-13	0.0041	0.0351	8.00E-13	0.0039	0.034	7.44E-13
1650-2000	0.041	0.1073	1.16E-10	0.2325	0.6528	3.91E-10	0.1125	0.4139	2.05E-10	9.33E-04	0.0161	7.24E-11	0.0056	0.03	7.63E-11	0.002	0.0219	8.16E-11	0.0036	0.0261	7.45E-11
2500-2700	0.0302	0.2256	1.37E-05	0.1868	0.7581	1.54E-04	0.1276	0.4172	4.68E-05	0.1276	0.4177	4.69E-05	0.01	0.1392	5.21E-06	0.0103	0.1378	5.11E-06	0.0111	0.1472	5.82E-06
3400-3800	0.0068	0.0869	2.03E-06	0.0221	0.288	2.23E-05	0.0057	0.0876	2.06E-06	0.0019	0.0255	1.74E-07	0.0043	0.0636	1.09E-06	0.0044	0.0622	1.04E-06	0.0045	0.0637	1.09E-06
3800-4400	0.0354	0.4717	5.98E-05	0.0309	0.47	5.94E-05	0.0374	0.4322	5.02E-05	0.0272	0.3115	2.61E-05	0.0284	0.314	2.65E-05	0.0254	0.3163	2.69E-05	0.0268	0.3245	2.83E-05
10-50	0.018	0.2263	6.53E-05	0.0467	0.5791	4.28E-04	0.0467	0.5794	4.28E-04	0.0045	0.0338	1.46E-06	0.0498	0.5781	4.26E-04	0.0312	0.3829	1.87E-04	0.0451	0.5751	4.22E-04
50-150	0.0167	0.1179	1.77E-05	0.0433	0.2722	9.45E-05	0.0433	0.2719	9.43E-05	0.003	0.0239	7.29E-07	0.0394	0.2574	8.45E-05	0.0278	0.1796	4.12E-05	0.0388	0.2485	7.87E-05
400-650	0.0109	0.0744	6.47E-12	0.015	0.1397	2.29E-11	0.0113	0.0828	7.91E-12	0.0059	0.0234	6.05E-13	0.004	0.0231	5.86E-13	0.0081	0.0252	7.06E-13	0.0083	0.0258	7.40E-13
100-6000	0.1372	0.3456	1.51E-05	0.3425	0.8865	7.61E-05	0.1239	0.3593	1.32E-05	0.0072	0.1044	2.95E-06	0.0216	0.1157	3.50E-06	0.0114	0.11	3.07E-06	0.0722	0.2232	1.33E-05
Total	-	0.6065	1.59E-04	-	1.7398	7.58E-04	-	1.0532	6.22E-04	-	0.5247	7.53E-05	-	0.7245	5.44E-04	-	0.5515	2.61E-04	-	0.7253	5.36E-04

Table 6.10: Radiometric survey LF overview with RMS detector type.

Freq Sweep	Bar			DEI			Entrance Atrium			Parking			Study Aisle			Tower B Terrace			Tower R		
	Max (T)	EBF (T)	ICNIRP	Max (T)	EBF (T)	ICNIRP	Max (T)	EBF (T)	ICNIRP	Max (T)	EBF (T)	ICNIRP	Max (T)	EBF (T)	ICNIRP	Max (T)	EBF (T)	ICNIRP	Max (T)	EBF (T)	ICNIRP
45-65	2.97E-08	1.22E-07	7.86E-06	3.92E-08	1.31E-07	5.91E-06	4.56E-08	1.79E-07	1.11E-05	1.46E-08	6.43E-08	4.57E-06	1.86E-08	8.28E-08	5.73E-06	5.92E-07	2.21E-06	1.31E-04	6.37E-08	3.59E-07	2.75E-05
65-110	4.69E-08	2.11E-07	2.47E-05	4.08E-08	2.02E-07	2.39E-05	4.26E-08	2.00E-07	2.33E-05	3.76E-08	2.07E-07	2.49E-05	3.75E-08	2.08E-07	2.50E-05	-	-	-	3.77E-08	2.07E-07	2.49E-05
110-200	9.14E-08	4.88E-07	1.03E-04	9.12E-08	4.86E-07	1.03E-04	9.11E-08	4.84E-07	1.02E-04	9.07E-08	4.82E-07	1.02E-04	9.09E-08	4.83E-07	1.02E-04	-	-	-	9.06E-08	4.82E-07	1.02E-04
200-500	1.09E-08	1.85E-08	2.91E-06	1.09E-08	1.92E-08	3.30E-06	1.14E-08	2.04E-08	3.63E-06	1.03E-08	1.75E-08	2.76E-06	1.11E-08	1.89E-08	2.93E-06	-	-	-	1.06E-08	1.79E-08	2.57E-06
500-1500	3.04E-07	5.69E-07	2.05E-04	2.93E-07	5.48E-07	1.98E-04	3.06E-07	5.69E-07	2.06E-04	2.94E-07	5.50E-07	1.99E-04	3.03E-07	5.66E-07	2.04E-04	-	-	-	2.93E-07	5.48E-07	1.98E-04
1.5k-150k	2.10E-09	5.47E-09	0.0023	2.10E-09	5.48E-09	0.0023	2.19E-09	5.51E-09	0.0021	2.08E-09	5.37E-09	0.0023	2.32E-09	5.65E-09	0.0024	-	-	-	2.33E-09	5.72E-09	0.0023
150k-1M	1.01E-09	1.88E-09	0.0061	6.33E-10	1.72E-09	0.0056	1.03E-09	1.77E-09	0.0056	9.87E-11	9.23E-10	0.0032	9.79E-11	1.21E-09	0.0047	3.22E-10	3.27E-09	0.0113	1.00E-09	2.08E-09	0.0072
Total	-	7.88E-07	8.74E-03	-	7.71E-07	8.23E-03	-	7.94E-07	8.05E-03	-	7.63E-07	5.83E-03	-	7.77E-07	7.44E-03	-	2.21E-06	1.14E-02	-	8.40E-07	9.85E-03

Table 6.11: Radiometric survey HF overview with RMS detector type.

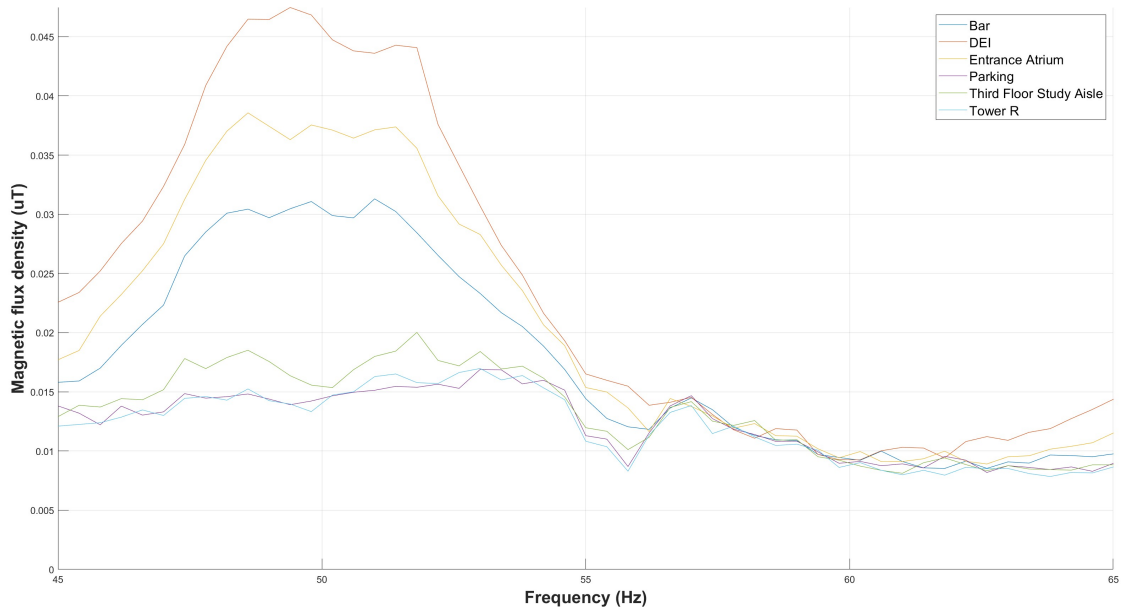
Freq Sweep	Bar			DEI			Entrance Atrium			Parking			Study Aisle			Tower B Terrace			Tower R		
	Max (V/m)	EEF (V/m)	ICNIRP	Max (V/m)	EEF (V/m)	ICNIRP	Max (V/m)	EEF (V/m)	ICNIRP	Max (V/m)	EEF (V/m)	ICNIRP	Max (V/m)	EEF (V/m)	ICNIRP	Max (V/m)	EEF (V/m)	ICNIRP	Max (V/m)	EEF (V/m)	ICNIRP
650-850	0.0295	0.0969	5.88E-12	0.145	0.3	5.83E-11	0.042	0.1372	1.17E-11	0.0012	0.0113	8.20E-14	0.0039	0.0213	2.89E-13	6.74E-04	0.0101	6.48E-14	0.0029	0.0215	3.05E-13
1650-2000	0.0422	0.1609	3.68E-11	0.0961	0.2268	4.63E-11	0.0268	0.0612	2.32E-11	5.59E-04	0.0091	2.29E-11	0.0014	0.0148	2.14E-11	4.83E-04	0.0078	2.06E-11	0.0281	0.0508	7.19E-11
2500-2700	0.0362	0.1143	3.51E-06	0.0527	0.2777	2.07E-05	0.02	0.0991	2.64E-06	0.0076	0.0734	1.45E-06	0.0067	0.0672	1.21E-06	0.0046	0.0634	1.08E-06	0.0056	0.071	1.35E-06
3400-3800	0.0028	0.0364	3.56E-07	0.0086	0.0885	2.11E-06	0.0037	0.0436	5.11E-07	0.0026	0.0336	3.04E-07	0.0021	0.033	2.92E-07	0.0026	0.0273	2.00E-07	0.0026	0.0337	3.04E-07
3800-4400	0.0174	0.2142	1.23E-05	0.014	0.2046	1.12E-05	0.0163	0.2012	1.09E-05	0.0149	0.1851	9.20E-06	0.0141	0.1815	8.86E-06	0.0111	0.1437	5.55E-06	0.0134	0.1775	8.47E-06
10-50	0.0117	0.1478	2.79E-05	0.0123	0.1487	2.82E-05	0.0171	0.2191	6.13E-05	0.0071	0.0882	9.92E-06	0.0132	0.1548	3.06E-05	0.0098	0.0711	6.45E-06	0.0126	0.1529	2.98E-05
50-150	0.009	0.0651	5.41E-06	0.0109	0.074	6.98E-06	0.0166	0.1047	1.40E-05	0.0067	0.0444	2.52E-06	0.0108	0.0693	6.13E-06	-	-	-	0.0115	0.0722	6.66E-06
400-650	0.0081	0.0184	4.02E-13	0.0086	0.0707	6.01E-12	0.0073	0.0311	1.14E-12	0.0063	0.0123	1.73E-13	0.0063	0.0135	2.11E-13	-	-	-	0.0041	0.011	1.35E-13
100-6000	0.0322	0.1241	2.62E-06	0.1153	0.3576	1.64E-05	0.0466	0.1497	3.18E-06	0.0051	0.057	8.87E-07	0.0088	0.0655	1.05E-06	0.0027	0.0516	7.24E-07	0.0092	0.0639	9.86E-07
Total	-	0.3492	4.95E-05	-	0.5485	6.93E-05	-	0.3670	8.93E-05	-	0.2256	2.34E-05	-	0.2611	4.71E-05	-	0.1750	1.33E-05	-	0.2635	4.66E-05

The figures 6.9, 6.13, 6.12 and 6.11 exhibit, respectively, the spectrum signature of **mains power preset**, the 65-130 Hz, 200-500 Hz and 0.15-1 MHz frequency sweeps for both of the detector types. For the ULF Magnetic Fields, it is noted that the external environments have higher magnitude levels, as well as B-field in the power frequency harmonics. And for the sweep between 150 kHz and 1 MHz, a series of B-field peaks centered at 500 kHz, 600 kHz, 750 kHz and 900 kHz might be noticed, whose most likely sources would be from an AM radio base.

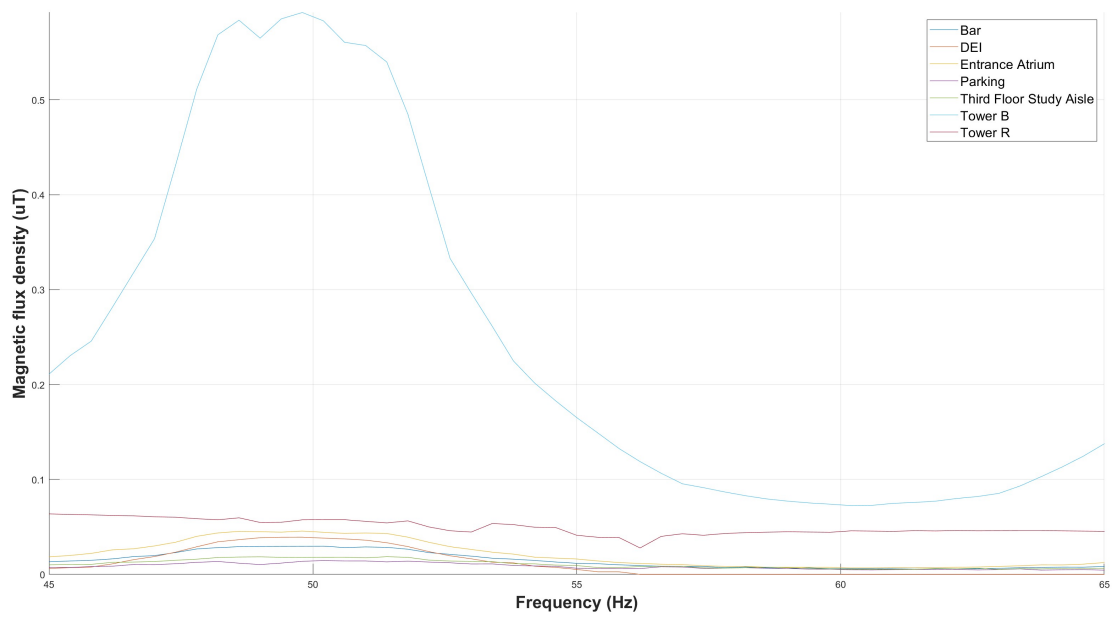
Moreover, the figure 6.10 consists on the global HF spectrum signature for both of the detector types, using a 0.15-6 GHz frequency sweep. As can be seen, a series of E-field peaks centered in the range of 800 MHz and 900 MHz are noticed, as well as in 1.8 GHz, 2.3 GHz and 2.7 GHz, probably due to EMF emitting sources in different telecommunication technologies, such as UMTS, DCS, GSM, LTE-A and 5G. Electric field peaks centered at 2.4 GHz, 2.5 GHz and 4.7 GHz, communication ranges used by Wi-Fi Access Points, are also observable. There are also peaks centered between 150 MHz and 300 MHz, whose probable sources are DTV and FM radio transmitters. There were no significant signals detected for the Medium Wave and Short Wave ranges, respectively to a 1 MHz and 10 MHz region.

The multitude of HF EMF sources present in the department makes the resulting spectrum signature exceed the CISPR 32 limits for radiated **Emissions**, whose Detector Type are Quasi-peak, Average or Peak, according to the desired frequency range. It is also noteworthy that the presence of a signal with triangular signature and peak in 97 dB/m , centered at 4 GHz, which lacks applications that could be EMF sources in such range.

Lastly, the spectrum signature also verify that the highest levels of HF electric fields are found in the DEI promenade, which may be indicative of preponderance of external sources, such as telecommunication bases installed nearby.

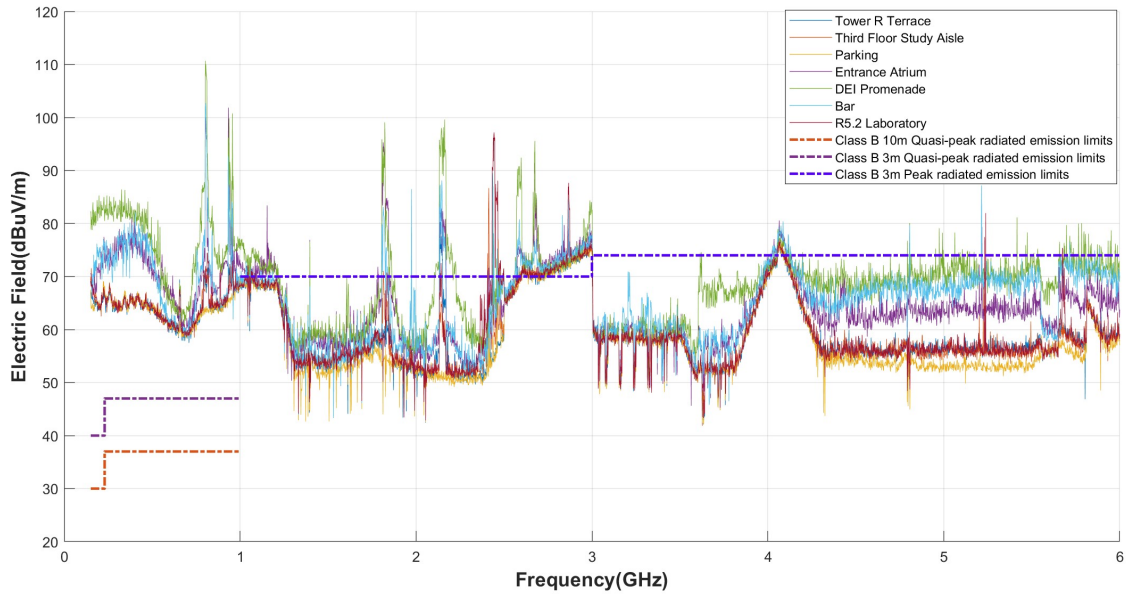


(a) MinMax.

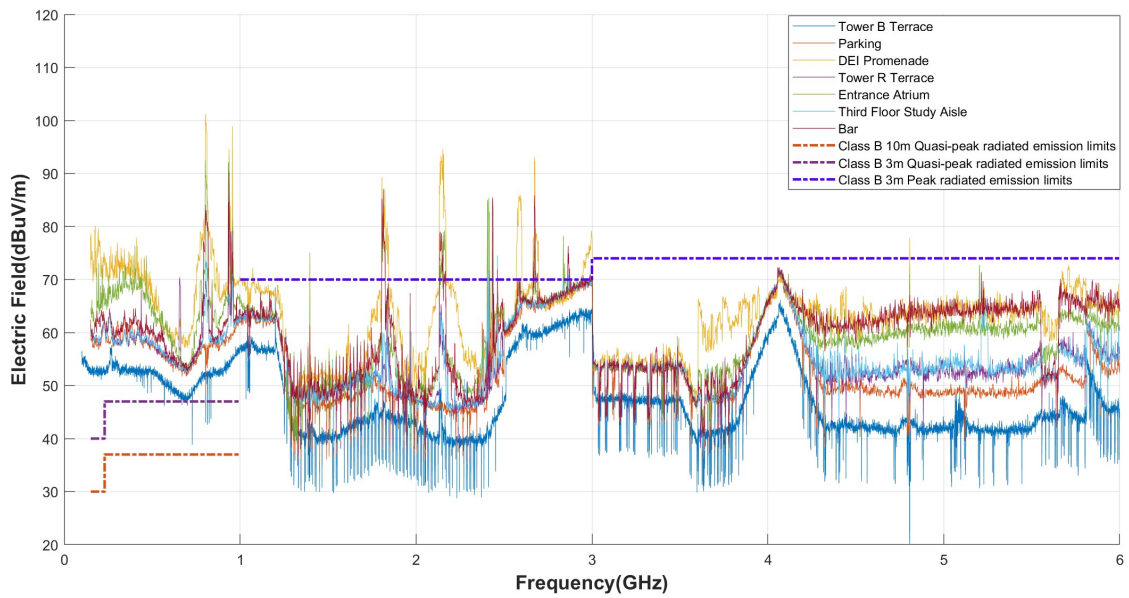


(b) RMS.

Figure 6.9: Power frequency spectrum signatures with MinMax and RMS detector type at different locations in DEEC.

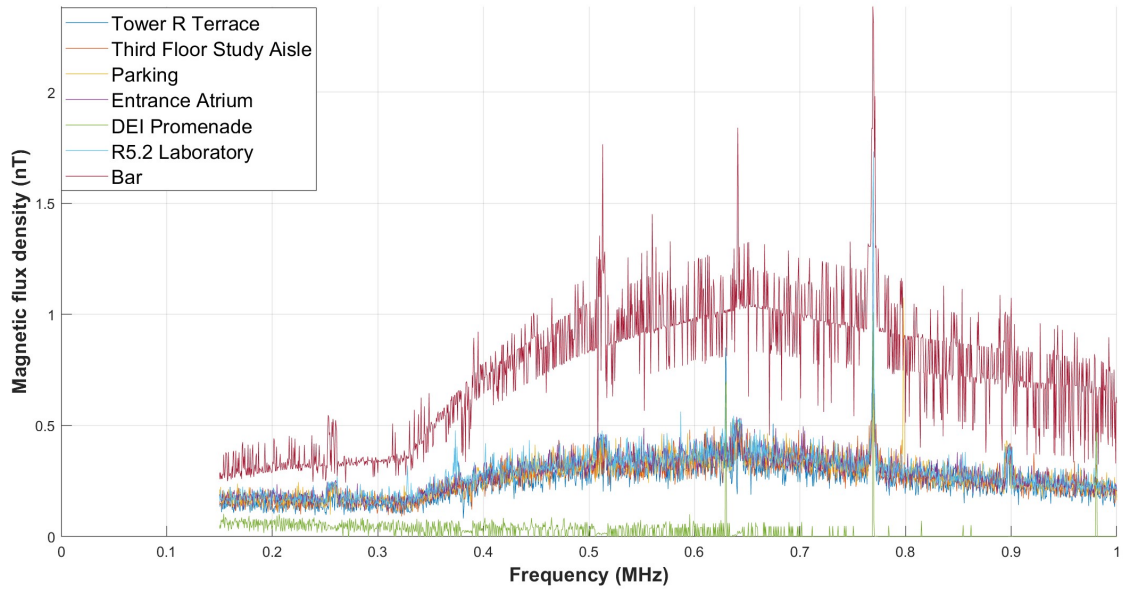


(a) MinMax.

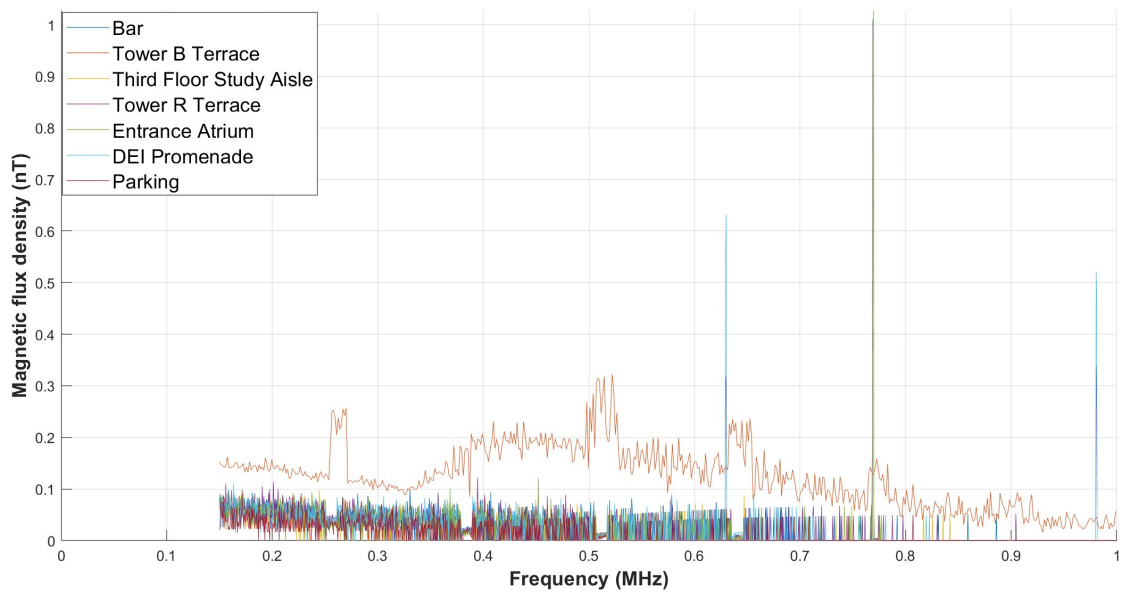


(b) RMS.

Figure 6.10: HF spectrum signatures with MinMax and RMS detector type at different locations in DEEC at different locations in DEEC.

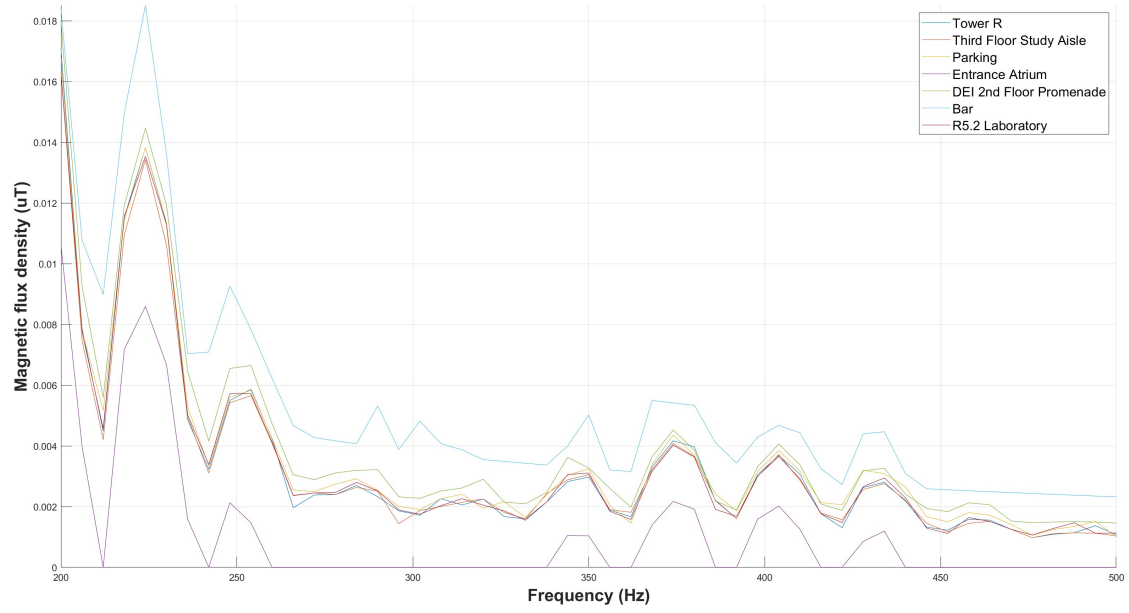


(a) MinMax.

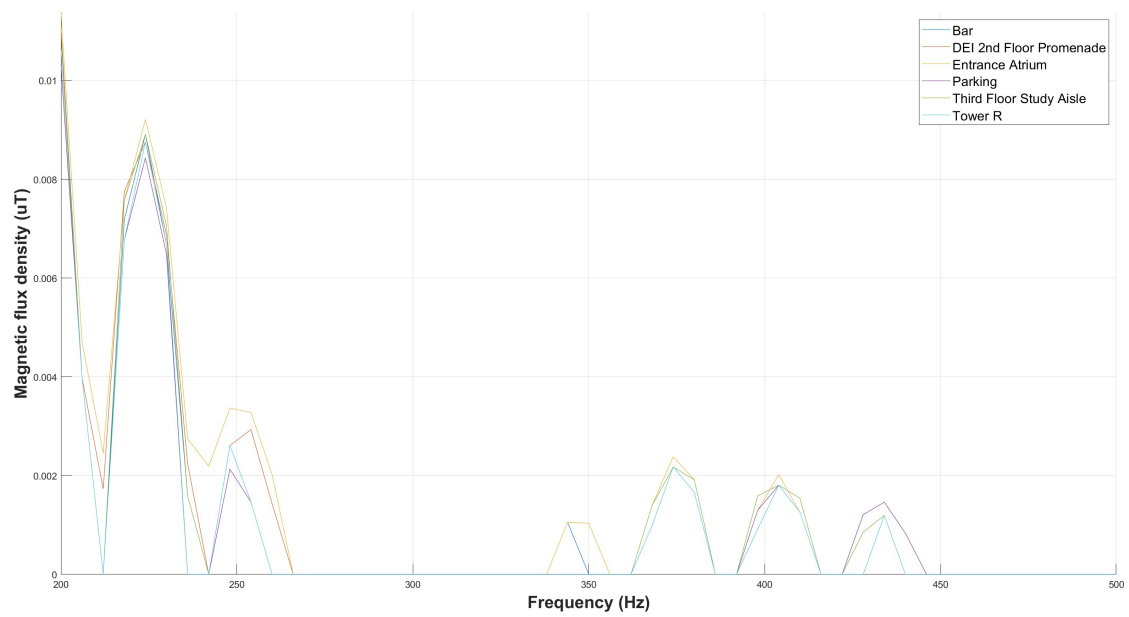


(b) RMS.

Figure 6.11: 0.15-1 MHz spectrum signatures with MinMax and RMS detector type at different locations in DEEC.

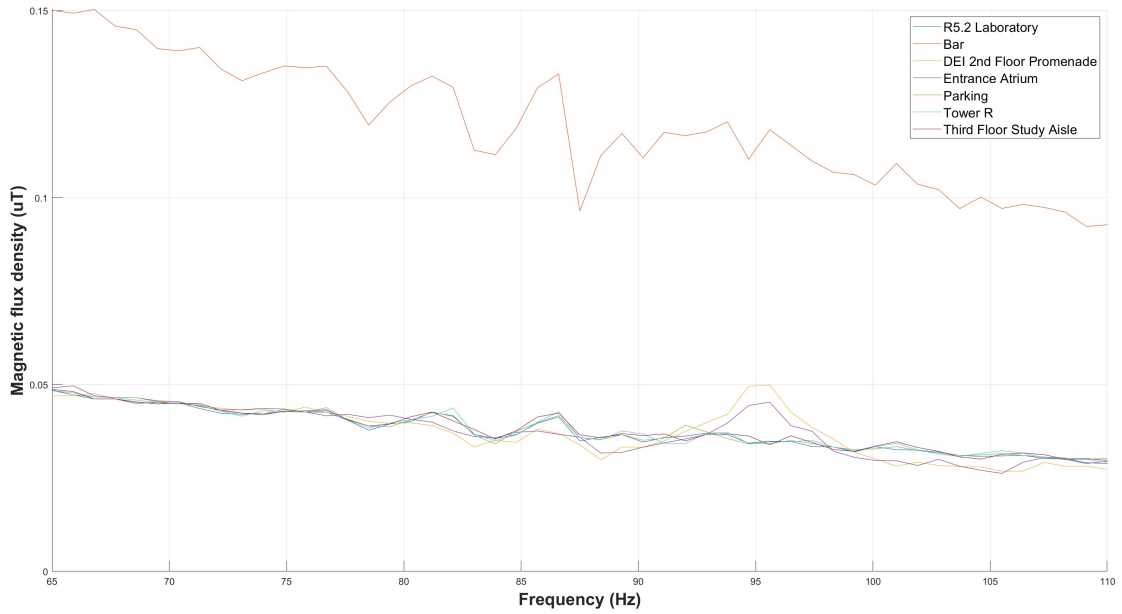


(a) MinMax.

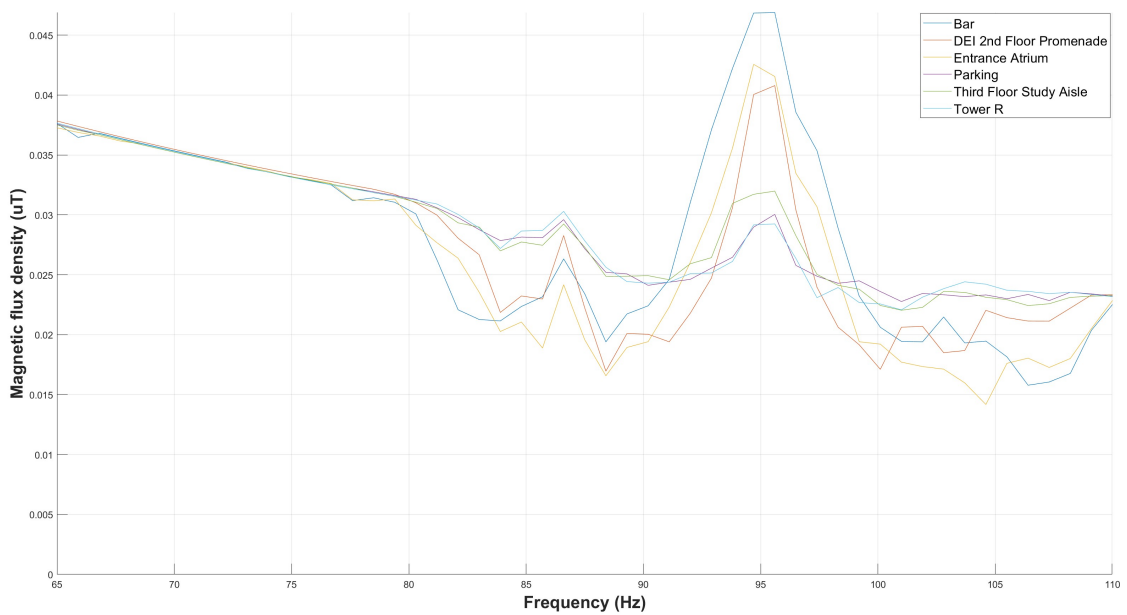


(b) RMS.

Figure 6.12: 200-500 Hz spectrum signatures with MinMax and RMS detector type at different locations in DEEC.



(a) MinMax.



(b) RMS.

Figure 6.13: 65-110 Hz spectrum signatures with MinMax and RMS detector type at different locations in DEEC.

Moreover, the table 6.12 indicates the results of Spatial Averaging at power frequency for human exposition compliance, in accordance with the EN 50492 standard. The research was conducted in the geometric center of the Bar, 3A.23 office and classroom T4.4, either in the

position of the professor’s desk, as in a student desk geometrically centered in the room.

According to the results obtained, the magnetic flux density at 50 Hz at head height does not tend to be higher than in the abdomen or trunk. Furthermore, all spatial averaged results are far below the power-frequency ICNIRP 100 μT limit for general occupation, presented in table B.1. However it is noted that the 3A.23 Office would be classified as a 0.4 μT limit, exposed previously in chapter 2.

Table 6.12: Spatial-averaging power frequency human exposure assessment magnetic flux density.

Location	EBF (μT)							ICNIRP
	Point 1	Point 2	Point 3	Point 4	Point 5	Point 6	Spatial Avg	
Bar	3.57E-01	3.68E-01	3.76E-01	3.64E-01	3.72E-01	3.56E-01	3.66E-01	1.70E-05
3A1.23 Office	8.36E-01	8.06E-01	8.26E-01	7.99E-01	7.87E-07	7.69E-07	8.05E-01	3.95E-05
T4.4 Classroom (Student)	4.20E-02	4.87E-02	3.75E-02	4.66E-02	4.62E-02	5.64E-02	4.66E-02	3.35E-06
T4.4 Classroom (Professor)	5.16E-02	5.33E-02	4.73E-02	5.89E-02	6.63E-02	5.39E-02	5.55E-02	3.85E-06

In the sequence, the figures 6.14 and 6.15 illustrate the results for the Long-range temporal variation Survey of power frequency magnetic flux density and HF global sweep, respectively.

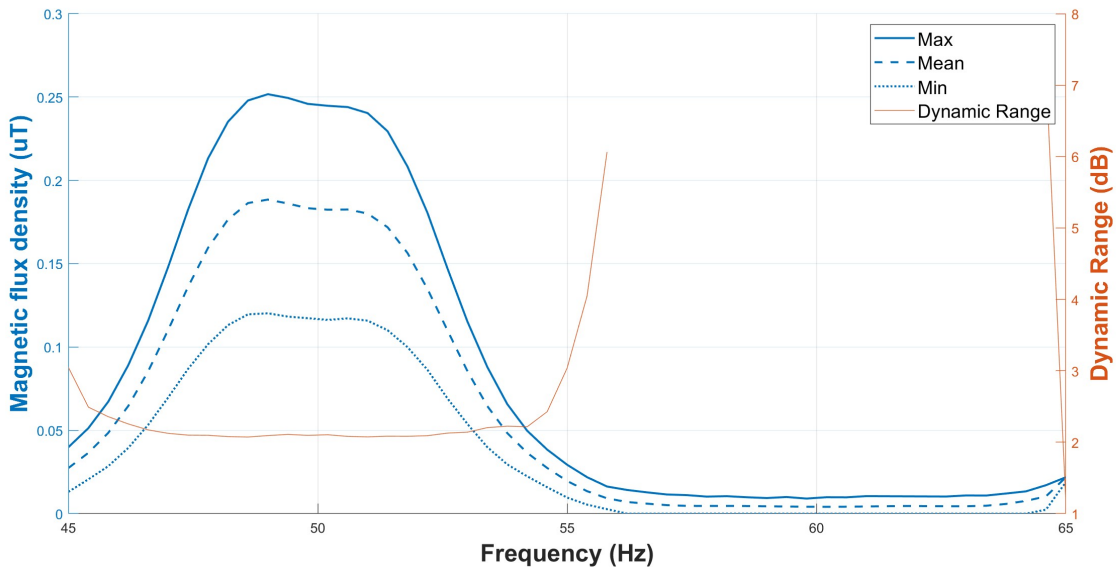


Figure 6.14: Dynamic range in 50 Hz 24 hour temporal variation Survey in 3A.23 office.

Regarding the first case, it is possible to observe a 2 dB Dynamic Range factor, probably due to variability of power flows in the power line over the Tower B. The maximum EBF obtained was 0.89 μT and maximum ICNIRP cumulative sum was 4.37E-05, in conformity with EMC and human dosimetric compliance. Nonetheless, if the DR factor was used a Safety Factor and

applied the values read in the Five-point method, the environments located in tower B and the points further west of the corridors would be in the $0.4 \mu T$ limit.

Furthermore, the HF Long-range temporal survey has a Dynamic Range floor of 10dB, with peaks centered on the frequency bands of telecommunications transmission. Considering only the maximum values recorded in each frequency, it was obtained an EEF of 1.79 V/m and a dosimetric exposure of 8.25E-04, levels below the limits of the 3V/m Compatibility Level of IEC 61000-2-5 and ICNIRP general-public exposure compliance.

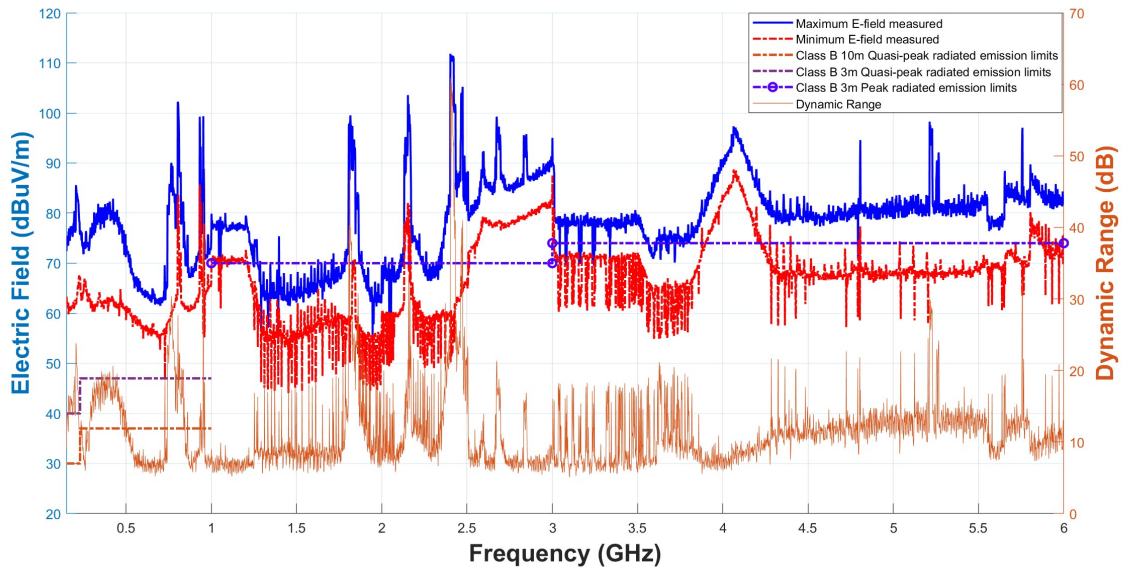


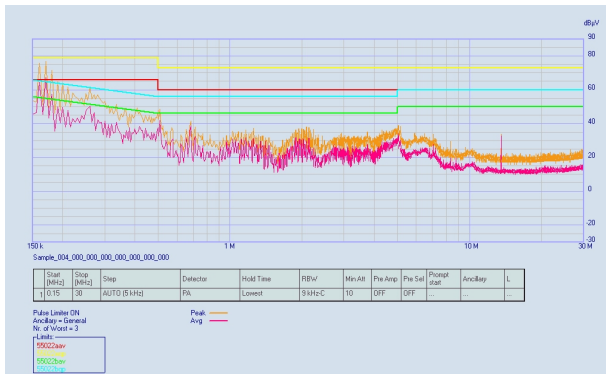
Figure 6.15: Dynamic range in the HF 24 hour temporal variation Survey in 3A.21 office.

6.3 EMC conducted noise measurements

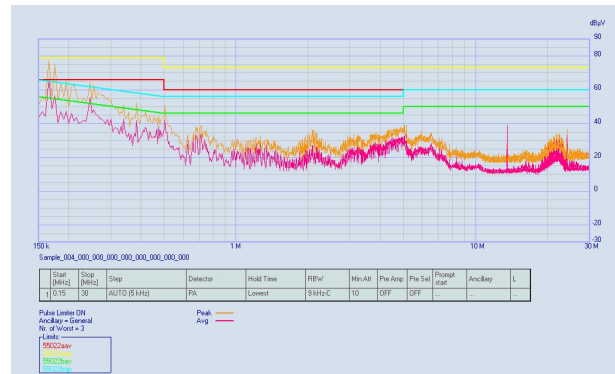
In this subsection, the results verified for EMC conducted noise at common 220 V/50 Hz outlets are cited, at different points of DEEC on September 8, 2022. For this purpose, the LISN+I device was connected to the outlet under study with its internal High-Pass filter turned off. Through the methodology described in the subchapter 4, the LISN+I was then connected to the NARDA PMM EMI 7010 spectrum analyzer, thus obtaining the values of noise conducted between 150 kHz and 1 MHz for the Phase and Neutral of the outlet under study. All measurements were made without electrical equipment connected to the outlets in the vicinity.

The figures 6.16 and 6.17, respectively, demonstrate the results for an outlet located immediately outside the Shielded Chamber, without filter, and another inside such chamber, with an

EMC filter to be investigated. In addition, the figure 6.18 illustrates the values recorded in an outlet in the T4.2 classroom, as well as the figures E.1 and E.2, in the Appendix E, show the results for an outlet in the Bar and in the Third Aisle Study Room, respectively. Lastly, the figures E.3 and E.4 show the EMC conducted noise results in the same outlet in R1.2 Laboratory at different times of the day.

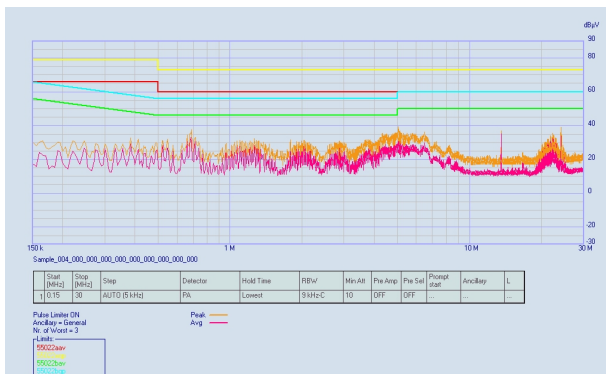


(a) Noise in Phase output

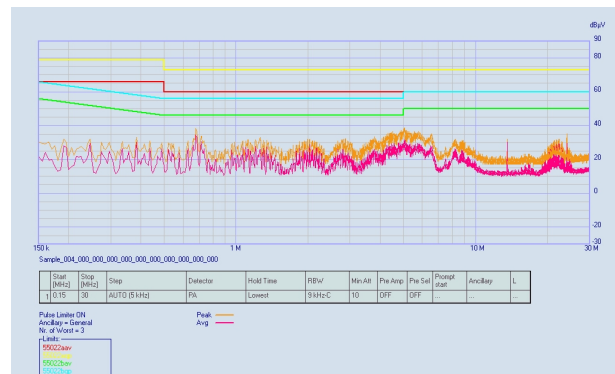


(b) Noise in Neutral output

Figure 6.16: EMC conducted noise at power outlet outside Shielded Chamber along with the EN 55022 class A and class B limits.



(a) Noise in Phase output



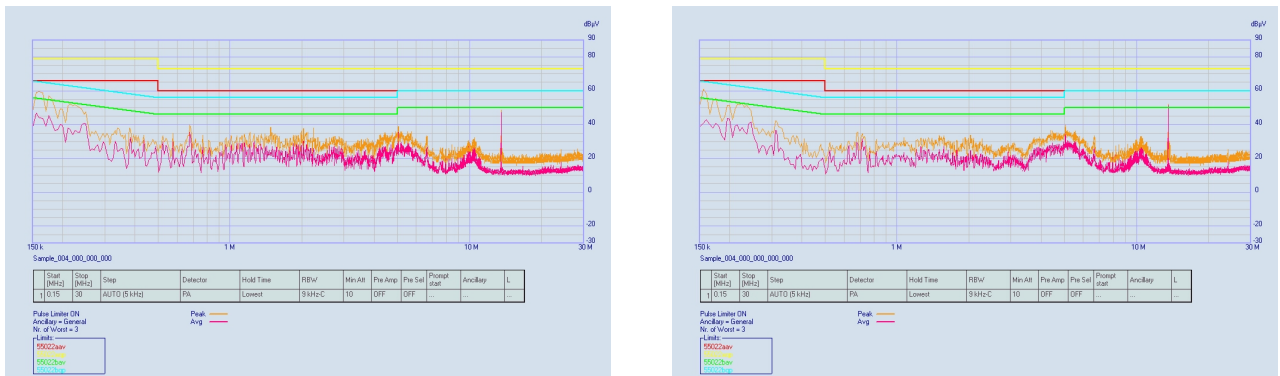
(b) Noise in Neutral output

Figure 6.17: EMC conducted noise at power outlet with filter inside Shielded Chamber along with the EN 55022 class A and class B limits.

In general, the results obtained for the Peak and Average noise conducted in the frequency range between 150 kHz and 1 MHz approach, and in some cases exceed, the CISPR 32 Class B Quasi-Peak and Average Emission limits. In the case of the outlet with filter inside the Chamber, the voltage levels observed in this range are attenuated, with an EMC conducted noise floor of approximately 20 dBµV.

Moreover, voltage peaks centered at 5 MHz, 10 MHz, 15 MHz, 22 MHz and 25 MHz were observed in all outlets for Phase and Neutral conductors. In the case of the neutral conductor of T4.2, there is an Avg and Peak maximum recordings above the 46 dB μ V CISPR-32 Class B average limit.

Therefore, due to the outlets of the same power circuit not having any equipment connected, it is inferred that there is pollution in the EMC frequency range to be injected downstream in the DEEC distribution circuits. All results obtained in LISN+I were declared credible and passive to be visualized in the spectrum analyzer.



(a) Noise in Phase output

(b) Noise in Neutral output

Figure 6.18: EMC conducted noise at power outlet in T4.2 classroom along with the EN 55022 class A and class B limits.

6.4 Chamber's Shielding Effectiveness measurement

The determination process of Chamber's Shielding Effectiveness was carried out on August 27 and 28, 2022, having the power frequency SE assessment being done on the first day and HF SE assessment made on the second. For all cases, the chamber's door was not opened in the interval between the first and the last measurement.

In the first case, the power frequency SE testing routine for the door, corner and chamber's wall was assembled, in accordance with the prescribed in subchapter 5.1. To this end, the perpendicular of the center of the coil was directed to each of the three points assessed, and different load current configurations were applied, according to the table D.2, and then comparing with the measured values at the same distance outside the chamber. The power frequency magnetic flux density was registered the Aaronia NF-5020 device, and the results were considered

from the highest value recorded within a 30s measurement period. The results of the SE as a function of the incident magnetic flux density can be found in the figure 6.19.

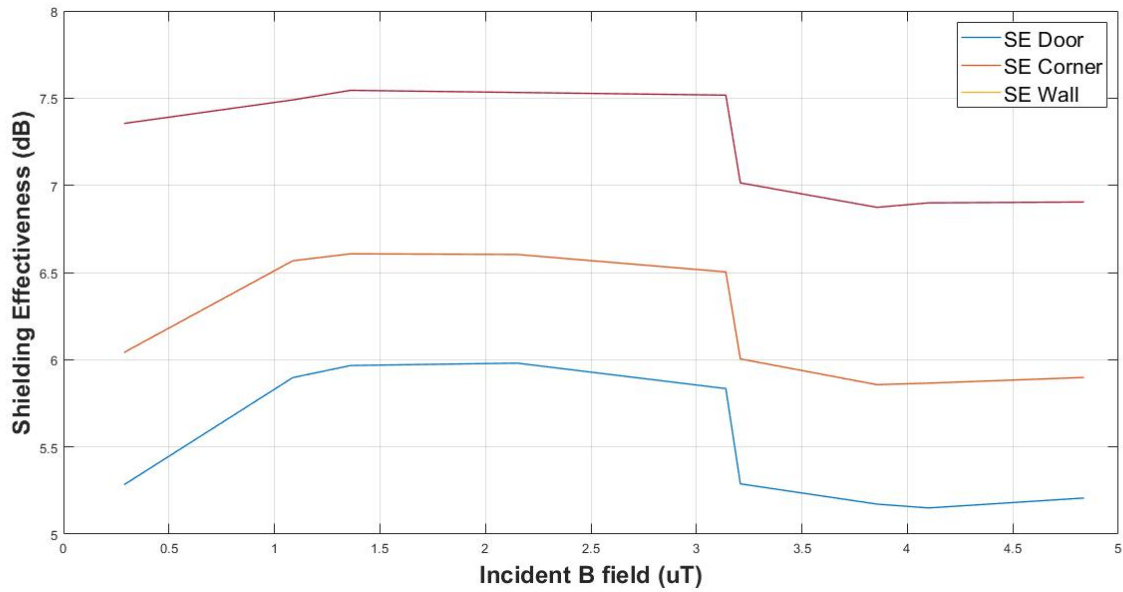


Figure 6.19: ULF Power frequency SE versus incident \vec{B} field.

Table 6.13: HF Shielding Effectiveness results per location.

Frequency (MHz)	RF signal generator power: +1 dBm			RF signal generator power: +7 dBm			RF signal generator power: +12 dBm			RF signal generator power: +15 dBm			RF signal generator power: +18 dBm		
	Without Shielding (dBm)	With Shielding (dBm)	Shielding Effectiveness (dB)	Without Shielding (dBm)	With Shielding (dBm)	Shielding Effectiveness (dB)	Without Shielding (dBm)	With Shielding (dBm)	Shielding Effectiveness (dB)	Without Shielding (dBm)	With Shielding (dBm)	Shielding Effectiveness (dB)	Without Shielding (dBm)	With Shielding (dBm)	Shielding Effectiveness (dB)
Location: Chamber's door															
200	-32.367	-49.798	17.431	-30.11	-48.63	18.52	-30.433	-49.16	18.727	-30.284	-49.294	19.01	-30.789	-47.646	16.857
450	-34.113	-69.436	35.323	-28.103	-62.63	34.527	-20.988	-57.41	36.422	-18.257	-53.581	35.324	-20.369	-52.63	32.261
900	-25	-37.098	12.08	-20	-30.502	10.21	-15	-24.995	10.14	-12	-22.512	10.29	-11	-18.246	7.73
1800	-24	-45	20.81	-20	-41	21.02	-13	-35	21.55	-12	-34	22.27	-12	-34	21.95
3000	-32	-69.584	37.83	-30	-69.604	39.49	-25	-69.658	45.06	-21	-69.631	48.88	-19	-69.606	51.02
4500	-34.618	-89	54.382	-34.08	-89.059	54.979	-28.254	-52.123	23.869	-27.123	-50.212	23.089	-27.917	-51.46	23.543
6000	-26.463	-64.05	37.587	-21.57	-57.566	35.996	-18.619	-56.478	37.859	-18.215	-56.822	38.607	-18.249	-56.898	38.649
Location: Chamber's corner															
200	-32.367	-48.81	16.443	-30.11	-49.043	18.933	-30.433	-48.122	17.689	-30.284	-47.276	16.992	-30.789	-47.691	16.902
450	-34.113	-62.218	28.105	-28.103	-53.097	24.994	-20.988	-46.428	25.44	-18.257	-43.023	24.766	-20.369	-43.322	22.953
900	-25	-80.769	55.75	-20	-80.751	60.46	-15	-80.894	66.04	-12	-80.904	68.68	-11	-80.967	70.46
1800	-24	-88	64.42	-20	-88	68.70	-13	-88	75.24	-12	-88	76.07	-12	-88	76.29
3000	-32	-69.032	37.28	-30	-69.051	38.94	-25	-69.028	44.43	-21	-69.098	48.35	-19	-69.048	50.46
4500	-34.618	-90.291	55.673	-34.08	-90.357	56.277	-28.254	-90.213	61.959	-27.123	-90.294	63.171	-27.917	-90.269	62.352
6000	-26.463	-86.891	60.428	-21.57	-87.499	65.929	-18.619	-87.334	68.715	-18.215	-85.984	67.769	-18.249	-89.58	71.331
Location: Chamber's wall															
200	-32.367	-51.206	18.839	-30.11	-50.099	19.989	-30.433	-50.448	20.015	-30.284	-50.419	20.135	-30.789	-50.282	19.493
450	-34.113	-55.211	21.098	-28.103	-49.408	21.305	-20.988	-44.209	23.221	-18.257	-41.289	23.032	-20.369	-41.651	21.282
900	-25	-80.114	55.09	-20	-79.991	59.70	-15	-80.152	65.30	-12	-80.162	67.94	-11	-80.205	69.69
1800	-24	-86.281	62.47	-20	-86.303	66.74	-13	-86.328	73.26	-12	-86.318	74.19	-12	-86.314	74.36
3000	-32	-68.672	36.92	-30	-68.713	38.60	-25	-68.653	44.05	-21	-68.736	47.99	-19	-68.709	50.12
4500	-34.618	-89.974	55.356	-34.08	-89.981	55.901	-28.254	-90	61.746	-27.123	-90.004	62.881	-27.917	-90.09	62.173
6000	-26.463	-85.565	59.102	-21.57	-81.028	59.458	-18.619	-79.305	60.686	-18.215	-78.593	60.378	-18.249	-78.796	60.547

For tests performed for high-frequency SE purposes, the reference source EMF was generated from the Aaronia BPSG5 signal generator, attached into a BicoLOG or HyperLOG antenna, where the emission power of this set was varied in a range of +1 dBm, +7 dBm, +12 dBm, +15 dBm and +18 dBm. For each one of the three points assessed, the SE was evaluated for EMF of 200 MHz, 450 MHz, 900 MHz, 1800 MHz, 3 GHz, 4.5 GHz and 6 GHz. The table 6.13 is a

summary of all high frequency SE results, as well as the figure 6.20 illustrates the minimum and maximum values, by frequency surveyed, for the door, corner and wall.

Regarding the power frequency results, there is a noticeable decay when the incident magnetic flux density is above $3 \mu T$. In addition, the door is the site with the worst SE (with a minimum of 5.2 dB), followed by the wall (minimum of 5.7 dB) and corner (minimum of 6.8 dB). This may be indicative that the door gaskets are oxidized or in bad conditions, and the chamber is not being properly electromagnetically shielded or electrically continuous. The door also has the worst maximum and minimum SE results for 900 MHz, 1800 MHz, 4.5 GHz and 6 GHz frequencies. The maximum SE of the Door at no time is more than 40 dB.

For the frequencies of 200 MHz, 450 MHz and 3 GHz, the three locations have similar values of maximum and minimum SE. For the surveyed frequencies of 900 MHz, 1800 MHz, 4500 MHz and 6 GHz, the SE results for the Wall and Corner are similar, where the maximum values of the first are slightly smaller. The largest difference is at 6 GHz, between 60.6 dB and 71 dB respectively.

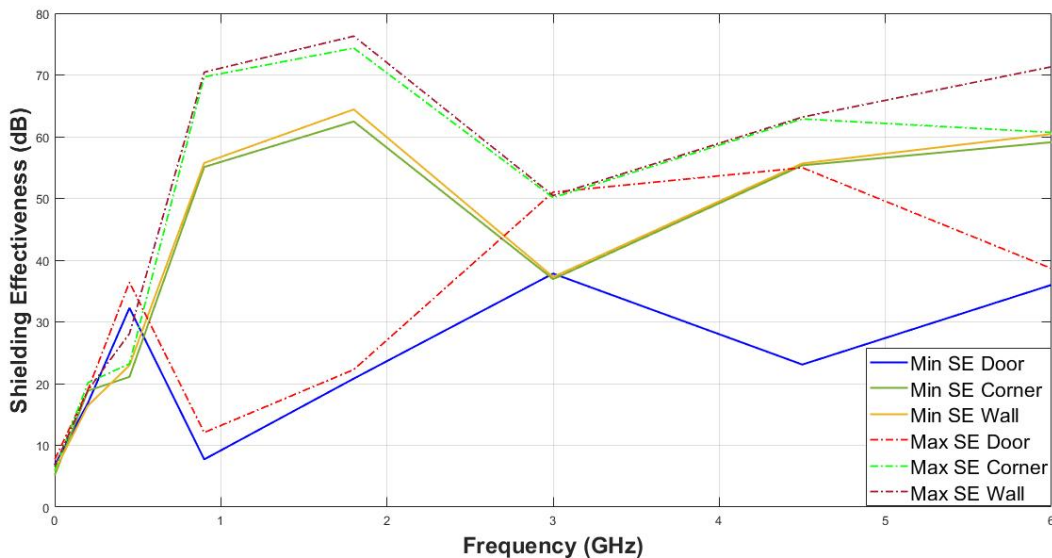


Figure 6.20: Maximum and minimum chamber's SE per frequency and location.

Finally, the trend of SE growing as higher levels of EMF incidents is not verified in some cases, as in the testing frequency at 6 GHz for the Wall and Door. Thus, it is not possible to draw conclusions about the electromagnetic saturation of the chamber shielding material.

Chapter 7

Conclusion

7.1 Conclusions

The work presented in this Dissertation was aimed to characterize the DEEC building for EMC purposes, and also to evaluate the human exposure levels of the department's population, due to the multitude of electronic equipment and the HV power line over Tower B. For these purposes, the Compatibility level concept of IEC 61000-2-5 and the guidelines of 1998 ICNIRP general-public exposure reference were used.

Only non-ionizing EMF were assessed, with measurements of electric and magnetic fields from 45 Hz to 6 GHz. For a complete characterization of this spectrum, as well as to evaluate the EMF spatial and temporal variation, a set of non-overlapping Broadband and Frequency Analysis methods were employed. All DEEC environments are below the ICNIRP guidelines of human exposure and are in conformity with the compatibility levels of IEC 61000-2-5. However, the rooms and corridors located near Tower B are above the Finnish Radiation safety Authority $0.4 \mu T$ limit mentioned in the subchapter 2.2, which raises safety concerns to the DEEC population who works in these areas.

Another conclusion is that further east and higher a certain location is, the higher are the 50 Hz magnetic induction levels observed. This is probably due to the transmission power line over Tower B. Regarding the magnetic field power frequency, the highest measurement was $1.97 \mu T$ at Tower B Terrace.

It also found a correlation factor of 0.94 between the measurements at the geometric center and at each corner of the rooms surveyed with the Five-point method. This indicates that the

measurement at the room geometric center is a good snapshot of the B-field distribution in a given environment. In the locations with a long length or with electrical distribution boards, however, there is a greater dispersion of measurements.

Regarding the power frequency electric fields, all majorant E-field measurements have intensity below 5 V/m, except for the external measurement in the outside of the main entrance of the department, with a majorant E-field of 36.2 V/m.

The graphical interpolation representation obtained from data measured in the Five-point method, was compared with the more traditional technique of Mapping and produced reliable and easily visible results. In this way, the five point interpolation is a robust alternative for an easy and fast representation of ULF B-field in a given environment, being also effective in showing trends from external sources and the influence of distribution board in magnetic induction.

The HF frequency sweep results also indicate that there is a clear spectrum signature in the department, common for all environments surveyed, although higher levels have been found in the external spots. The maximum EEF is 1.74 V/m, found at DEI promenade. In addition, the occupation of the spectrum basically consists on telecommunications transmission bands, with the highest values of electric fields being found in the GSM900 and 4G bands. However, there is an intense triangular signal, with a 97 dB/m peak centered on the frequency of 4 GHz, whose source is unknown.

For both Broadband Measurements and Frequency Sweeps, there was a temporal variation recorded in the electromagnetic fields surveyed. The Dynamic Range factor shows a 2 dB variation for power frequency magnetic fields, and approximately a 10 dB variation for high-frequency electric fields.

In addition, the projected LISN+I device was able to produce credible results of EMC conducted noise in a spectrum analyzer. Measuring at different power outlets around DEEC, there is a clear indication of peak and average values, in the frequency ranges of 150 kHz-1 MHz and 15 MHz-30 MHz, whose magnitude is higher than the CISPR-32 Class B limits for Quasi-peak and Average detectors. In this way, there is EMC conducted disturbance injected downstream in the DEEC distribution circuits, whose influence should be thoroughly investigated. It is intended to publish this study in an EMC journal or conference in 2022.

Finally, the measurement of the Shielded Chamber's SE, according to the adapted guidelines of IEEE 299-2006 standard, indicates low levels of shielding for power frequency magnetic fields,

with a maximum of 7.5 dB. There is a noticeable improvement in performance for incident HF EMF, notoriously those above 450 MHz. The maximum SE measured was 76.3 dB, obtained in the Chamber's corner at 1800 MHz. It is not possible to obtain conclusions regarding the saturation of the chamber shielding material.

Among the three measured chamber locations, the door is the one with the lowest SE for all frequencies surveyed. This may indicate that the gaskets are not performing properly and may require maintenance or replacement.

7.2 Future Work

For a more comprehensive assessment of electric fields in the department, it is recommended to acquire LF and HF E-electric broadband probes, today non-existent in the EMC laboratory. Also investigate how ULF magnetic induction and electric fields behave in the underground parking lot, according to the charge and discharge cycles of the batteries attached to the inverters.

Furthermore, the Long-range temporal variation Survey should be performed in winter, to assess temporal variation in different building occupancy and climate regimes. If the transmission line power flows data are available, verify the correlation between these and the temporal variation.

Regarding the built LISN+I, characterize its high pass filter, aiming at other applications for such equipment. And subsequently carry out a more exhaustive research on the source of EMC conducted noise in DEEC electric circuits.

Lastly, performing Crosstalk studies in the corridors. For this, intentional sources of disturbance must be inserted to the principle of these, investigating the levels of susceptibility of the accessible rooms. As well as the attenuation and reflection factors between successive floors due to the constructive materials used in the facilities[35, 36].

References

- [1] T. Williams. *EMC for Product Designers*. Elsevier Science/Newnes, 5th edition, 2016. 1.1, 2, 2
- [2] European Parliament and Council of European Union. Directive 2014/30/EU of the European Parliament and of the Council, of 26 february 2014, on the harmonisation of the laws of the Member States relating to electromagnetic compatibility, 3 2014. 1.1, 2, 2, 2.1
- [3] V. Rajamani, C. Bunting, and G. Freyer. Why consider EMC testing in a reverberation chamber. In *2008 10th International Conference on Electromagnetic Interference Compatibility*, pages 303–308, 2008. 1.1, 5
- [4] Z. Sienkiewicz. Biological effects of electromagnetic fields and radiation. *Journal of Radiological Protection*, 18(3):185–193, Sep 1998. 1.1
- [5] A. Vorst, A. Rosen, and Y. Kosuka. *RF/Microwave Interaction with Biological Tissues*. Wiley-IEEE Press, first edition, Jan 2006. 1.1, 2.2
- [6] ICNIRP guidelines for limiting exposure to time-varying electric, magnetic and electromagnetic fields (up to 300ghz). *Health Physics*, 74(3):494–525, Apr 1998. 1.1, 2, 2.2, 2.3, 2.4, 3.1.3, 3.2.1, 3.2.3
- [7] R. Stam. Comparison of international policies on electromagnetic fields. Technical report, Dutch National Institute for Public Health and the Environment, Jan 2018. 1.1, 2.2, 2.2
- [8] United States National Cancer Institute. Electromagnetic fields and cancer, May 2022. 1.1
- [9] D. Kljajic and N. Djuric. Comparative analysis of EMF monitoring campaigns in the campus area of the university of Novi Sad. *Environmental Science and Pollution Research*, 27(13):14735–14750, Feb 2020. 1.1, 3, 3.1.1, 3.2.1

- [10] World Health Organization. *WHO Research Agenda for Radiofrequency Fields*. WHO Library Cataloguing-in-Publication Data, 2010. 1.1
- [11] M. Feychting. Non-cancer EMF effects related to children. *Bioelectromagnetics*, 26(S7):S69–S74, 2005. 1.1
- [12] P. Bienkowski. Electromagnetic fields measurements – Methods and accuracy estimation. *Studies in Applied Electromagnetics and Mechanics*, 29:229 – 237, October 2002. 1.1
- [13] P. Bienkowski. Interlaboratory comparisons in EMF survey measurements. *The Environmentalist*, 29(2):130–134, Feb 2009. 1.1, 3.1.1
- [14] D. Amaripadath, R. Roche, L. Joseph-Auguste, D. Istrate, D. Fortune, J.P. Braun, and F. Gao. Measurement and analysis of supraharmonic emissions in smart grids. In *2019 54th International Universities Power Engineering Conference (UPEC)*. IEEE, Sep 2019. 1.1
- [15] B. Jaekel, A. Ogunsola, and L. Sandrolini. Recent development regarding IEC 61000-2-5, description and classification of electromagnetic environments. In *International Symposium on Electromagnetic Compatibility, EMC'09 Kyoto*, pages 813–816, 2009. 1.1, 2.1, 2.2
- [16] S.M. Malta, J.C.M. Sales, M.I. Martins, and A.O. Rodrigues. Medição de blindagem eletromagnética adaptada a realidade dos laboratórios. *Exacta*, 1:1–10, 2008. 1.1, 5, 5, 5.1, 5.1, 5.1, 5.1
- [17] Aaronia AG. Manual SPECTRAN V4. techreport, Aaronia AG, Strickscheid, Germany, 2013. 2, 2, 3, 3.1.1, 3.1.2, 3.1.2, 3.4, 3.1.2, 3.2.1, 3.2.1, 3.2.4, 3.2.4, 5.1
- [18] J. Shepard. EMI, EMC, EMS, and the ITU, Jun 2020. Accessed: 2022-08-25. 2, 2.1
- [19] M. Kaur, S. Kakar, and D. Mandal. Electromagnetic interference. In *2011 3rd International Conference on Electronics Computer Technology*, volume 4, pages 1–5, 2011. 2
- [20] D. Hoolihan. CISPR 32: New international standard on electromagnetic emissions from multimedia equipment. In *EMC DIRECTORY DESIGN GUIDE*, pages 1–5. Interference Technology, 2012. 2
- [21] B. Jaekel. Electromagnetic environments - phenomena, classification, compatibility and immunity levels. In *IEEE EUROCON 2009*, pages 1498–1502, 2009. 2.1

- [22] Technical Committee 77. IEC 61000-2-5 environment : Description and classification of electromagnetic environments. Technical report, International Electrotechnical Commission, 2017. 2.1
- [23] P. Lyttkens. Electromagnetic field and neurological disorders. alzheimer’s disease, why the problem is difficult and how to solve it. Master’s thesis, Uppsala University, Uppsala, Sweden, 2018. 2.2
- [24] A. Balaji. Effect of High voltage transmission lines on human health, plant life, and animal activity. volume 56. International Research Journal of Engineering and Technology, Jun 2015. 2.2
- [25] IEEE International Committee on Electromagnetic Safety. IEEE recommended practice for measurements and computations of radio frequency electromagnetic fields with respect to human exposure to such fields, 100 kHz 300 GHz. Technical report, IEEE, New York, United States of America, 2008. 2.2, 3.1.2, 3.1.2, 3.1.2, 3.2.2, 3.2.3, 3.2.4
- [26] Y. W. Weldu, M. Mannan, and S. G. Al-Ghamdi. Monitoring electromagnetic radiation emissions in buildings and developing strategies for improved indoor environmental quality. *Health Physics*, 117(6):648–655, jul 2019. 2.2
- [27] EMFs.info. Limits in the rest of the world. Exposure limits country by country., Jun 2022. Accessed: 2022-08-24. 2.2, 2.2
- [28] Lennart Hardell and Cindy Sage. Biological effects from electromagnetic field exposure and public exposure standards. *Biomedicine & Pharmacotherapy*, 62(2):104–109, Feb 2008. 2.2
- [29] M. Misakian, G.K. Bell, T.D. Bracken, L.H. Fink, K.C. Holte, J.E. Hudson, G.B. Johnson, T.J. McDermott, R.C. Mukherji, R.G. Olsen, G.B. Rauch, S.A. Sebo, J.M. Silva, and P.S. Wong. A protocol for spot measurements of residential power frequency magnetic fields. *IEEE Transactions on Power Delivery*, 8:1386–1394, 7 1993. 3, 3, 3.1.1, 3.1.3, 3.2.2
- [30] M. G. Yost, G. M. Lee, D. Duane, J. Fisch, and R. R. Neutra. California protocol for measuring 60 Hz magnetic fields in residences. *Applied Occupational and Environmental Hygiene*, 7(11):772–777, Nov 1992. 3, 3.1.1, 3.1.1

- [31] J. Vehmaskoski, M. Suojanen, S. Kuusiluoma, P. Trygg, T. Keikko, and L. Korpinen. Measurement of power frequency magnetic fields in buildings from EMC point of view. In *PowerCon 2000. 2000 International Conference on Power System Technology. Proceedings (Cat. No.00EX409)*, pages 1377–1381. IEEE, 8 2000. 3.1.1, 3.1.3
- [32] IEEE International Committee on Electromagnetic Safety. IEEE standard for safety levels with respect to human exposure to electric, magnetic, and electromagnetic fields, 0 hz to 300 GHz. Technical report, The Institute of Electrical and Electronics Engineers, Inc., New York, United States, 2019. 3.1.1, 3.3
- [33] P. Bienkowski and H. Trzaska. Interlaboratory comparisons in emf survey measurement - methods and results. *International Conference and COST 281 Workshop on Emerging EMF Technologies*, 29(2):130–134, Apr 2006. 3.1.1
- [34] J Vehmaskoski, M Suojanen, S Kuusiluoma, P Trygg, T Keikko, and L Korpinen. Measurement of power frequency magnetic fields in buildings from emc point of view. *Power System Technology*, pages 1377–1381, 8 2000. 3.2
- [35] D. Davis, B. Segal, A. Cinquino, K. Hoege, R. Mastrocola, and T. Pavlasek. Electromagnetic compatibility in hospital corridors. In *1999 IEEE International Symposium on Electromagnetic Compatibility. Symposium Record*, volume 1, pages 268–272. Institute of Electrical and Electronics Engineers Inc., 1999. 3.1.1, 7.2
- [36] D. Davis, B. Segal, C. W. Trueman, R. Calzadilla, and T. Pavlasek. Measurement of indoor propagation at 850 MHz and 1.9 GHz in hospital corridors. In *2000 IEEE-APS Conference on Antennas and Propagation for Wireless Communications (Cat. No.00EX380)*, pages 77–80. Institute of Electrical and Electronics Engineers Inc., 2000. 3.1.1, 7.2
- [37] P. Vlach, B. Segal, J. Lebel, and T. Pavlasek. Cross-floor signal propagation inside a contemporary ferro-concrete building at 434, 862, and 1705 MHz. *IEEE Transactions on Antennas and Propagation*, 47:1230–1232, 1999. 3.1.1
- [38] EFM Company. EFM160 power frequency electric field sensor application notes. Technical report, EFM Company, W. Stockbridge, Massachusetts, United States, 2003. 3.1.2, 3.1.2
- [39] I. Souza and L. Gamberini. Análise dos níveis de radiação não ionizante em diferentes ambientes na faixa de 100 kHz até 3 GHz. Niterói, Brazil, Universidade Federal Fluminense, July 2018. 3.1.3

- [40] T.A. Richard, A.P. Coimbra, and F. R. Antunes. Low frequency electromagnetic fields in power transformer rooms. In *9th Spanish-Portuguese Congress on Electrical Engineering*, 2005. 3.1.3
- [41] Associação Brasileira de Compatibilidade Eletromagnética. Medição dos níveis de radiações não ionizantes emitidas pelas estações rádio base de telefonia celular que se sujeita a população da cidade de Campinas. Technical report, ABRICEM, May 1994. 3.2.1
- [42] M. Shalaby, M. Shokair, and N. W. Messiha. Electromagnetic field measurement instruments: Survey. *Iranian Journal of Science and Technology, Transactions of Electrical Engineering*, 43(S1):1–14, Aug 2018. 3.2.1, 3.2.1
- [43] P. Slobodyanyuk and V. Blagodarnyy. Monitoring of the electromagnetic environment by distributed spectrum monitoring system in Ukraine. In *10th International Symposium on Electromagnetic Compatibility*, pages 796–800, 9 2011. 3.2.1
- [44] O. Genç, M. Bayrak, and E. Yaldız. Analysis of the effects of gsm bands to the electromagnetic pollution in the RF spectrum. *Progress In Electromagnetics Research, PIER*, 101:17–32, 2010. 3.2.1, 3.2.1
- [45] P. Boisvert. The ambient electromagnetic environment in metropolitan hospitals. Master’s thesis, McGill University, Montreal, Canada, May 1991. 3.2.1
- [46] UNIKLINIK RWTH Aachen. Sources of EMF. Accessed in 24.09.2022. 3.2.1
- [47] L. Verloock, W. Joseph, F. Goeminne, L. Martens, M. Verlaek, and K. Constandt. Temporal 24-hour assessment of radio frequency exposure in schools and homes. *Measurement*, 56:50–57, 2014. 3.2.2
- [48] NARDA Safety Test Solutions. Applications for spatial averaging complying with EN 50492 - technical note 11. Technical report, NARDA. 3.2.3, 3.7
- [49] D. Pereira. Design and implementation of a lisen for measuring conducted emissions. Master’s thesis, University of Coimbra, Coimbra, Portugal, 2016. 4, 4.1, 4, 4
- [50] C. Vitek R. A. McConnell. Calibration of fully anechoic rooms and correlation with OATS measurements, 1996. 5.1

- [51] IEEE Electromagnetic Compatibility Society. IEEE std 299-2006 standard method for measuring the effectiveness of electromagnetic shielding enclosures. Technical report, New York, United States of America, 2 2006. 5, 5.1, 5.1, 5.1

Appendix A

IEC 61000-2-5 overview of compatibility levels, disturbance degrees and levels for location classes

Tables A.1 to A.10 represent the maximum compatibility levels for each disturbance Degree at their respective frequency range and physical quantity. With the exception of the table A.3, which shows the disturbances degree per physical phenomenon for the commercial/public location class. Table A.11 shows all eight types of Location class cited in IEC 61000-2-5.

Table A.1: Disturbance degrees and maximum compatibility levels for LF magnetic fields at various frequencies

Disturbance Degree	DC	50Hz/60Hz POW freq	POW harmonics	POW not related
1	3	3	$3/n$	0.015
2	10	10	$10/n$	0.05
3	30	30	$30/n$	0.15
4	100	100	$100/n$	0.5

NOTE: n is the order of the harmonic. Values in A/m. RMS for AC

For overhead lines, measured at 1 m above ground.

For household or commercial environments, measured at 0.3m from the source.

Table A.2: Disturbance degrees and maximum compatibility levels for LF electric fields

Disturbance Degree	DC lines	50 Hz/60 Hz POW frequency
	Disturbance levels	
1	0.1	≤ 0.1
2	1	≤ 1
3	10	≤ 10
4	20	≤ 20

NOTE: Values in kV/m. RMS for AC.
 For overhead lines, measured at 1 m above ground.
 For household or commercial environments, measured at 0.3 m from the source.

Table A.3: Disturbance degrees in the commercial/public location class

	Phenomenon	Enclosure	AC power	Signal
LF - radiated	Magnetic Fields	2	-	-
LF - radiated	Electric Fields	1	-	-
HF - conducted	Induced Continuous Wave	-	3	3
HF - conducted	Medium Frequency	-	2	1
HF - conducted	High Frequency	-	2	1
HF - radiated	Mobile units of phones	4	-	-
HF - radiated	External Radio and Base stations of phones	3	-	-
HF - radiated	Other RF services	5	-	-

Table A.4: Disturbance degrees and maximum compatibility levels of induced CW conducted voltages with GND reference

Disturbance Degree	10 kHz to 150 MHz	
	V	mA
1	0.3	0.7
2	1	7
3	3	21
4	10	70
5	30	210

NOTE: Values in RMS

Table A.5: Disturbance degrees and maximum compatibility levels for conducted oscillatory transients in LV AC power systems

Disturbance Degrees	Building response to impulsive disturbances	Local system response to impulsive disturbances
	Disturbance levels of Oscillatory transients frequency range	
	Medium Frequency 5 kHz to 500 kHz	High Frequency 0.5 MHz to 30 MHz
	Rise time: 0.5 μs Duration time: 20 μs	Rise time: 5 ns to 50 ns Rise time: 0.5 ns to 5 ns
	Occasional	Frequent
1	1 kV	0.5 kV
2	2 kV	1 kV
3	4 kV	2 kV
4	6 kV	4 kV

NOTE: Values shown are open-circuit voltages for 120 V to 690 V RMS power systems. They reflect the external origin and the coupling mechanisms of these transients, which are which are essentially independent of the system voltage.

Table A.6: Disturbance degrees, maximum compatibility levels for HF RF wideband devices and distance to source

Disturbance Degrees and Corresponding Fields	WDTS and HIPERLAN	WDTS and HIPERLAN	WDTS and HIPERLAN
	P=0.1W _{ERP}	P=0.2W _{ERP}	P=1W _{ERP}
	Transmitter frequencies [GHz]		
	2.4-2.4835	5.15-5.35	5.47-5.715
	Distance to source [m]		
1 and 0.3 V/m	58	83	183
2 and 1 V/m	17	24	55
3 and 3 V/m	5.8	8.2	18
4 and 10 V/m	1.7	2.5	5.5
5 and 30 V/m	0.58	0.82	1.8

Table A.7: Disturbance degrees, maximum compatibility levels for HF RF terminal wideband devices and distance to source.

Disturbance Degrees and Corresponding Fields	WDTS	WDTS	WDTS
	and	and	and
	HIPERLAN	HIPERLAN	HIPERLAN
	Terminal	Terminal	Terminal
	$P=0.1W_{ERP}$	$P=0.2W_{ERP}$	$P=1W_{ERP}$
Transmitter frequencies [GHz]			
	2.4-2.4835	5.15-5.35	5.47-5.715
Distance to source [m]			
1 and 0.3 V/m	7.4	10	23
2 and 1 V/m	2.2	3	7
3 and 3 V/m	0.74	1	2.3
4 and 10 V/m	0.22	0.3	0.7
5 and 30 V/m	0.074	0.1	0.23

Table A.8: Disturbance degrees, maximum compatibility levels for Base stations and distance to source

Disturbance degrees and and corresponding fields	GSM	DECT	DCS1800	3G/UMTS	3.5G/HSPA	4G/LTE-A
	$P=320W$	$P=0.25W$	$P=0.2kW$	$P=0.4kW$	$P=20W$	$P=10W$
	Transmitter frequencies [MHz]					
	935-960	1880-1960	1805-1880	761-862	1749.9-1784.9	2570-2620
	Distance to source [m]					
1 and 0.3 V/m	2060	57	1630	2304	515	364
2 and 1 V/m	620	17	490	691	154	109
3 and 3 V/m	206	5.7	163	230	51.5	36
4 and 10 V/m	62	1.7	49	69	15.4	10.9
5 and 30 V/m	21	0.57	16	23	5.15	3.6
6 and 100 V/m	6.5	0.17	4.9	6.9	1.54	1.08

NOTE: Power transmission values in Effective Radiated Power

Table A.9: Disturbance degrees, levels for Mobile and portable phones and distance to source

Disturbance degrees and and corresponding fields	GSM	DECT	DCS1800	3G/UMTS	3.5G/HSPA	4G/LTE-A
	P=2W	P=0.25W	P=4W	P=126mW	P=251mW	P=200mW
	Transmitter frequencies [MHz]					
	935-960	1880-1960	1805-1880	761-862	1749.9-1784.9	2570-2620
	Distance to source [m]					
1 and 0.3 V/m	104	12	47	8.3	12	10
2 and 1 V/m	31	3.5	14	2.5	3.5	3.1
3 and 3 V/m	10.5	1.2	4.7	0.83	1.2	1
4 and 10 V/m	3.2	0.35	1.4	0.24	0.34	0.29
5 and 30 V/m	1.1	0.12	0.47	0.073	0.1	0.11
6 and 100 V/m	0.31	0.031	0.14	0.044	0.047	0.067

Table A.10: Disturbance degrees, maximum compatibility levels for HF radiated electric fields and distance to source

Disturbance Degrees and Field Corresponding	FM	DTV	DTV	Non-specific
	Broadcast	VHF	UHF	short range equip.
	$P = 100kW$	$P = 10kW_{ERP}$	$P = 120kW_{ERP}$	$P = 25mW_{PEP}$
	Transmitter frequencies [GHz]			
	76-108	174-202	470-862	2.400-2.4835/5.725-5.875
	Distance to source [m]			
1 and 0.3 V/m	7390	58	200	129
2 and 1 V/m	2216	17	60	38.5
3 and 3 V/m	39	5.8	20	12.9
4 and 10 V/m	221.6	17.3	6	3.85
5 and 30 V/m	73.9	5.8	2	1.29
6 and 100 V/m	-	1.73	0.59	-

Table A.11: Types of Location Classes

Location class type	
1	Residential-rural location
2	Residential-urban location
3	Commercial location (including densely populated public areas)
4	Light industrial location
5	Heavy industrial location
6	Traffic area
7	Telecommunication centre
8	Hospital

Appendix B

ICNIRP reference levels for general-public exposure to time-varying EMF

Table B.1: ICNIRP reference levels for general-public exposure to time-varying EMF.

Frequency range	E-field strength	H-field strength	B-field	EPW power density Seq
Up to 1 Hz	—	$3.2 * 10^4$	$4 * 10^4$	—
1-8 Hz	10000	$3.2 * 10^4 / f^2$	$4 * 10^4 / f^2$	—
8-25 Hz	10000	$4000 / f$	$5000 / f$	—
25-800 Hz	$250000 / f$	$4000 / f$	$5000 / f$	—
0.8-3 kHz	$250000 / f$	5	6.25	—
3-150 kHz	87	5	6.25	—
0.15-1 MHz	87	$0.73 / f$	$0.92 / f$	—
1-10 MHz	$87000 / \sqrt{f}$	$0.73 / f$	$0.92 / f$	—
10-400 MHz	28	0.073	0.092	2
0.4-2 GHz	$13750\sqrt{f}$	$0.0037\sqrt{f}$	$0.0046\sqrt{f}$	$f/200$
2-300 GHz	61	0.16	0.45	10

Appendix C

EMF radiated survey equipment characteristic and additional results

Parametros característicos dos Aparelhos: Frequency Range, Measurement Range, Linearity and Frequency Sensitivity

Table C.1: Aaronia SPECTRAN NF-5020 Spectrum Analyzer

Frequency Range	Typ. E-field level range	Typ. B-field level range	Lowest Sampletime	Accuracy	Magnetic Axis	Electric Axis
1Hz to 1MHz	0.1 V/m to 5k V/m	1 pT to 500 T	1ms	Typ. 3%	X/Y/Z	X

Table C.2: Aaronia SPECTRAN HF-6060V4 Spectrum Analyzer

Frequency Range	Min Power at RF input	Max Power at RF input	Lowest Sampletime	Accuracy
10MHz to 6GHz	-135dBm	+50dBm	1ms	$\pm 2dBm$

Table C.3: SYPRIS 4080 ELF handheld meter characteristic

Frequency response	Measurement Range	Sampling Interval	Measurement Type	Accuracy Error	Directionality Error	Overall Error
25 Hz-1 kHz	0.1 mG-511 mG	0.4s	True RMS	2% typ.	1% typ.	$\pm 5\%$

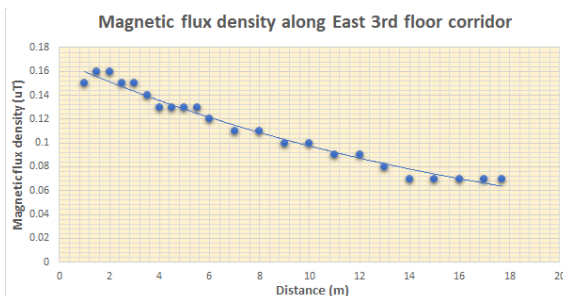
Table C.4: EFM 160 Power Frequency Electric Field Sensor

Frequency response	Measurement Range	Measurement Type	Input Impedance
15 Hz-20kHz	0.1 V/m-750 V/m	True RMS	1MΩ – 15pF

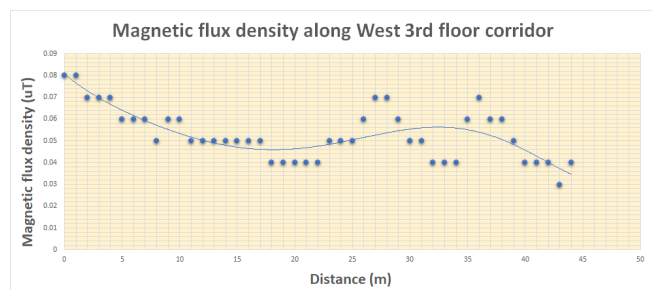
Table C.5: Electric field survey at power frequency at different locations with EFM160 and Aaronia NF5020.

Date	Time	Equipment	Axis X			Axis Y			Axis Z			Equivalent Majorant Electric Field (EMEF)		
			Min (V/m)	Avg (V/m)	Max (V/m)	Min (V/m)	Avg (V/m)	Max (V/m)	Min (V/m)	Avg (V/m)	Max (V/m)	Min (V/m)	Avg (V/m)	Max (V/m)
Location: Bar. Measured at the geometrical center														
19/07/2022	18:00	EFM 160	0.89	0.94	1.00	0.89	1.33	1.78	1.00	1.56	2.11	1.61	2.26	2.94
02/08/2022	12:15	NF-5020	-	-	2.78	-	-	2.58	-	-	2.67	-	-	4.64
25/08/2022	17:40	NF-5020	-	-	2.71	-	-	2.45	-	-	2.29	-	-	4.32
Location: Terrace 4th floor. Measured 3m away from Bar's entrance, centered on the perspective of the door														
19/07/2022	18:10	EFM 160	1.33	1.61	1.89	1.00	1.61	2.22	0.89	1.33	1.78	1.89	2.64	3.42
02/08/2022	12:25	NF-5020	-	-	3.10	-	-	2.76	-	-	1.79	-	-	4.52
25/08/2022	17:50	NF-5020	-	-	2.78	-	-	2.80	-	-	2.86	-	-	4.87
Location: Entrance Atrium. Measured at the geometrical center														
19/07/2022	18:20	EFM 160	0.00	0.39	0.78	0.00	0.33	0.67	0.00	0.39	0.78	0.00	0.64	1.29
02/08/2022	12:30	NF-5020	-	-	1.28	-	-	1.42	-	-	1.39	-	-	2.37
25/08/2022	18:00	NF-5020	-	-	2.52	-	-	2.37	-	-	2.22	-	-	4.11
Location: 3A Corridor. Measured 1m from the eastend of corridor 3A														
19/07/2022	18:50	EFM 160	0.11	0.22	0.33	0.67	1.17	1.67	1.11	1.50	1.89	1.30	1.91	2.54
02/08/2022	12:50	NF-5020	-	-	2.95	-	-	2.31	-	-	2.89	-	-	4.73
25/08/2022	18:30	NF-5020	-	-	2.80	-	-	2.41	-	-	3.24	-	-	4.91
Location: East Terrace. Measured at the geometrical center														
19/07/2022	18:40	EFM 160	0.00	0.44	0.89	0.11	0.56	1.00	0.78	0.89	1.00	0.79	1.14	1.67
02/08/2022	12:50	NF-5020	-	-	1.21	-	-	1.62	-	-	1.67	-	-	2.63
25/08/2022	18:20	NF-5020	-	-	3.86	-	-	3.21	-	-	2.76	-	-	5.73
Location: DEEC's main entrance - Outdoor. Measured 3m away from DEEC's main Entrance, centered on the perspective of the door														
19/07/2022	18:30	EFM 160	23.89	24.33	24.78	22.11	22.33	22.56	11.89	12.78	13.67	34.65	35.41	36.19
02/08/2022	12:40	NF-5020	-	-	29.33	-	-	39.68	-	-	17.87	-	-	52.48
25/08/2022	18:10	NF-5020	-	-	28.26	-	-	36.44	-	-	7.86	-	-	46.78
Location: R1.2 Laboratory. Measured at the geometrical center.														
19/07/2022	19:00	EFM 160	0.00	0.11	0.22	0.00	0.11	0.22	0.78	0.83	0.89	0.78	0.85	0.94
02/08/2022	12:25	NF-5020	-	-	3.73	-	-	4.23	-	-	3.38	-	-	6.57
02/08/2022	17:50	NF-5020	-	-	1.49	-	-	1.62	-	-	1.79	-	-	2.84
25/08/2022	17:50	NF-5020	-	-	5.39	-	-	4.09	-	-	3.50	-	-	7.62
Location: Tower R Terrace. Measured at the geometrical center.														
25/08/2022	17:30	NF-5020	-	-	5.62	-	-	5.64	-	-	5.40	-	-	9.62

Additional information: All measurements were taken 1m above the ground



(a) East Third Floor corridor chart.



(b) West Third Floor corridor chart.

Figure C.1: Magnetic field density obtained in the survey along the East and West Third Floor corridors.

Table C.6: Five-point method measurements summary

Location	Min(uT)	Max(uT)	SEMONT _{MIN}	SEMONT _{MAX}	X _{AVG}	$\delta 1(\%)$	$\delta 2(\%)$
Entrance Atrium	0.04	0.15	1.00E-04	3.20E-03	0.88	4.95	11.43
3A.23 Office	0.22	0.48	2.40E-03	7.68E-02	2.53	4.32	11.88
2 nd West Terrace	0	0.02	1.00E-04	3.20E-03	0.09	28.86	66.66
2 nd East Terrace	0.01	0.03	1.50E-04	4.80E-03	0.21	22.37	48.57
2 nd floor corridor	0.01	0.13	5.50E-04	1.76E-02	1.10	0	0
3 rd floor East corridor	0.11	0.34	1.70E-03	5.44E-02	1.55	7.21	19.35
3A floor East corridor	0.12	0.77	3.85E-03	1.23E-01	2.18	8.83	22.99
3 rd floor East Study Aisle	0.02	0.05	2.50E-04	8.00E-03	0.28	16.28	37.61
3 rd floor West Study Aisle	0	0.03	1.50E-04	4.80E-03	0.11	17.32	40
Bar	0.05	0.32	1.60E-03	5.12E-02	0.69	8.68	23.11
T4.2	0.02	0.11	1.00E-04	3.20E-03	0.10	0	0
4 th floor East corridor	0.03	0.41	2.05E-03	6.56E-02	1.83	8.10	21.92
4 th floor West corridor	0	0.09	4.50E-04	1.44E-02	0.2	0.0	0.0
S5.4	0.01	0.01	5.00E-05	1.60E-03	0.1	0	0
S6.4	0.03	0.05	2.50E-04	8.00E-03	0.38	11.55	26.66
NEEC	0	0.13	6.50E-04	2.08E-02	0.05	100	200
R5.2 Lab	0	0.14	2.00E-04	6.40E-03	0.1	0	0
Tower B Roof - Indoor	0	0.04	2.00E-04	6.40E-03	0.3	0	0
Tower B Roof - Outdoor	0.27	1.97	9.85E-03	3.15E-01	17.28	21.42	31.88
Shielded Chamber	0	0	0	0	-	-	-
Parking - Inverters zone	0.01	0.03	1.50E-04	4.80E-03	0.1	0	0
Electric vehicle parking lot	0.02	0.1	5.00E-04	1.60E-02	0.38	12.35	27.37
Parking - Power Station Room	0.03	0.09	1.95E-03	6.24E-02	0.51	12.17	33.02
Tower A 6 th floor Study Room	0.09	0.72	5.00E-04	1.60E-02	0.425	19.51	47.06
R1.2	0	0.02	1.00E-04	3.20E-03	0.09	55.27	133.33
Tower B Study Room	0.03	0.1	3.60E-03	1.15E-01	6.63	7.34	19.62
DEEC's Secretary	0.12	0.28	1.40E-03	4.48E-02	1.4	0	0
Tower R 6 th floor Terrace	0.01	0.02	1.00E-04	3.20E-03	0.13	34.64	80

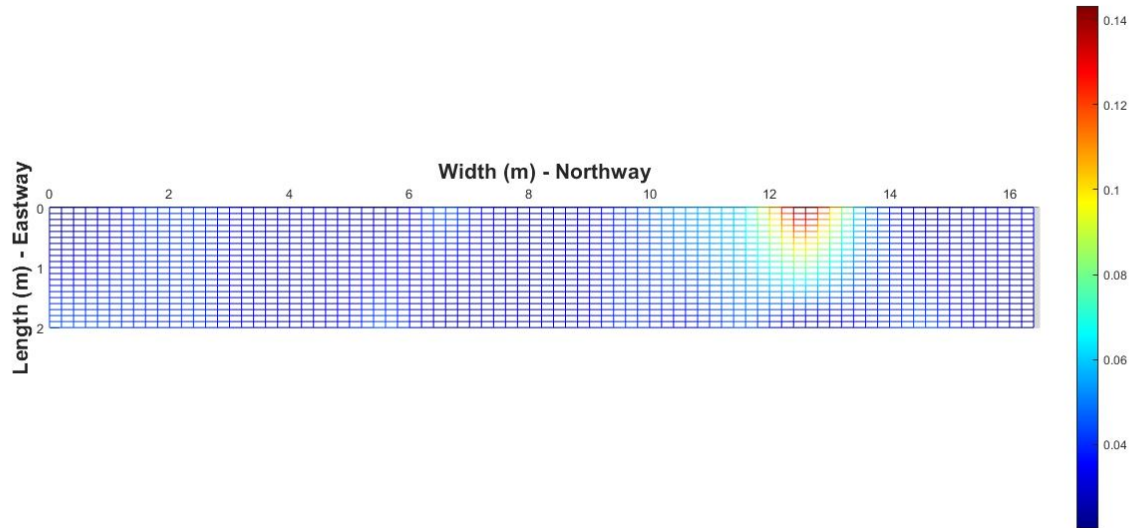


Figure C.2: 28-point Mapping grid in Bar's lateral

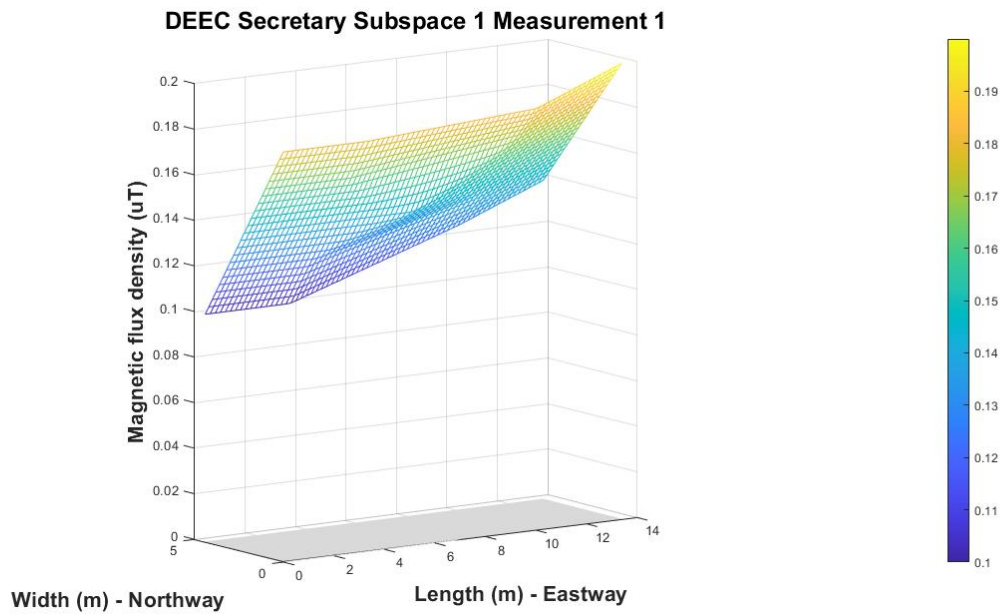


Figure C.3: Power frequency B-field interpolation and extrapolation at the Secretary first subspace.

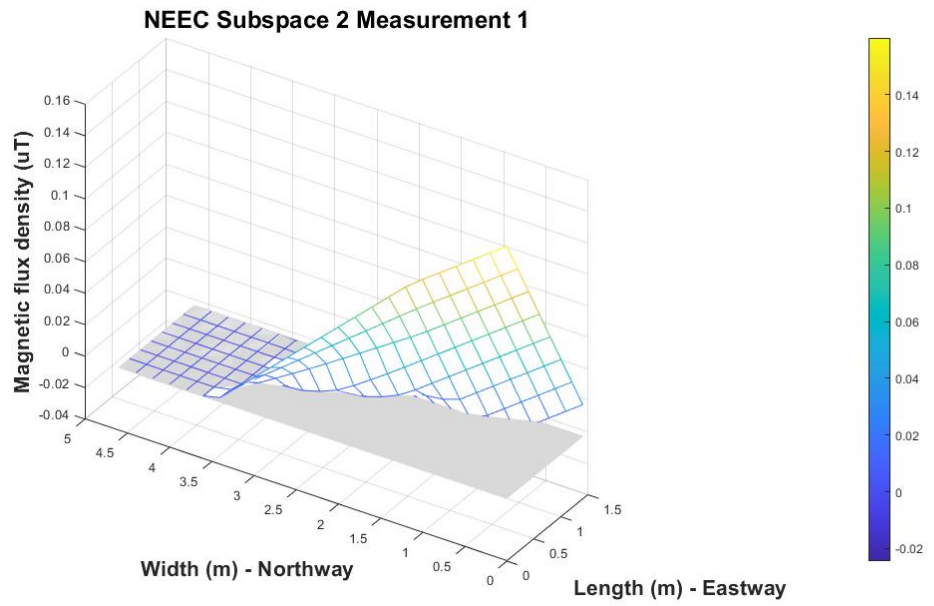


Figure C.4: Power frequency B-field interpolation and extrapolation at the NEEC second subspace.

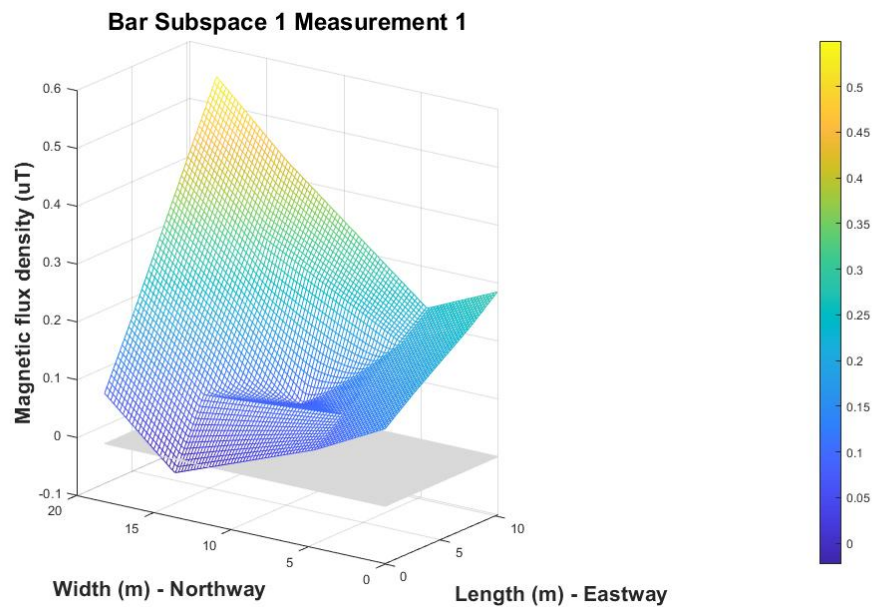


Figure C.5: Power frequency B-field interpolation and extrapolation at the Bar.

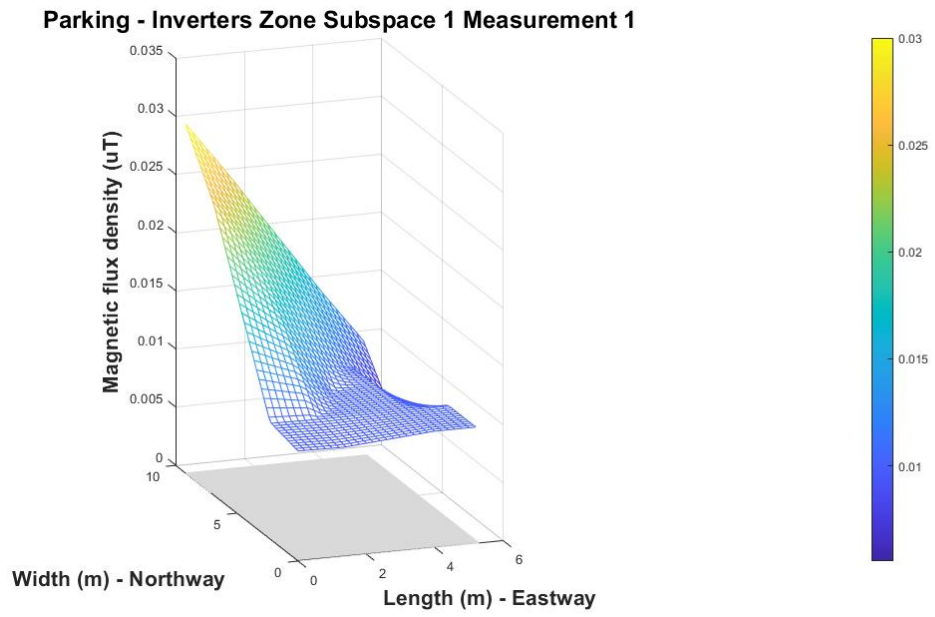


Figure C.6: Power frequency B-field interpolation and extrapolation at the Parking - Drivers Zone.

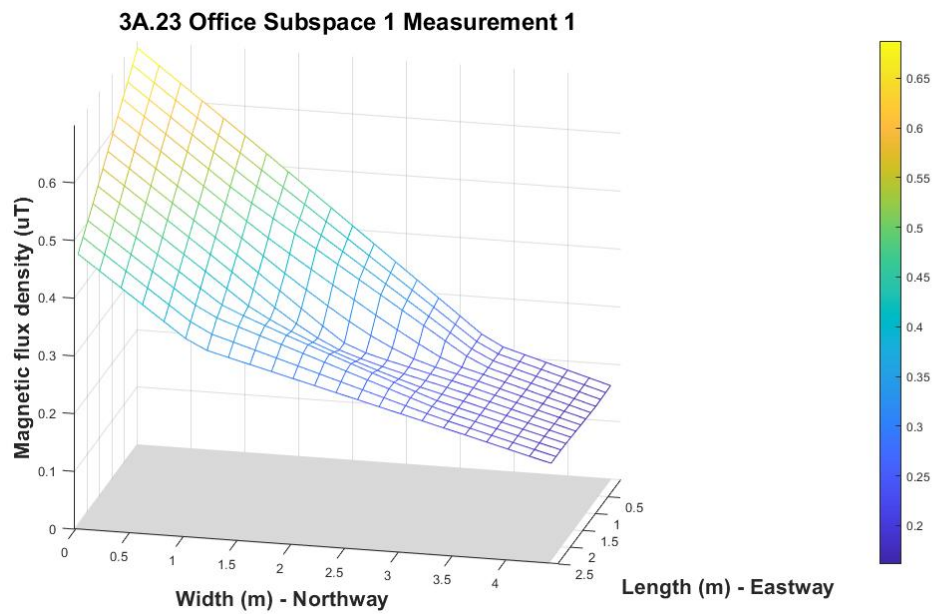


Figure C.7: Power frequency B-field interpolation and extrapolation at the 3A.23 Office.

Appendix D

Shielding Effectiveness testing site configurations and additional results

Table D.1: Shielding effectiveness frequency test specifications.

Frequency	Motivation	Antenna
50Hz	Power frequency equipment	30-spiral Coil
200MHz	Television broadcasting	BicoLOG 30100
450MHz	Intermediate UHF band	BicoLOG 30100
900MHz	GSM900 band	HiperLOG 7060
1.8GHz	GSM1800 and UMTS band	HiperLOG 7060
3GHz	WLAN band	HiperLOG 7060
4.5GHz	Peak observed in Radiometric survey	HiperLOG 7060
6GHz	Possible telecommunications range futurely available	HiperLOG 7060

Table D.2: Power-frequency Shielding effectiveness incandescent load configuration.

Power (W)	I(A)	Predicted B(uT)
25	0.108	0.463
100	0.435	1.87
125	0.543	2.33
200	0.870	3.73
225	0.978	4.20
300	1.31	5.59
325	1.41	6.06
400	1.74	7.46
520	2.25	9.65

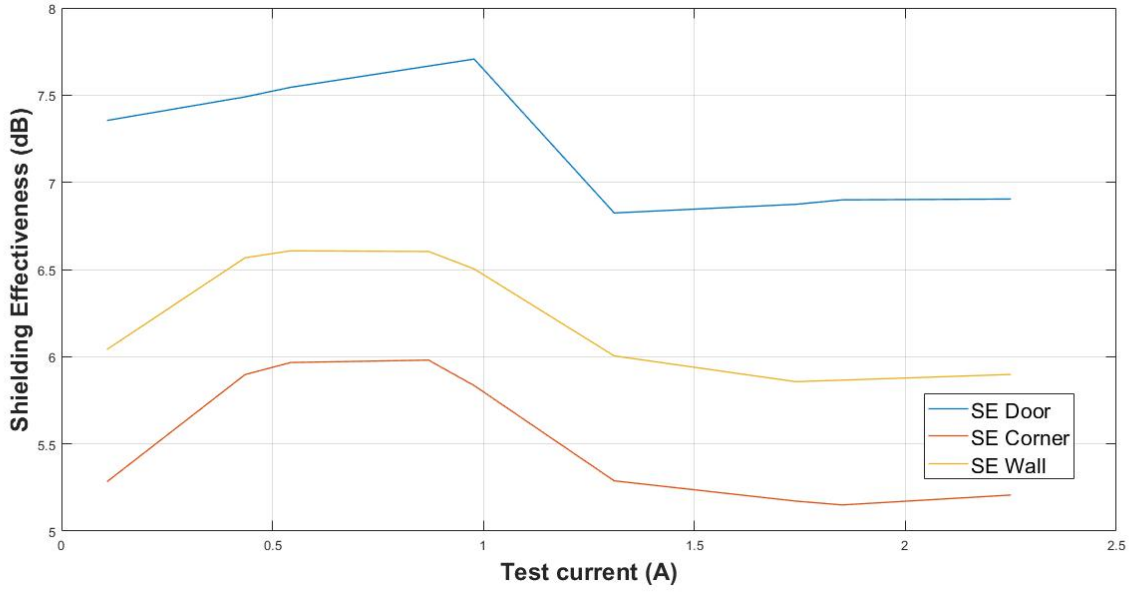


Figure D.1: ULF Power frequency SE in different loading test configurations.

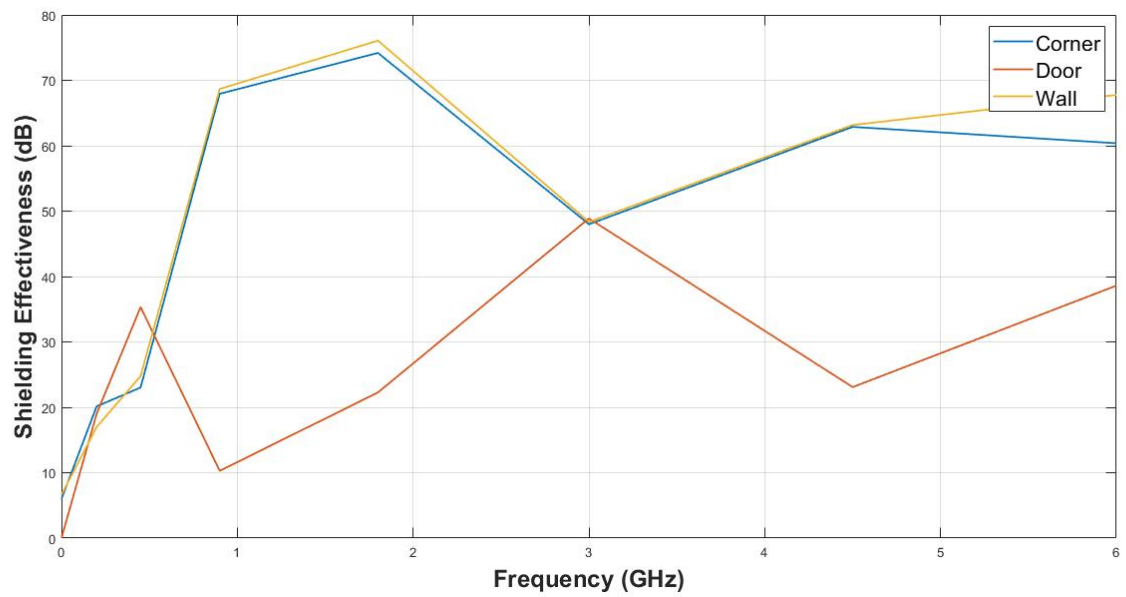


Figure D.2: Chamber's SE scenario with Signal generator emitting fields with a strength of 15dBm.

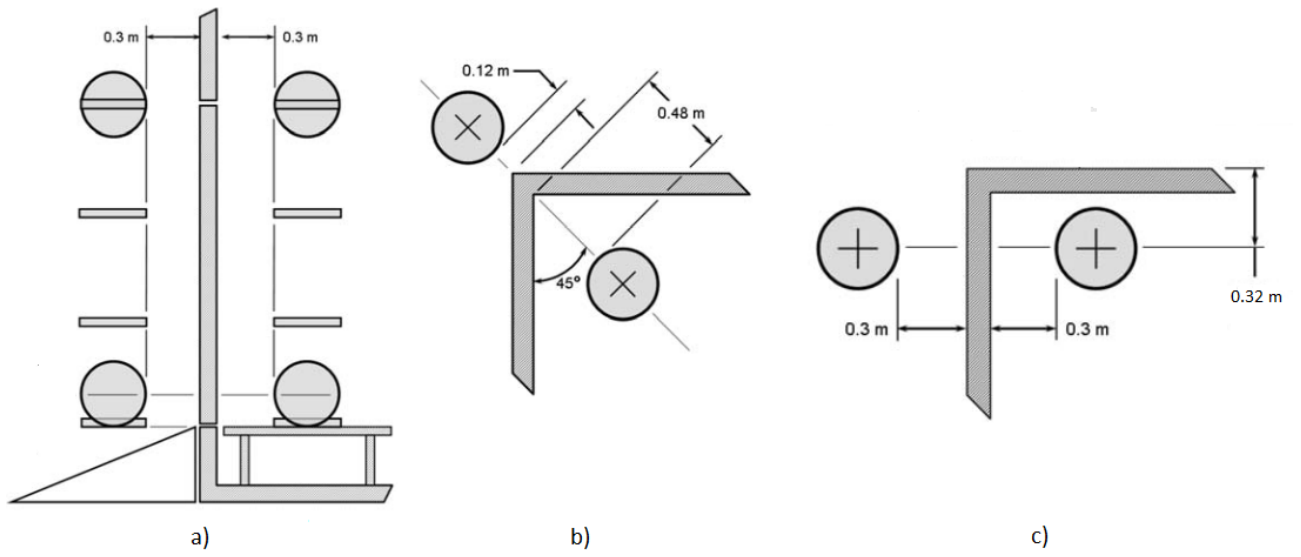
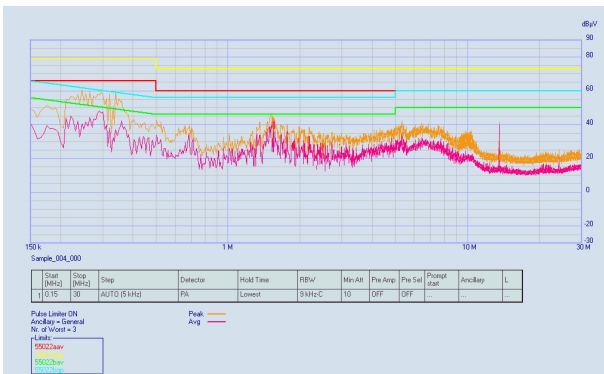


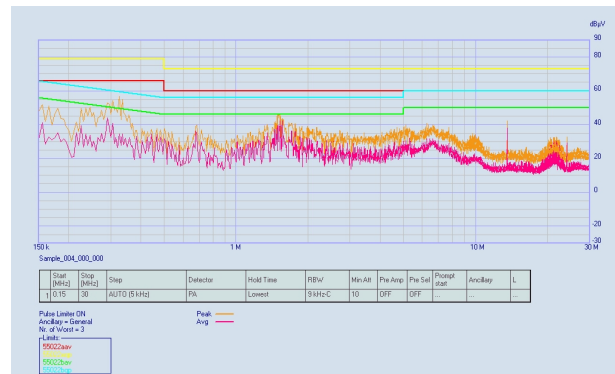
Figure D.3: Shielding effectiveness tests configuration protocol for Chamber's door (a), corner (b) and wall (c).

Appendix E

Additional results and Datasheet

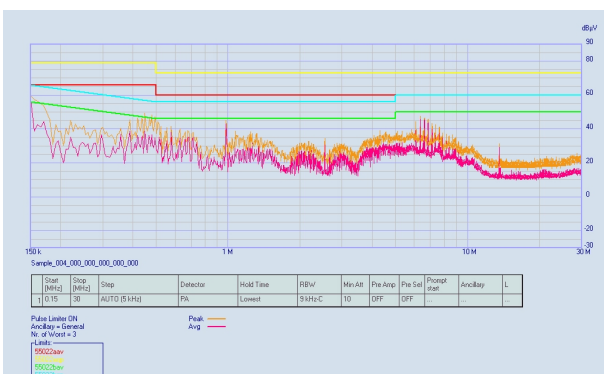


(a) Noise in Phase output

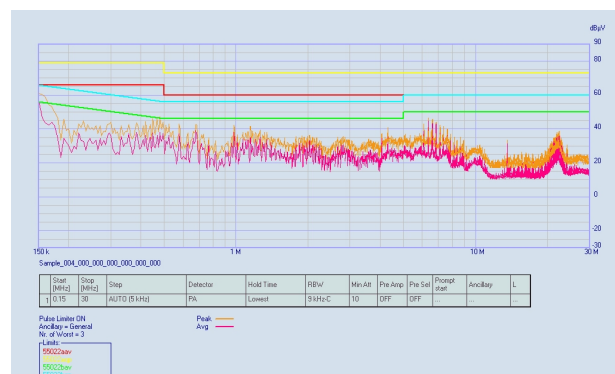


(b) Noise in Neutral output

Figure E.1: EMC conducted noise at power outlet in Bar along with the EN 55022 class A and class B limits.

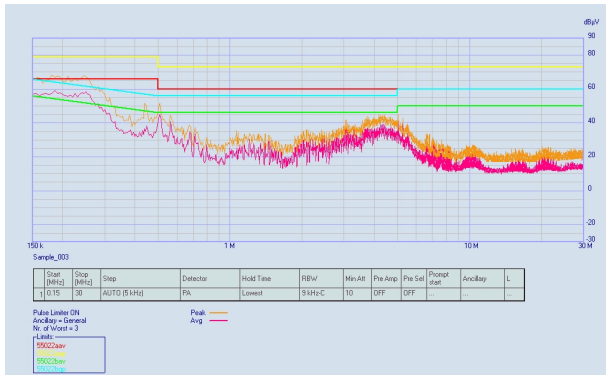


(a) Noise in Phase output

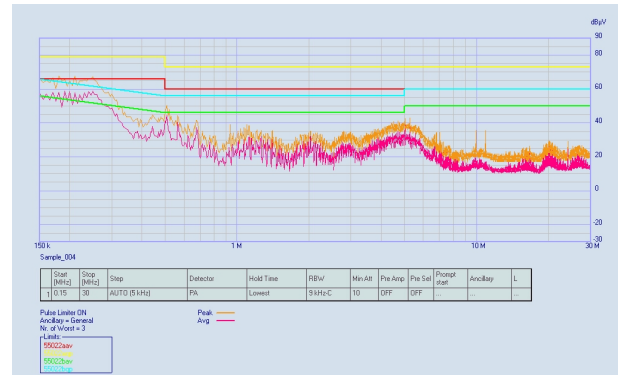


(b) Noise in Neutral output

Figure E.2: EMC conducted noise at power outlet in Third floor Study Aisle along with the EN 55022 class A and class B limits.

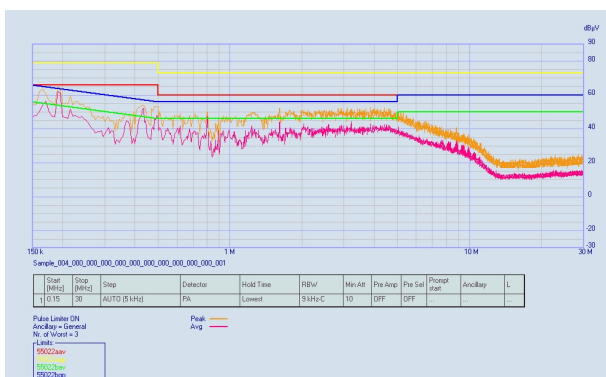


(a) Noise in Phase output

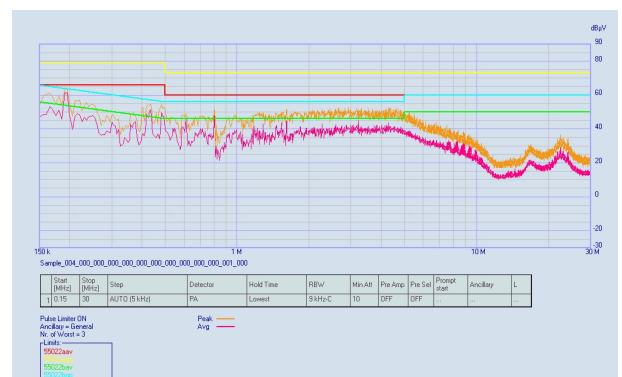


(b) Noise in Neutral output

Figure E.3: EMC conducted noise at power outlet in R1.2 laboratory at 17:41h along with the EN 55022 class A and class B limits.



(a) Noise in Phase output



(b) Noise in Neutral output

Figure E.4: EMC conducted noise at power outlet in R1.2 laboratory at 22:54h along with the EN 55022 class A and class B limits.



Figure E.5: Example of expansion joint in DEEC.

Table E.1: LISN+I toggle switches configuration modes

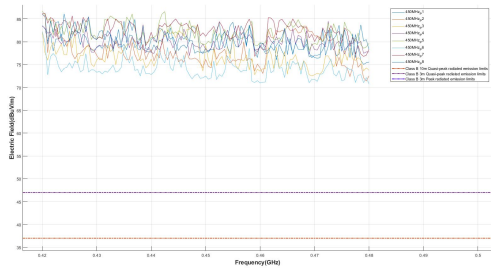
1st switch		2nd switch		3rd switch	
Power OFF	Power ON	Neutral Selected	Phase Selected	Filter OFF	Filter ON
Up	Down	Up	Down	Left	Right

Table E.2: LISN+I insulation verification tests.

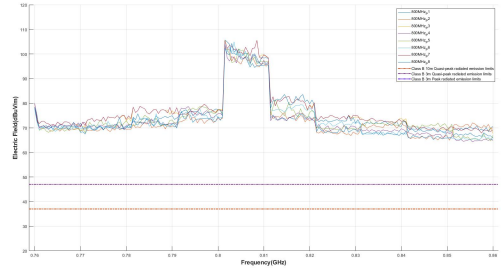
Insulation tests		Toggle switches configuration			
		1 st UP 2 nd UP 3 rd LEFT	1 st UP 2 nd UP 3 rd RIGHT	1 st UP 2 nd DOWN 3 rd LEFT	1 st UP 2 nd DOWN 3 rd RIGHT
I	Resistance between Phase and Neutral (Ω)	infinite	infinite	infinite	infinite
II	Resistance between Phase and BNC ground (Ω)	infinite	infinite	infinite	infinite
III	Resistance between Phase and BNC signal (Ω)	infinite	infinite	infinite	infinite
IV	Resistance between Neutral and BNC ground (Ω)	infinite	infinite	infinite	infinite
V	Resistance between Neutral and BNC signal (Ω)	infinite	infinite	infinite	infinite
VI	Resistance between BNC ground and BNC signal (Ω)	497.3	infinite	497.69	infinite
Insulation tests		1 st DOWN 2 nd UP 3 rd LEFT	1 st DOWN 2 nd UP 3 rd RIGHT	1 st DOWN 2 nd DOWN 3 rd LEFT	1 st DOWN 2 nd DOWN 3 rd RIGHT
I	Resistance between Phase and Neutral (Ω)	infinite	infinite	infinite	infinite
II	Resistance between Phase and BNC ground (Ω)	infinite	infinite	infinite	infinite
III	Resistance between Phase and BNC signal (Ω)	infinite	infinite	infinite	infinite
IV	Resistance between Neutral and BNC ground (Ω)	infinite	infinite	infinite	infinite
V	Resistance between Neutral and BNC signal (Ω)	infinite	infinite	infinite	infinite
VI	Resistance between BNC ground and BNC signal (Ω)	497.52	infinite	497.29	infinite

Table E.3: Wavelength spatial-variation hypothesis results.

Frequency (MHz)	PI		PII		PIII		PIV		PV		PVI		PVII		PVIII	
	Max (V/m)	MEF (V/m)	Max (V/m)	MEF (V/m)	Max (V/m)	MEF (V/m)	Max (V/m)	MEF (V/m)	Max (V/m)	MEF (V/m)	Max (V/m)	MEF (V/m)	Max (V/m)	MEF (V/m)	Max (V/m)	MEF (V/m)
100	0.0047	0.026	0.0094	0.0489	0.0057	0.0293	0.0099	0.0534	0.009	0.0493	0.009	0.0501	0.0056	0.0329	0.0045	0.0207
450	0.0164	0.1129	0.0203	0.1016	0.0149	0.0891	0.0168	0.1138	0.0216	0.1479	0.013	0.0593	0.0206	0.1537	0.0202	0.1249
800	0.1922	0.4941	0.1409	0.3722	0.189	0.5617	0.1553	0.3801	0.1938	0.438	0.1756	0.4513	0.189	0.5601	0.1641	0.4



(a) 450MHz Chart.



(b) 900MHz Chart.

Figure E.6: Wavelength spatial-variation hypothesis graphic results.

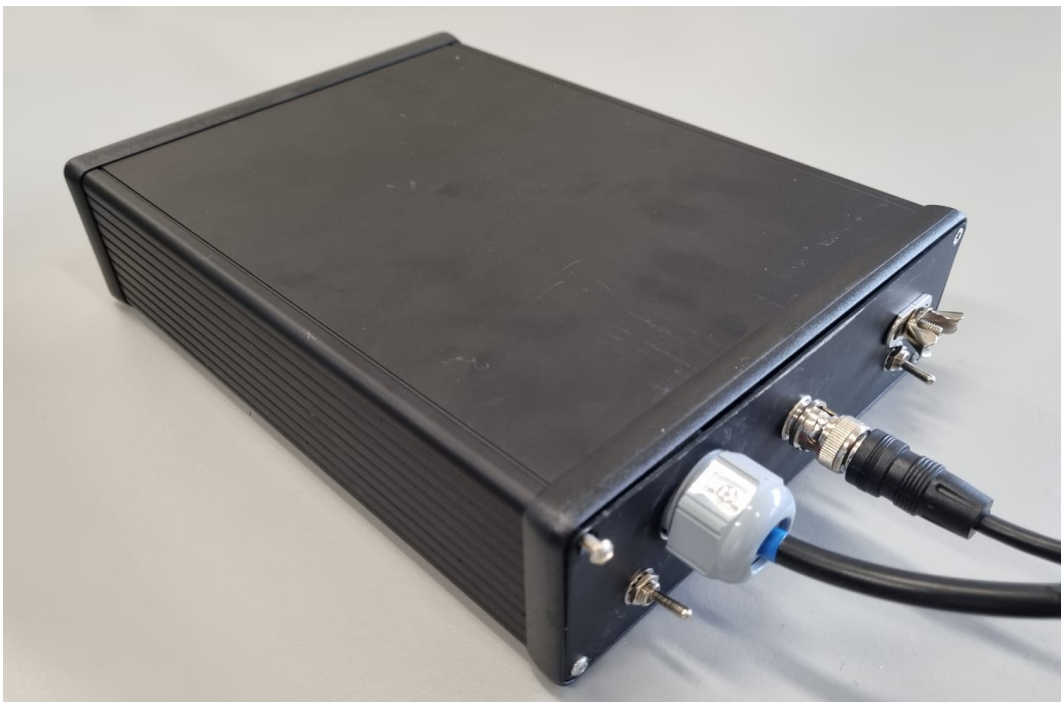


Figure E.7: LISN+I equipment.

Measurement Report (Same Site at Different Spots)

Surveyor: Felipe Ferreira		Electrical and Computer Engineering Department of University of Coimbra	
Manufacturer: Syrpris		Date: 202 - - Start Time: :	
Model: 4080		Date of Last Calibration: 202 - -	
Serial Number: 359193			
Probe: Triaxial ELF Meter		Antenna:	
Surveying Site:			
Address:		DEEC, Pólo II, 3030-290 Coimbra	
Metric used		True RMS (Cummulative)	
Statistical information:		> 4mG: $\pm 5\%$ of rdg max < 4mG: $\pm 2\%$ of digit, max	
Acquisition Time:		0.4 sec	
Physical quantity:	miliGauss	Condition:	
Temperature:		Humidity:	
Antenna factor (dB):		Cable Loss (dB):	
Geometric description (Number of subspaces):			
Frequency Range:	25 Hz – 1kHz		
Data available in file:			
Measured Values			
Spot	Height (m)	Magnetic field (mG)	Description / Obs.
Additional Info:			
# of measurements:	Max:		Min: Avg:
Obs.:			

Measurement report_v17_Syrpris

Figure E.8: Front page of Five-point method Datasheet.

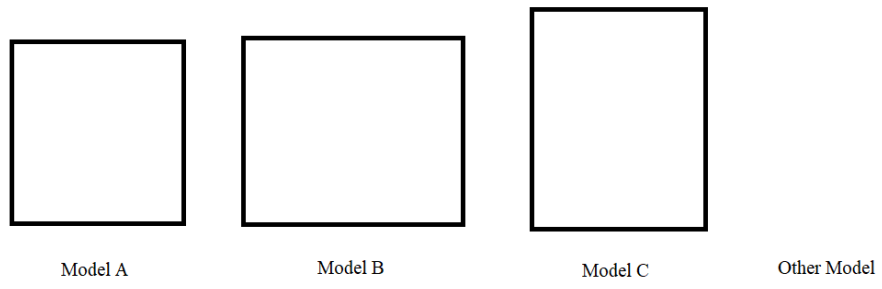
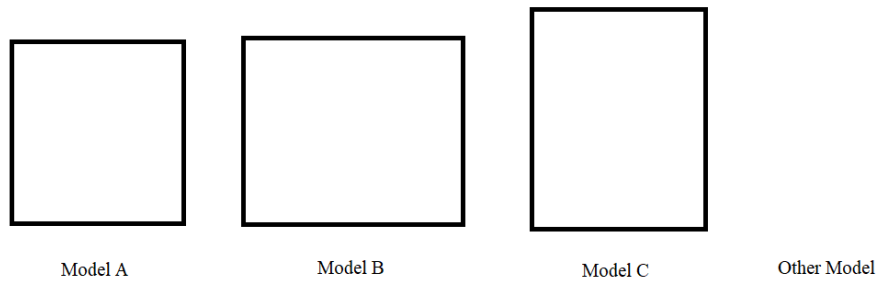


Figure E.9: Back page of Five-point method Datasheet.



Measurement report_v17_Syrpris

Figure E.11: Back page of ULF B-field time-variation Datasheet.

Measurement Report (Frequency Screening)

Surveyor: Felipe Ferreira		Electrical and Computer Engineering Department of University of Coimbra			
Manufacturer: Aaronia		Date: 2022 - - Start Time: :			
Model: NF-5020		Date of Last Calibration: 2022 - 03 - 16			
Serial Number: 05093					
Probe:		Antenna:			
Metric used and statistical information:					
Statistical Information					
Acquisition Time:					
Physical quantity:		Condition:			
Temperature:		Humidity:			
Antenna factor (dB):		Cable Loss (dB):			
Resolution Bandwidth (RBW)		Sampletime (ms):			
Number of Rooms measured:					
Measured Values					
Name of the Room	Height (m)	Room Model / Location	Frequency Range	File name	Add. Info:
P1			Power 50 Hz		
P2			100 Hz-300 Hz		
P3			300Hz-1000Hz		
P4			1kHz-30kHz		
P5			30kHz-150 kHz		
P6			150kHz-1MHz		
P7					
P8					
P9					
P10					
P11					
P12					
P13					
P14					
P15					
P16					
P17					
P18					
P19					
P20					
P21					
P22					
P23					
P24					
P25					
P26					
P27					
P28					
P29					
P30					
Additional Info:					

Measurement report_v17_AaroniaNF

Figure E.12: LF Radiometric Survey Datasheet.

Measurement Report (Frequency Screening)

Surveyor: Felipe Ferreira		Electrical and Computer Engineering Department of University of Coimbra			
Manufacturer: Aaronia		Date: 2022 - - Start Time: :			
Model: HF-6065		Date of Last Calibration: 2022 - 03 - 16			
Serial Number: 38360					
Probe:		Antenna:			
Metric used and statistical information:					
Statistical Information					
Acquisition Time: 0.4 sec					
Physical quantity:		Condition:			
Temperature:		Humidity:			
Antenna factor (dB):		Cable Loss (dB):			
Resolution Bandwidth (RBW):		Sampletime (ms):			
Number of Rooms measured:					
Measured Values					
Name of the Room	Height (m)	Room Model / Location	Frequency Range	File name	Add. Info:
P1			650MHz-950MHz		
P2			1650MHz-2000MHz		
P3			2500MHz-2700MHz		
P4			3400MHz-3800MHz		
P5			3800MHz-4400MHz		
P6			10Mhz-50MHz		
P7			50MHz-150MHz		
P8			400MHz-650MHz		
P9			150MHz-6000MHz		RBW = 3MHz
Additional Info:					

Measurement report_v17_AaroniaHF

Figure E.13: HF Radiometric Survey Datasheet.

